

**Misfits of wheat stem rust resistance-
Unusual solutions to a consistent problem**

A DISSERTATION
SUBMITTED TO THE FACULTY OF THE
UNIVERSITY OF MINNESOTA

BY:

Jordan J. Briggs

IN PARTIAL FULFILLMENT OF THE REQUIREMENTS
FOR THE DEGREE OF
DOCTOR OF PHILOSOPHY OF PLANT PATHOLOGY

ACADEMIC ADVISORS:

MATTHEW ROUSE

JAMES KURLE

ROBERT STUPAR

MELANIA FIGUEROA

DECEMBER 2016

Copyright Page

JORDAN J. BRIGGS 2017 ©

Acknowledgements

I would like to acknowledge my primary academic advisor and committee members: Dr. Matthew Rouse, Dr. James Kurle, Dr. Melania Figueuroa, and Dr. Robert Stupar. Thank you for the advice and assistance in my studies.

Thank you to all the members of the Rouse laboratory: Sam Stoxen, Dr. Nirmala Jayaveeramuthu, Dr. Shaun Curtin, Dr. Erena Edae, Garima Singh, Zennah Kosgey, Kelly Sidla, Zachary Blankenheim, and Eleanor McNairy. In addition to the assistance you have provided in the field and laboratory you have also provided a great deal of emotional support throughout my education.

I would also like to also thank Dr. Matthew Rouse, Dr. Colin Hiebert, and Dr. Wolfgang Spielmeier for their advice on professional and educational matters. You have stood out as examples of the scientist I hope to become.

Dedication

To my family, friends, and anyone who walked with me along the path to my degree.

Abstract

Rust fungi include some of the most economically damaging pathogens of wheat. They are notorious for their ability to quickly spread in susceptible host populations and greatly reduce grain yield potential and quality when managed improperly. *Puccinia graminis* f. sp. *tritici* (Pgt), the causal agent of wheat stem rust, can cause yield losses exceeding 50%. Stem rust is controlled in the U.S.A. using several methods including the introduction of genetic resistance, selection for earlier maturing varieties, removal of the alternate host *Berberis vulgaris*, and the application of fungicides. Subsequently, epidemics of stem rust causing greater than 10% yield losses have not been observed in the U.S.A. since the mid 1950's. Together, removal of *B. vulgaris* from wheat growing regions and the introduction of genetic resistance have accounted for much of the control of stem rust. Genetic resistance remains the dominant method of controlling stem rust in regions where removing *B. vulgaris* is not applicable. In more recent years, races of Pgt have been identified that overcome most widely deployed resistance genes. In 1999 race TTKSK was identified in Uganda that overcame stem rust resistance gene Sr31. Following deployment of Sr24 in Kenya, further selection for virulence resulted in the identification of race TTKST, then TTTSK (Sr36 virulence), and more recently TTKTT and TTKTK (SrTmp virulence). Major resistance genes have continually proven to not provide a durable form of resistance to wheat stem rust. Some resistance genes however have proven the test of time and remain effective to date. These resistance genes include Sr2, Lr34, Lr46, and Lr67. Each gene functions in an additive, minor-effect, and in some cases recessive manner, atypical of standard major genes, and provides and/or enhances resistance to multiple diseases including stem rust, leaf rust, stripe rust, and powdery mildew. Additionally Lr34 and Lr67 do not have the NB-LRR protein domains consistent with major genes. Durable genetic resistance to stem rust may require sources of resistance that deviate from standard mechanisms. This dissertation describes such sources

of resistance. SrTm4 is a major gene identified in *Triticum monococcum* that functions in a recessive manner, is broadly effective, and elicits a mesothetic (intermediate-effect) infection type. The adult plant resistance observed in 'Morochito Blanco' was found to have two underlying QTL, Qsr.cdl.2BS.2 and Qsr.cdl.6AS.1. These two loci comprise much of the adult plant resistance in 'Morochito Blanco' and exhibit interactions with environment or pathogen race. The Sr12 mutants created in this dissertation were made to characterize the disease reducing capabilities of Sr12: a recessive, race specific major gene that co-locates with adult plant resistance to Sr12 virulent races. Lastly, this dissertation also describes the identification of putative susceptibility genes for rust pathogens in barley, maize, soybean, and *Brachypodium distachyon*. The putative susceptibility gene in *B. distachyon* was tested with a T-DNA insertion mutant and exhibits enhanced rust resistance, however, may be linked to changes in overall plant growth and development. Each source of rust resistance defies standard systems of characterization and includes some traits that are less desirable along with their resistance capabilities, for example: unstable expression due to environmental interactions, race specificity, or recessive gene action. However, the benefit of these sources of stem rust resistance may compensate for their less desirable traits.

Table of Contents

List of Tables.....	vii
---------------------	-----

List of Figures.....	xii
----------------------	-----

Chapter 1

Mapping of *SrTm4*, a recessive stem rust resistance gene from diploid wheat effective to Ug99

a. Synopsis.....	1
b. Introduction.....	1
c. Materials and Methods.....	4
d. Results.....	6
e. Discussion.....	8

Chapter 2

Mapping of stem rust resistance QTL in the Ecuadorian bread wheat cultivar Morocho Blanco

a. Synopsis.....	18
b. Introduction.....	18
c. Materials and Methods.....	20
d. Results.....	24
e. Discussion.....	25

Chapter 3

Race specific analysis of adult plant resistance

a. Synopsis.....	37
b. Introduction.....	37
c. Materials and Methods.....	40
d. Results.....	43
e. Discussion.....	v

.....45

Chapter 4

Comparative differential expression of compatible rust infections

a. Synopsis.....	57
b. Introduction.....	57
c. Materials and Methods.....	60
d. Results.....	64
e. Discussion.....	67

Chapter 5

Creation of *Sr12* mutants derived from ‘Thatcher’ wheat

a. Synopsis.....	79
b. Introduction.....	79
c. Materials and Methods.....	82
d. Results.....	85
e. Discussion.....	88

Bibliography.....	97
--------------------------	-----------

List of Tables

Mapping of *SrTm4*, a Recessive Stem Rust Resistance Gene from Diploid Wheat Effective to Ug99

Table 1	13
----------------------	----

Infection types of *Triticum monococcum* lines and wheat cultivar Arina to selected races of *Puccinia graminis* f. sp. *tritici*.

Table 2	16
----------------------	----

Primer sequences, annealing temperatures, and restriction enzymes used for markers in the *SrTm4* region.

Supplementary Table S1	17
-------------------------------------	----

SrTm4 colinear region in *Brachypodium*: the two flanking markers BQ461276 and DR732348 of *SrTm4* define a colinear region in *Brachypodium* that includes 29 genes.

Mapping of stem rust resistance QTL in the Ecuadorian bread wheat cultivar Morocho Blanco

Table 1	31
----------------------	----

Percentage of variation and additive effects conferred by *Qsr.cdl.2BS.2* and *Qsr.cdl.6AS.1* on stem rust IR factor in the three populations across three years.

Table 2	31
----------------------	----

Recombinant lines from the DH 90K, DH KASP, and RIL KASP populations that retain a high level of resistance consistent with *Qsr.cdl.2BS.2* and retain maturity

similar or earlier than the average populations members without *Qsr.cdl.2BS.2*.

Table 332

P-values for single marker ANOVA of *Qsr.cdl.2BS.2* and *Qsr.cdl.6AS.1* associated SNP markers for severity and IR phenotypes in the 2013-2015 Kenyan screening seasons.

Table 432

Percentage of variation and additive effects conferred by *Qsr.cdl.2BS.2* and *Qsr.cdl.6AS.1* on stem rust disease severity in the three populations across three years.

Table 533

Haplotype analysis of SNPs associated with *Qsr.cdl.2BS.2*.

Table 633

Interval mapping logarithm of odds (LOD) scores for *Qsr.cdl.2BS.2* associated SNP markers and their correlation with disease severity in the DH 90K population.

Table 733

Interval mapping logarithm of odds (LOD) scores for *Qsr.cdl.2BS.2* associated SNP markers and their correlation with IR in the DH 90K population.

Table 834

Haplotype analysis of SNPs associated with *Qsr.cim.6AS.1*.

Supplemental

Table 1	34
DNA sequences for SNP markers associated with ‘Morocho Blanco’ resistance loci.	
Supplemental Table 2	35
Genetic map of chromosomes 2B and 6A, including positions of <i>Qsr.cdl.2BS.2</i> and <i>Qsr.cdl.6AS.1</i> .	
Race specific Analysis of adult plant resistance	
Table 1	51
The genetic map for chromosome 4A of the DH 90K population.	
Table 2	52
Significant QTL (pvalue <0.05) for all race/environments.	
Table 3	53
Correlation values of BLUP performance rank for the disease severity phenotype.	
Table 4	53
Correlation values of BLUP performance rank for the infection response phenotype.	
Table 5	53
Disease severity and Infection response exhibited by ‘Morocho Blanco’ in the Kulumsa, Ethiopia in single race nurseries of TTKSK, TKTTF, TRTTF, and JRCQC.	
Table 6	55
ANOVA analysis of the linear model for disease severity in Rosemount, MN to stem rust races RCRSC and TPMKC.	
Table 7	56
ANOVA analysis of the linear model for IR in Rosemount, MN to stem rust races	

RCRSC and TPMKC.

Comparative differential expression of compatible rust infections

Table 1	70
----------------------	----

Primers used to verify the presence of the T-DNA insertion in *BRADI3G28410*.

Table 2	70
----------------------	----

The total number of differentially expressed genes per time-point and change in regulation for each host; barley, soybean, and maize.

Table 3	70
----------------------	----

The total non-redundant differentially expressed genes and non-redundant differentially expressed genes that are homologous to at least one other host expressed as a proportion of the total number of gene models assessed in this study.

Table 4	72
----------------------	----

Differentially expressed homologues that exhibit similar changes in expression at the same time points.

Table 5	73
----------------------	----

Three putative nitrate transporter homologues were identified in *B. distachyon* using TBLASTX to compare the maize, soybean, and barley nitrate transporter gene models to the *B. distachyon* genome. Two *B. distachyon* homologues were found to have insertions within exonic sequences and only one homologue could be found in multiple T-DNA stock genetic backgrounds.

Creation of Sr12 mutants derived from ‘Thatcher’ wheat

Table

1	93
'Thatcher' M1 families exhibiting lines indicative of a <i>Sr12 knockout</i> and the number of observed mutant lines per headrow.	
Table 2	94
Observed IT's to SCCSC for progeny of mutant lines.	
Table 3	95
Results of the NB-LRR3 KASP assay used to identify the presence of <i>Sr12</i> .	
Table 4	95
Percent similarity of <i>Sr12</i> mutants to parental lines based on SNP marker alleles.	
Table 5	96
F ₁ allelism assay of M ₂ <i>Sr12</i> mutant crosses. IT 2+ is the expected phenotype for <i>Sr12</i> knockout mutants. Segregation of phenotypes indicates possible heterozygosity in <i>Sr12</i> mutants.	
Table 6	96
Proportion of susceptible (IT 2+) to resistant (IT 0;) progeny of F1 <i>Sr12</i> mutant crosses. Chi2 Tests were used to identify significant deviation from 3:1 susceptible to resistant segregation.	

List of Figures

Mapping of *SrTm4*, a Recessive Stem Rust Resistance Gene from Diploid Wheat Effective to Ug99

Figure 1.....13
Infection types of *Triticum monococcum* and *T. aestivum* lines.

Figure 2.....14
Infection types of *Triticum monococcum* and *T. aestivum* lines to races of *Puccinia graminis* f. sp. *tritici*: TPMKC, RKQQC, RCRSC, and SCCSC.

Figure 3.....15
Genetic maps of *SrTm4* on chromosome arm 2A^mL derived from two biparental mapping populations and their comparison with a physical map of *Brachypodium* chromosome 5.

Figure 4.....16
Relative map position of *SrTm4*, *Sr21*, and *Sr48*.

Mapping of stem rust resistance QTL in the Ecuadorian bread wheat

cultivar Morocho Blanco

Figure 1.....28

Logarithm of odds scores plotted for disease severity on chromosomes 6A and 2B for the DH 90K population. The significance threshold of 4.5 is indicated by the horizontal line spanning the graph.

Figure 2.....29

Logarithm of odds scores plotted for IR on chromosomes 6A and 2B for the DH 90K population. The significance threshold of 4.4 is indicated by the horizontal line spanning the graphs.

Figure 3.....30

Effect of QTL in the LMPG-6/'Morocho Blanco' DH population.

Supplemental Figure 1.....36

Logarithm of odds scores plotted for average maturity, severity and IR on chromosome 5A for the DH 90K population.

Race specific analysis of adult plant resistance

Figure 1.....50

Logarithm of odds scores for marker and the infection response phenotype associations mapped for chromosome 6A and 2B in Kenya, Ethiopia, and Rosemount single race nurseries.

Figure 2.....52

Logarithm of odds scores for marker and the severity phenotype associations mapped for chromosome 6A and 2B in Kenya, Ethiopia, and Rosemount single race nurseries.

Figure

3	53
BCCBC seedling infection types were converted to a 0-9 numerical score and compared to the 2013-2015 Kenyan infection response field data.	
Figure 4	54
(Top) Disease severity population density distribution curves for each race/environment. (Bottom) Kolmogorov-Smirnov pvalues for distribution correlations.	
Figure 5	55
(Top) Infection Response population density distribution curves for each race/environment. (Bottom) Kolmogorov-Smirnov pvalues for distribution correlations.	
Comparative differential expression of compatible rust infections	
Figure 1	71
A homologous set of putative nitrate transporters. All three genes were significantly differentially expressed at 12 hpi.	
Figure 2	73
Differentially expressed homologues with similar expression profiles identified through a TBLASTX of the soybean differentially expressed genes to the barley and maize differentially expressed genes.	
Figure 3	74
A) Line Bd21-3 and the mutant families 18123-1 through 18123-8 were screened with primers targeting the T-DNA insertion site for <i>BRADI3G28410</i> . B) The forward primer from (A) was used with the transposon specific T3 primer described by Bragg et al. (2012).	

Figure

4.....	75
The most significant BLAST alignment of the PCR product resulting from the 18123-F1 and T3 primer pair to the Bd21-3 genome sequence.	
Figure 5.....	76
<i>B. distachyon</i> line Bd21-3 and the JJ18123 mutant families inoculated with <i>Pga</i> race DBL. From left to right: Bd21-3; 18123-1; 18123-2; 18123-3; 18123-4; 18123-5; 18123-6; 18123-7; and 18123-8.	
Figure 6.....	77
Comparative growth of representatives lines from T-DNA mutant stock JJ18123 to Bd21-3.	
Figure 7.....	78
Pustule formation on T-DNA stock lines: JJ18133 and JJ18143.	
Creation of Sr12 mutants derived from ‘Thatcher’ wheat	
Figure 1.....	91
SCCSC infection response for A) ‘Prelude’, B) ‘Prelude’ (+Sr12), C) ‘Thatcher’, and D) <i>Sr16</i> (ISr-Sr16).	
Figure 2.....	92
BFBJC infection response for A) ‘Thatcher’, B) ‘Prelude’, C) ‘Prelude’ (+Sr12), D) IS-Sr9g, E) IS-Sr16, and F) IS-Sr5.	
Figure 3.....	93
SCCSC infection response on <i>Sr12</i> mutants. From left to right; ‘Thatcher’, 31-1, 35-1, 50-1, 83-1, 132-1, 150-1, 179-1, 234-1, 250-1, 272-1, 447-1, 520-1, and 547-1.	

Figure 4.....	94
BFBJC infection response on <i>Sr12</i> mutants. From left to right; ‘Thatcher’, 31-1, 35-1, 50-1, 83-1, 132-1, 150-1, 179-1 (IT 3), 179-1 (IT ;1), 234-1, 250-1, 272-1, 447-1, 520-1, and 547-1.	

Other Items (list of abbreviations etc.)

QTL: Quantitative Trait Locus

Pgt: Puccinia graminis f. sp. tritici

Pp: Phakopsora pachyrhizi

Ps: Puccinia sorghi

Pga: Puccinia graminis f. sp. avenae

T-DNA: Transfer DNA

IT: Infection Type

IR: Infection Response

cM: Centimorgan

SNP: Single Nucleotide Polymorphism

Mapping of *SrTm4*, a recessive stem rust resistance gene from diploid wheat Effective to Ug99

Abstract

Race TTKSK (04KEN156/04, Ug99) of *Puccinia graminis* f. sp. *tritici*, the causal agent of wheat stem rust, is a serious threat to wheat production worldwide. Diploid wheat, *Triticum monococcum* (genome Am), has been utilized previously for the introgression of stem rust resistance genes *Sr21*, *Sr22*, and *Sr35*. Multipathotype seedling tests of biparental populations demonstrated that *T. monococcum* accession PI 306540 collected in Romania contains a recessive resistance gene effective to all *P. graminis* f. sp. *tritici* races screened, including race TTKSK. We will refer to this gene as *SrTm4*, which is the fourth stem rust resistance gene characterized from *T. monococcum*. Using two mapping populations derived from crosses of PI 272557 × PI 306540 and G3116 × PI 306540, we mapped *SrTm4* on chromosome arm 2AmL within a 2.1 cM interval flanked by sequence-tagged markers BQ461276 and DR732348, which corresponds to a 240-kb region in *Brachypodium* chromosome 5. The eight microsatellite and nine sequence-tagged markers linked to *SrTm4* will facilitate the introgression and accelerate the deployment of *SrTm4*-mediated Ug99 resistance in wheat breeding programs. *

Introduction

Over 700 million metric tons of wheat, *Triticum aestivum* L. and *T. turgidum* ssp. *durum* (Desf.) Husn., are produced worldwide each year (FAO 2013), playing an important role in global food security. Reducing yield losses to pests and pathogens

* The chapter is the result of collaborative research. Collaborators include: Jordan Briggs, Shisheng Cheng, Wenjun Zhang, Sarah Nelson, Jorge Dubcovsky, and Matthew N. Rouse. The author contributed to designing and performing the experiments including: rating stem rust on seedling plants, extracting DNA, performing genetic marker assays, genetic mapping of *SrTm4*, drafting the manuscript, and editing. MNR and JD developed the populations. SC and WZ contributed to genetic mapping on of the two populations, developed the sequence-based markers, and identified critical recombinants for fine-mapping. SN contributed to performing genetic marker assays. MNR contributed rating stem rust on seedlings, approved experimental design, and supervised all analyses. JD supervised marker development and fine-mapping. All collaborators reviewed, commented, and improved the manuscript. This work was published in *Phytopathology*, 105(10): 1347-54, and titled, "Mapping of *SrTm4*, a Recessive Stem Rust Resistance Gene from Diploid Wheat Effective to Ug99." All dissertation committee members reviewed, commented, and approved this chapter. 1

is critical to maintain and increase wheat productivity. Historically, stem rust has produced large yield losses, which can exceed 50% in susceptible wheat cultivars during *Puccinia graminis* f. sp. *tritici* epidemics (Leonard 2001; Roelfs 1978). Breeding efforts to increase genetic resistance to stem rust, development of early maturing varieties, and efforts to remove the alternate host *Berberis vulgaris* L. near wheat-growing regions provided significant control of *P. graminis* f. sp. *tritici* in the past and reduced both severity and incidence of the stem rust disease (Peterson et al. 2005; Roelfs 1982, 1985). However, the emergence of the *P. graminis* f. sp. *tritici* Ug99 race group, composed of race TTKSK and variant races, allowed *P. graminis* f. sp. *tritici* to overcome many of the deployed stem rust resistance genes, making the pathogen again a threat to wheat production worldwide (Pretorius et al. 2000; Singh et al. 2011). The adaptation of the Ug99 race group to previously resistant cultivars has rendered three resistance genes (*Sr24*, *Sr36*, *Sr9h*) ineffective since the initial characterization of race TTKSK (Jin et al. 2008, 2009; Pretorius et al. 2012; Rouse et al. 2014), although these three genes remain effective against many *P. graminis* f. sp. *tritici* races. Over 50 wheat stem rust resistance genes have been identified (McIntosh et al. 1995, 2013), yet few of the ones present in current commercial wheat varieties are effective to the Ug99 race group (Jin and Singh 2006; Sharma et al. 2013; Singh et al. 2011).

Wheat wild relatives at different ploidy levels have been previously utilized for introgressing resistance genes effective against stem rust into cultivated varieties including *Sr21*, *Sr22*, and *Sr35* from *T. monococcum* L. (Gerechter-Amitai et al. 1971; McIntosh et al. 1984; The 1973); *Sr33*, *Sr45*, *Sr46*, *SrTA10171*, *SrTA10187*, and *SrTA1662* from *A. tauschii* Coss. (Kerber and Dyck 1979; Marais et al. 1998; McIntosh et al. 2013; Olson et al. 2013a,b); *Sr32*, *Sr39*, and *Sr47* from *A. speltooides* Tausch (Faris et al. 2008; Kerber and Dyck 1990; McIntosh et al. 1995); and *Sr36*, *Sr37*, and *Sr40* from *T. timopheevii* (Zhuk.) Zhuk. (Dyck 1992; McIntosh and Gyrfas 1971). Among these resistance genes only *Sr35* and *Sr33* have been cloned and both encode nucleotide-binding-site leucine-rich repeat proteins (NB-LRR) (Periyannan et

al. 2013; Saintenac et al. 2013).

This study focused on a resistance gene from *T. monococcum*, a species closely related to *T. urartu*, the donor of the A genome to the polyploid wheat species. *T. monococcum* and *T. urartu* are endemic to the same geographic regions, have identical karyotypes (Giorgi and Bozzini 1969), and have normal bivalent chromosome pairing in meiosis (Dvorak 1976; Nath et al. 1984), but their hybrids are sterile confirming that they are different species (Johnson and Dhaliwal 1976). The DNA sequences of these diploid species are sufficiently differentiated to greatly reduce pairing between the *T. monococcum* chromosomes and the A genome chromosomes from polyploid wheat when they are in the presence of the wild-type pairing homoeologous 1 (*Ph1*) gene (Dubcovsky et al. 1995; Luo et al. 1996).

The *T. monococcum* ssp. *monococcum* accession PI 306540 was identified in a previous study as possessing potentially new resistance genes based on seedling ITs to *P. graminis* f. sp. *tritici* races (Rouse and Jin 2011b). F_{2:3} families derived from a cross between PI 306540 and stem rust susceptible *T. monococcum* ssp. *monococcum* PI 272557 were screened with race TTKSK and *Sr21*-virulent races QFCSC and TTTTF. Segregation of resistance to race TTKSK indicated the presence of three resistance genes (Rouse and Jin 2011a). One of the three genes was predicted to be *Sr21*. The other two genes are different from known *T. monococcum* resistance genes *Sr22* and *Sr35* (Rouse and Jin 2011a). One of these two genes was effective to *P. graminis* f. sp. *tritici* races TTKSK and QFCSC, but ineffective to race TTTTF. The other gene we refer to as *SrTm4* produced a mesothetic IT (reaction with both resistant and susceptible ITs present) when present singly (Rouse and Jin 2011a). In a population derived from PI 306540, a low or mesothetic reaction was observed in environmentally controlled settings to races QFCSC and TTKSK in families predicted to carry *SrTm4* based on the presence of a mesothetic IT to race TTTTF. The objective of this study was to genetically map *SrTm4*, to identify the colinear regions in other sequenced genomes, and to develop molecular

markers closely linked to the gene that can be effectively used to monitor the introgression of a small segment of *T. monococcum* chromosome 2A^m carrying *SrTm4* into common wheat.

Materials and methods

Plant materials. Two F₂ mapping populations, including 89 individuals from the cross of PI 272557 × PI 306540 and 190 individuals from the cross of G3116 × PI 306540, were used to map *SrTm4* in diploid wheat. PI 306540 and PI 272557 are cultivated spring *T. monococcum* ssp. *monococcum* accessions obtained from the U.S. Department of Agriculture-Agricultural Research Service (USDA-ARS) National Small Grains Collection. PI 272557 was characterized as susceptible to five races of *P. graminis* f. sp. *tritici* in a previous study (Rouse and Jin 2011b). G3116 (PI 427992) is a wild *T. monococcum* ssp. *aegilopoides* and was selected as a parent of the second cross because of its high level of polymorphism compared with cultivated *T. monococcum* ssp. *monococcum* (Dubcovsky et al. 1996). Based on seedling tests with multiple *P. graminis* f. sp. *tritici* races, G3116 was postulated to possess resistance gene *Sr21* (Zhang et al. 2010). This hypothesis was confirmed in a recent study that mapped the *Sr21* resistance from G3116 to the long arm of chromosome 2A^m, roughly 50 cM from the centromere (Chen et al. 2015). Since both G3116 and PI 306540 carry *Sr21*, a *P. graminis* f. sp. *tritici* race virulent to *Sr21* (e.g., TTTTF) was used to map *SrTm4* in this population. The Swiss winter wheat cultivar Arina (obtained from the Australian Winter Cereals Collection, Tamworth, AUS-21732) was utilized as a check line for *Sr48* in some of our experiments.

Evaluation of stem rust resistance. Inoculation of seedlings with *P. graminis* f. sp. *tritici* isolates was performed at the USDA-ARS Cereal Disease Laboratory according to previously described methods (Rouse et al. 2011c). *P. graminis* f. sp. *tritici* race TTTTF (isolate 01MN84A-1-2) was used to inoculate the parents and 25 individuals from each F_{2:3} family. At least two replications were performed for each F_{2:3} family. After inoculation, plants were incubated in growth chambers maintained at

18°C day, 15°C night with a 16 h photoperiod. The lower incubation temperature was necessary to ensure consistent expression of *SrTm4* resistance. Infection types (ITs) were assessed 14 days after inoculation on the primary leaves using a 0 to 4 scale described by Stakman et al. (1962). ITs of 2 or lower including mesothetic (;3, 13, or ;23) ITs denote resistant reactions and ITs of 3 and greater denote susceptible reactions. The F₂ *SrTm4* genotypes were based on the phenotypes of their F_{2:3} families and classified as homozygous resistant (HR), heterozygous (Het), or homozygous susceptible (HS).

We also inoculated PI 306540, PI 272557, G3116, Einkorn (PI 10474), and wheat cultivar Arina with diverse *P. graminis* f. sp. *tritici* races that are virulent on *Sr21* including TTTTF, TPMKC, RKQQC, RCRSC, QTHJC, QFCSC, and SCCSC (isolates 01MN84A-1-2, 74MN1409, 99KS76A, 77ND82A, 75ND717C, 06ND76C, and 09ID73-2) to determine the effectiveness of *SrTm4* to different *P. graminis* f. sp. *tritici* races. The five lines were also inoculated with *Sr21*-avirulent race MCCFC (isolate 59KS19). Presence of ITs characteristic of *SrTm4* (IT ;3, 13, or ;23) were considered indicative of the effectiveness of *SrTm4* to each *P. graminis* f. sp. *tritici* race.

Molecular marker analyses. Genomic DNA from the F_{2:3} families was bulk extracted using a modified CTAB protocol (Yu et al. 2008) from a minimum of 10 F_{2:3} plants per family. Single sequence repeats (SSR) markers were selected to screen for polymorphism in regions associated with *SrTm4* using protocols described before (Röder et al. 1998; Somers et al. 2004; Song et al. 2005). Wheat ESTs that were previously mapped to the long arm of chromosome 2A were also tested for sequence polymorphism to develop sequence-based markers. ESTs linked to *SrTm4* were then used to search for the orthologous region in the *Brachypodium* genome. *Brachypodium* genes found in the targeted region were then used to find wheat orthologs and to develop new markers.

Genetic mapping. The linkage map of *SrTm4* was constructed using MapMaker

version 3.0b (Lander et al. 1987). The Kosambi mapping function was used to calculate map distances. The genetic linkage map was drawn with the software MapDraw V2.1 (Liu and Meng 2003).

RESULTS

Evaluation of *SrTm4* resistance. PI 306540 displayed resistant ITs characteristic of *SrTm4* to all of the *P. graminis* f. sp. *tritici* races tested (Table 1; Figs. 1 and 2). The ITs of G3116 and PI 10474 were consistent with the presence of *Sr21* in these lines (Table 1). PI 272557 was susceptible to all of the *P. graminis* f. sp. *tritici* races and wheat cultivar Arina was resistant to all of the races.

ITs in resistant $F_{2:3}$ families derived from the PI 272557 \times PI 306540 cross ranged from ;3 to 31, whereas susceptible families exhibited ITs ranging from 3 to 4 in response to race TTTTF (Fig. 1). Among the 89 F_3 families, we detected 11 homozygous resistant, 49 segregating for resistance, and 29 homozygous susceptible. This ratio deviated slightly from the expected 1:2:1 segregation ratio ($\chi^2 = 8.19$, $P = 0.017$). However, the segregation of resistance among 1,370 plants from the progeny of the 49 segregating $F_{2:3}$ families was 346 resistant plants and 1,024 susceptible, which fit a 1:3 segregation ratio expected for a single recessive resistance gene ($\chi^2 = 0.048$, $P = 0.82$).

ITs in resistant $F_{2:3}$ families derived from the G3116 \times PI 306540 cross ranged from ;3 to 31, whereas susceptible families exhibited ITs ranging from 3 to 4 in response to race TTTTF. Among the 190 $F_{2:3}$ families analyzed for this population, we detected 39 homozygous resistant families, 108 families segregating for resistance to race TTTTF, and 43 homozygous susceptible families. This ratio did not deviate significantly from the expected 1:2:1 segregation ratio expected for a single gene ($\chi^2 = 3.72$, $P = 0.155$). Analysis of 1,318 plants from the progeny of 60 segregating $F_{2:3}$ families in this population resulted in 363 (27.5%) resistant plants and 955 (72.5%) susceptible plants, which is close to the 1:3 segregation ratio expected for a single recessive resistance gene ($\chi^2 = 4.54$, $P = 0.033$).

Identification of SSR markers linked with *SrTm4*. Bulk segregant analysis (BSA) was used to identify SSR markers linked with *SrTm4*. Among the initial polymorphic SSR markers tested in population PI 272557 × PI 306540, *gwm265* showed significant linkage to *SrTm4*. Marker *gwm265* was previously mapped to chromosome arm 2AL in wheat (Röder et al. 1998; Song et al. 2005). Therefore, additional SSR markers from 2AL were screened on the parents for polymorphisms and all polymorphic markers were screened on the F_{2:3} population. A total of seven SSR markers in population PI 272557 × PI 306540 and six SSR markers in population G3116 × PI 306540 were found to be linked with *SrTm4* (Fig. 3; Table 2).

Development of sequenced-based markers linked to *SrTm4*. To saturate the chromosome region carrying *SrTm4* and to identify the collinear region in other cereal genomes like Brachypodium, we selected several wheat ESTs from the long arm of chromosome 2A to develop sequence based markers. Wheat EST BG313738 was found to be polymorphic in both populations and was mapped proximal to *SrTm4*. The sequence of BG313738 was used to identify a colinear region in chromosome 5 of Brachypodium where we selected thirty genes to develop additional markers for *SrTm4*. These efforts resulted in two additional sequence-tagged markers in the PI 272557 × PI 306540 population and eight in the G3116 × PI 306540 population linked with *SrTm4* (Fig. 3; Table 2). The two closest markers flanking *SrTm4* were BQ461276 (1.6 cM proximal to *SrTm4*) and DR732348 (0.5 cM distal to *SrTm4*, Fig. 2), which defined a 2.1 cM candidate region for *SrTm4* in the G3116 × PI 306540 population. Marker DR732348 was developed from the same contig as SSR markers *gwm526* and *gdm93*, which amplify the same SSR locus. The flanking SSR sequences were used to identify the *T. aestivum* contig (IWGSC_2AL_contig 6401556, The International Wheat Genome Sequencing Consortium 2014), and then a gene within this contig was used to develop marker *DR732348*.

SrTm4 colinear region in *Brachypodium*. The proximal marker *BQ461276* was identified to be orthologous to *Brachypodium* gene *Bradi5g25720* (Bd5: 26,907,758 bp to 26,910,587 bp), whereas the distal marker *DR732348* was 91% identical at the DNA level with *Bradi5g26020* (Bd5: 27,127,725 bp to 27,147,892 bp) (Fig. 2C). The *SrTm4* flanking markers define a 240-kb genomic region in *Brachypodium* chromosome 5 (Bd5: 26,907,758 bp - 27,147,892 bp) that includes 29 putative *Brachypodium* genes (*Bradi5g25730* to *Bradi5g26010*). The functional annotation of these 29 genes (Supplementary Table S1) does not include any NB-LRR resistance gene.

The relative map position of *SrTm4* with other *Sr* genes on chromosome 2AL.

Two previously characterized wheat stem rust resistance genes, *Sr21* and *Sr48*, have been mapped before on chromosome arm 2AL (Bansal et al. 2008, 2009; Chen et al. 2015). *Sr21* was mapped roughly 50 cM from the centromere and 29.1 cM proximal to marker *BG313738*, whereas *SrTm4* was mapped 5.8 cM distal to the same sequence-tagged marker and ~85 cM from the centromere. This result clearly indicates that *SrTm4* and *Sr21* are two different loci, located ~35 cM apart (Fig. 4).

Sr48 has been previously mapped 22.1 cM distal to marker *gwm382* (Bansal et al. 2008, 2009; Fig. 3B) on the long arm of chromosome 2A from 'Arina'. Initially, no common markers were available between the *Sr48* and *SrTm4* maps, complicating the comparative analysis. To generate a common reference point, we first sequenced the PCR product of *gwm382* and identified *T. aestivum* contig IWGSC_2AL_contig 6435092 (The International Wheat Genome Sequencing Consortium 2014) that includes the *gwm382* SSR flanking sequences. From this contig we developed marker *BG907495* that was mapped 11.7 cM distal to *SrTm4*. Based on these distances, *SrTm4* is located 29.9 cM proximal to *Sr48* (Fig. 4).

DISCUSSION

A previous survey of *T. monococcum* for resistance to race TTKSK (Rouse and

Jin 2011b) postulated that most of the resistant accessions carry the mapped genes Sr21 (Chen et al. 2015), Sr22 (Periyannan et al. 2011), and Sr35 (Saintenac et al. 2013). However, accession PI 306540, a cultivated *T. monococcum* ssp. *monococcum* collected in Romania, possessed two different resistance genes (Rouse and Jin 2011a).

We focused on one of these genes, namely *SrTm4*, that is effective to the virulent race TTTTF because of the interesting recessive nature of the resistance and its broad resistance to all the *P. graminis* f. sp. *tritici* races tested so far. The initial study showed that *SrTm4* confers resistance to Ug99 race TTKSK, and additional races TTTTF, TRTTF, QFCSC, and MCCFC (Rouse and Jin 2011a). We showed here that PI 306540 also displayed mesothetic resistant ITs to four additional races that are virulent on *Sr21* (TPMKC, RKQQC, RCRSC, and SCCSC) (Fig. 2). The mesothetic type of resistance observed to these races suggests that *SrTm4* is effective to these races. Though the presence of ITs characteristic of a particular gene is not necessarily diagnostic of the presence of that gene, the presence of the mesothetic ITs provides preliminary evidence of the spectrum of effectiveness of *SrTm4*. The broad-spectrum resistance of *SrTm4* makes it a valuable resource for breeding resistance to Ug99 and other virulent *P. graminis* f. sp. *tritici* races. However, *SrTm4* only confers partial resistance and therefore it should be deployed in combination with other *P. graminis* f. sp. *tritici* resistance to achieve economically useful levels of resistance.

We have initiated the introgression of *SrTm4* from PI 306540 into polyploid wheat. These crosses require the use of a tetraploid bridge because direct crosses between *T. monococcum* and hexaploid wheat are frequently sterile.

When the complete *T. monococcum* complement is present, some recombination is observed between the *T. monococcum* and the A genome chromosomes, but that recombination is reduced to very low levels when only single chromosomes or

chromosome pieces of *T. monococcum* are present in hexaploid wheat (Dubcovsky et al. 1995, Luo et al. 1996). Fortunately, recombination between the A and A^m chromosomes is restored to normal levels in the presence of the *ph1b* mutation (Dubcovsky et al. 1995). Using the *ph1b* mutation and the multiple markers linked to *SrTm4* developed in this study, it will be possible to engineer a small *T. monococcum* introgression carrying only *SrTm4*.

Sr21 and *SrTm4* present very different resistance profiles that suggest that they are different genes. Resistance conferred by *Sr21* is dominant, ineffective at lower temperatures (16°C), and ineffective to several *P. graminis* f. sp. *tritici* races (TTTTF, QFCSC, TPMKC, RKQQC, RCRSC, QTHJC, and SCCSC). By contrast, resistance conferred by *SrTm4* is recessive, effective at lower temperatures, and screening data suggest *SrTm4* is effective against all 10 *P. graminis* f. sp. *tritici* races tested so far, including several that are virulent on *Sr21* (e.g., TTTTTF). The genetic map of *SrTm4* presented here confirmed that this gene is different from *Sr21*, and that the two genes are roughly 38 cM apart (Fig. 4) (Chen et al. 2015).

The relationship of *SrTm4* and *Sr48* is not as clear as the relationship between *SrTm4* and *Sr21* described above. *Sr48* was mapped to chromosome arm 2AL of the bread wheat cultivar Arina (Bansal et al. 2008), and was first designated as *SrAn1* using Australian *P. graminis* f. sp. *tritici* isolates 98-1,2,3,5,6 and 34-1,2,7+*Sr38*. Subsequent mapping placed *Sr48* 16.5 cM distal to the stripe rust resistance locus *Yr1* (Bansal et al. 2009). A comparative analysis of shared marker *gwm382* (BG907495, is from the same contig as *gwm382*) between the *T. monococcum* 2A^m genetic map in our present study and the hexaploid wheat 2A genetic map (Bansal et al. 2009) indicates *SrTm4* is located approximately 30 cM proximal to *Sr48* (Fig. 3A and B).

However, *P. graminis* f. sp. *tritici* isolates used to map *Sr48* do not possess comparable virulence to those used in this study or previously by Rouse et al.

(2011). Therefore, further screening with *P. graminis* f. sp. *tritici* isolates covering a broad range of virulence phenotypes or a more precise map of *Sr48* sharing common markers with the *SrTm4* map will be necessary to determine if *SrTm4* and *Sr48* are different genes or different alleles of the same gene. Once *SrTm4* is transferred to hexaploid wheat, a direct allelism test in a ph1b background may provide a definitive answer to this question.

The fourth resistance gene from *T. monococcum*, *SrTm4*, confers resistance to diverse isolates of *P. graminis* f. sp. *tritici* and is an interesting target to be combined with other Ug99 effective stem rust resistance genes. Pyramids of broadly effective resistance genes are expected to confer more durable resistance, but only the test of time will confirm or reject this hypothesis. Since *SrTm4* and *Sr21* are on the same chromosome arm, it should be possible to introgress both genes simultaneously in hexaploid wheat. However, additional studies will be required to test if the large *T. monococcum* segment required to introgress both *T. monococcum* genes carries any detrimental gene to hexaploid or tetraploid wheat agronomic performance or quality. If *SrTm4* and *Sr48* are different genes, coupling both genes on chromosome arm 2AL should also be possible.

The two stem rust resistance genes cloned so far (Periyannan et al. 2013; Saintenac et al. 2013) are NB-LRR, and both confer resistance to Ug99 with dominant inheritance. The recessive nature of *SrTm4* and the mesothetic IT may be indicative of a different resistance mechanism, providing an additional incentive for the cloning of this gene. The absence of NB-LRR genes in the colinear region of *Brachypodium* provides indirect support for this hypothesis. However, the final identification of the *SrTm4* gene will be required to fully test this hypothesis.

The use of two diploid wheat populations with contrasting levels of polymorphism seems to be a viable strategy to clone this resistance gene. The more polymorphic cross between wild and cultivated *T. monococcum* can be used to rapidly

develop markers in the initial stages of the high density mapping (as demonstrated in this study), whereas the cross between the two cultivated *T. monococcum* accessions can be used in the later stages of the project to identify the causal polymorphisms. A similar strategy was used successfully to clone the Ug99 resistance gene *Sr35* (Saintenac et al. 2013). The cloning of *SrTm4* will add additional tools to generate cisgenic resistance cassettes that can combine different resistance genes (e.g., *Sr33* and *Sr35*). In the meantime, the closely linked markers to *SrTm4* identified in this study will be useful tools to initiate the introgression of this gene into polyploid wheat and to deploy the natural *SrTm4* allele in wheat commercial varieties.

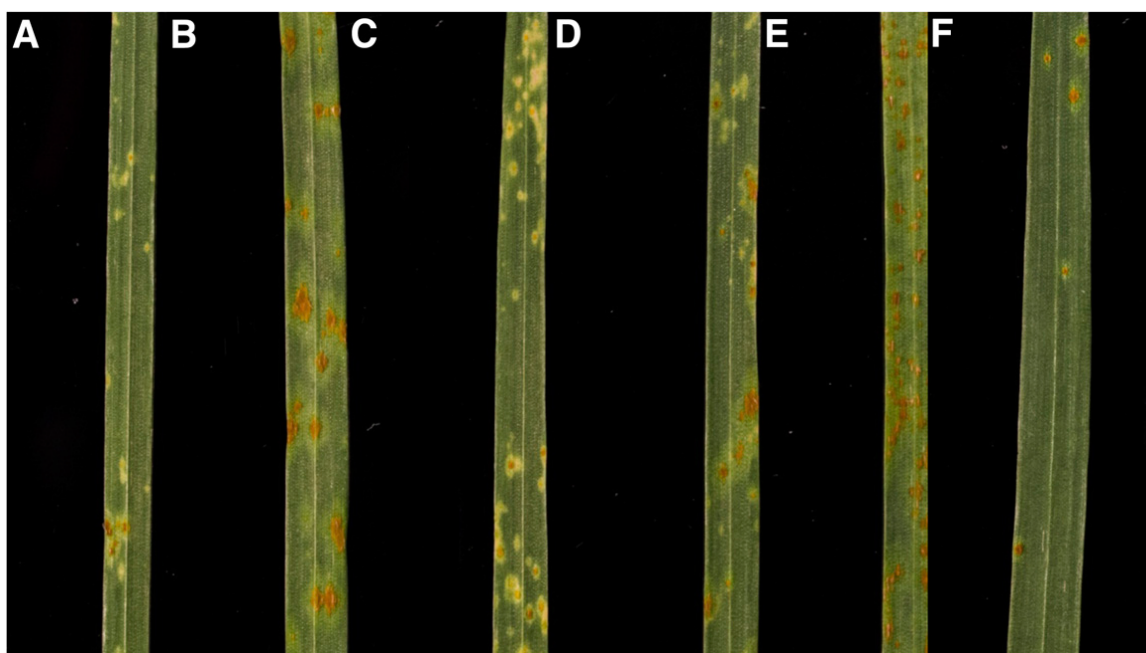


Figure 1. Infection types of *Triticum monococcum* and *T. aestivum* lines A, PI 306540 (*SrTm4*); B, PI 272557; C, PI 272557/PI 306540 F2:3 family 42 (*SrTm4*); D, PI 272557/PI 306540 F2:3 family 70 (*SrTm4*); E, PI 10474 (*Sr21*); and F, Arina (*Sr48*) in response to pathotype TTTTF of *Puccinia graminis* f. sp. *tritici*.

<i>P. graminis</i> f. sp. <i>tritici</i> race	Line				
	PI 306540	PI 272557	G3116	PI 10474	Arina
TTTTF	;13	33+	3	33+	13- LIF
TPMKC	;	33+	3	33+	13- LIF
RKQQC	;13	33+	3	3	13-
RCRSC	;13	33+	3	33+	3-LIF
QTHJC	;12+	33+	3	33+	13- LIF
QFCSC	;1	33+	3	33+	13- LIF
SCCSC	;13	33+	3	33+	13- LIF
MCCFC	;1	33+	;1	;1	3-LIF

Table 1. Infection types of *Triticum monococcum* lines and wheat cultivar Arina to selected races of *Puccinia graminis* f. sp. *tritici*.

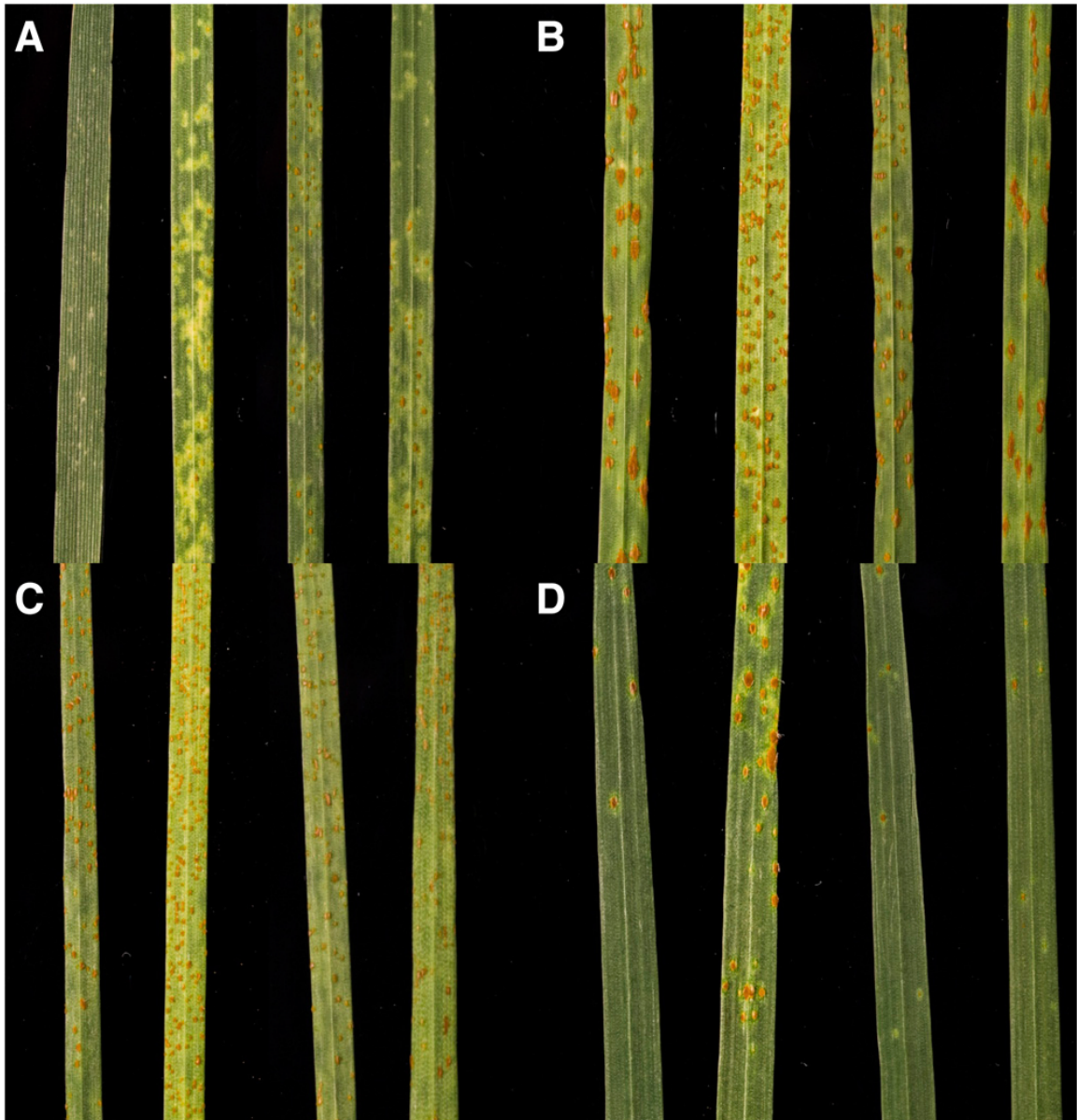
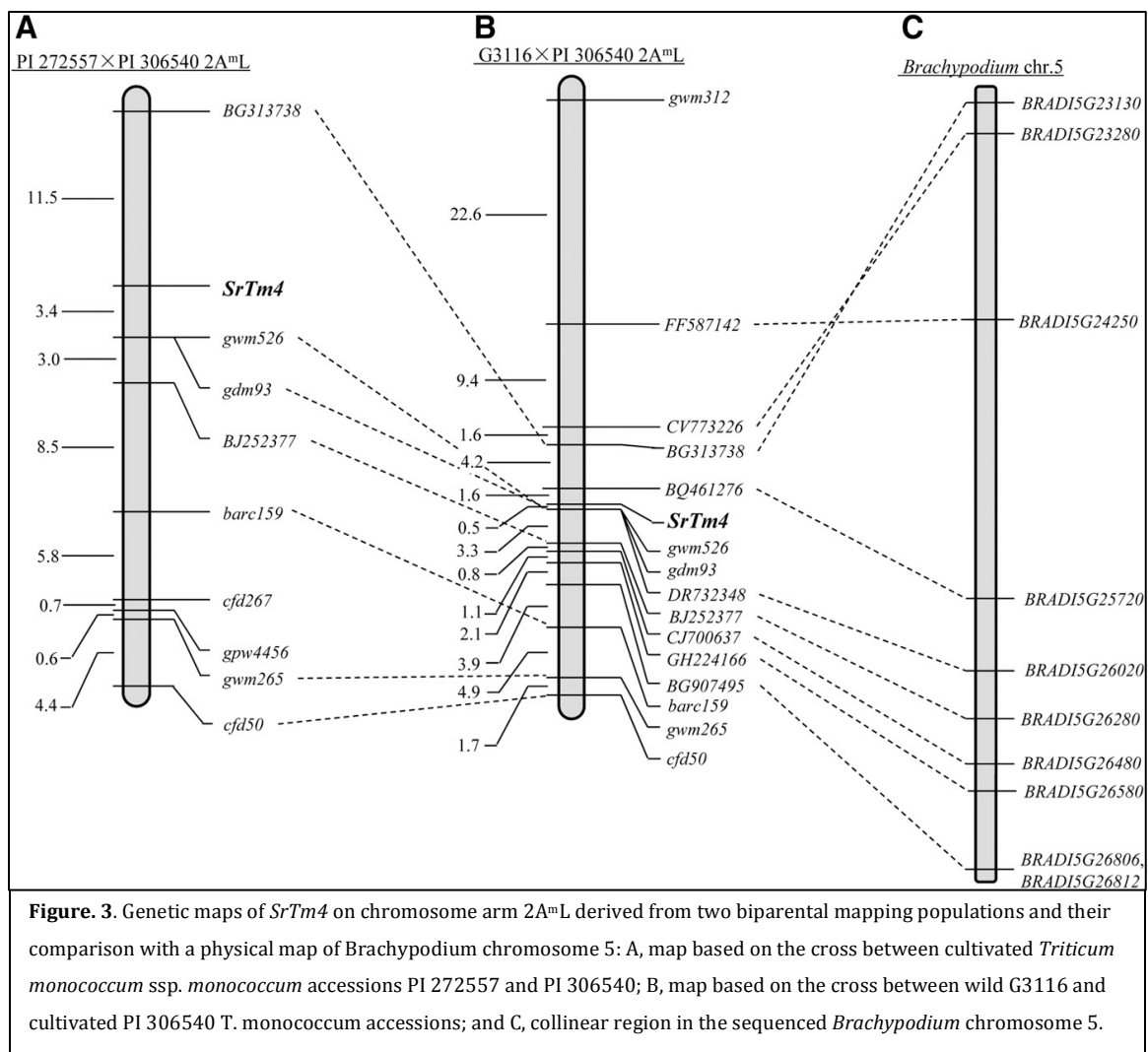


Figure. 2. Infection types of *Triticum monococcum* and *T. aestivum* lines A, PI 306540 (*SrTm4*); B, PI 272557; C, G3116 (*Sr21*); and D, Arina (*Sr48*) in response to physiologic races of *Puccinia graminis* f. sp. *tritici*: TPMKC, RKQQC, RCRSC, and SCCSC (from left to right within each frame).



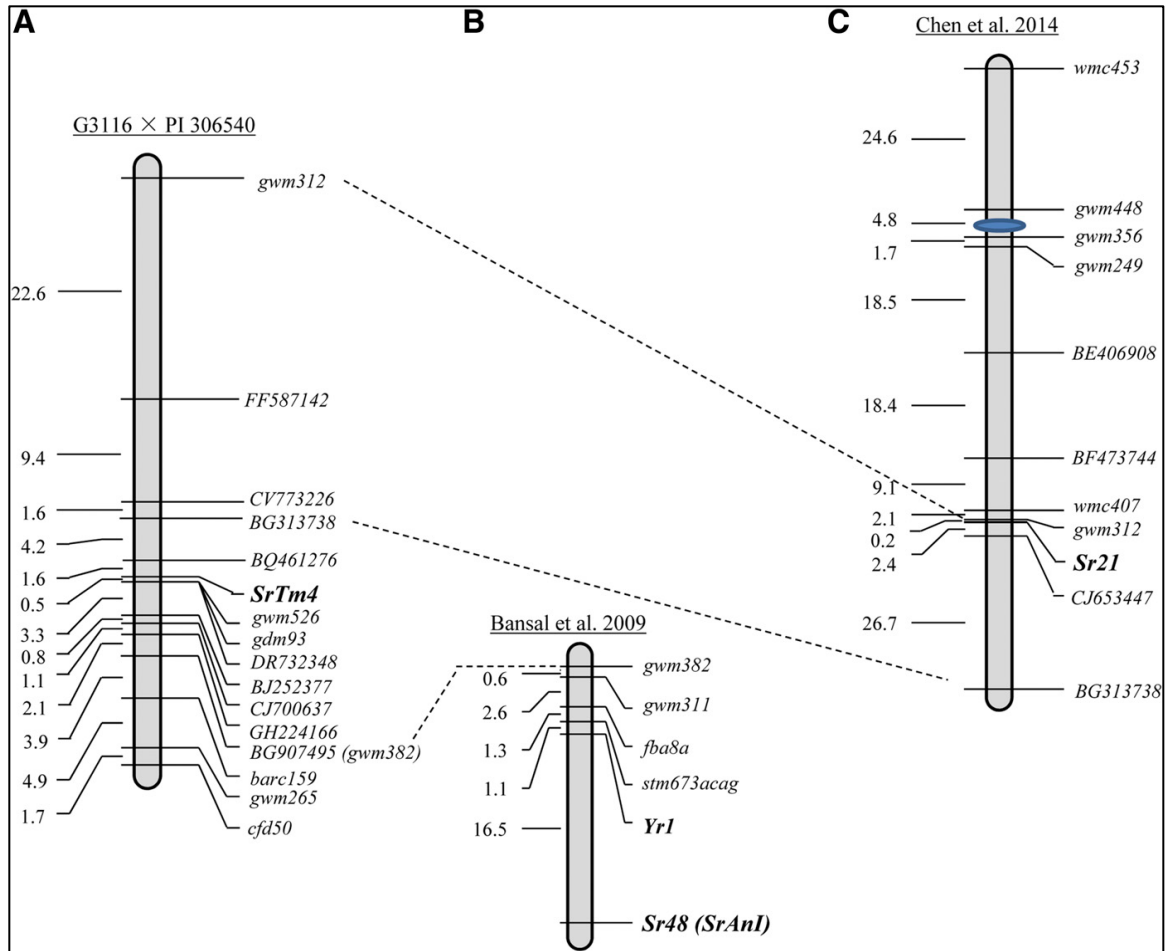


Figure 4. Relative map position of SrTm4, Sr21, and Sr48. A, Genetic map of SrTm4 derived from G3116 × PI 306540 in this study; B, genetic map of Sr48 (SrAnI) from hexaploid wheat 2A (Bansal et al. 2009); and C, genetic map of Sr21 from Triticum monococcum (Chen et al. 2015).

Markers	Marker type	Forward primer (5'-3')	Reverse primer (5'-3')	Restriction enzyme	Annealing temperature (°C)
<i>gwm312</i>	SSR	ATCGCATGATGCACGTAGAG	ACATGCATGCCTACCTAATGG	—	56
<i>gwm526</i>	SSR	CAATAGTTCTGTGAGAGCTGCG	CCAACCCAAATACACATTCTCA	—	55
<i>gdm93</i>	SSR	AAAAGCTGCTGGAGCATACA	GGAGCATGGCTACATCCTTC	—	55
<i>barc159</i>	SSR	CGCAATTTATTATCGGTTTTAGGAA	CGCCCGATAGTTTTCTAATTTCTGA	—	50
<i>gwm265</i>	SSR	TGTTGCGGATGGTCACTATT	GAGTACACATTTGGCCTCTGC	—	55
<i>gpm4456</i>	SSR	ATTAGTCTCCTCCTCCCTTTGG	AGTAGCCGGGCGAGAAATAG	—	60
<i>cfd267</i>	SSR	GTGCGTCGTGTAGCAGCTC	CTCTCTGTCTCCAGGTCGT	—	60
<i>cfd50</i>	SSR	TTCTGCAACATTTTGTCCCA	CGTATGATCCTAACGAGGGC	—	60
<i>FF587142</i>	Indel	TGGAGAAAGTTACGAGGAACGC	TTATGGGCTGTTAATGGGCAAA	—	59
<i>CV773226</i>	CAP	AGGTGCCCTGAGCAGCGAGAC	GCCATGTCTTGGCCGTAGCG	<i>ApoI</i>	56
<i>BG313738</i>	CAP	CTGACTGCGCCTTATGTTGA	GTGCCATGGCTTGATGGAGCCG	<i>SacII</i>	56
<i>BQ461276</i>	Indel	GAGGAAACTTCAATGTGGC	CAGTAATGCTTATCGGGTAAC	—	50
<i>DR732348</i>	CAP	TGAGACCATCTACAGCGG	TCTTCATCATTTGGACACCT	<i>AccI</i>	54
<i>BJ252377</i>	Indel	ATCAGGTAATCCCAAGA	TTCAGAAATCAGATCAACAAGAC	—	50
<i>CJ700637</i>	CAP	CACCACCATCCAATCCTAC	CTTCATCACCCGAGACAAC	<i>BspI</i>	54
<i>GH224166</i>	CAP	AAATTGTTGTTCTGCTAGAC	AAATCACTGAAAGTCTCTG	<i>FokI</i>	48
<i>BG907495</i>	Indel	AAAGAAAGTTGTGCAGCAAA	TGTCATAGAGTTCAAACAGTGG	—	51

° SSR, simple sequence repeat; CAP, cleavage amplification polymorphism; Indel, insertion/deletion.

Table 2. Primer sequences, annealing temperatures, and restriction enzymes used for markers in the SrTm4 region.

Brachypodium#	Top BLASTP	Wheat EST	Comment on function	Rice gene&
<i>Bradi5g25720</i>	XP_003580793	<i>BQ461276</i>	Proximal flanking marker	<i>Os04g57540</i>
<i>Bradi5g25730</i>	XP_003580794	<i>CJ879961</i>	probable polyamine oxidase 4-like	<i>Os04g57550</i>
<i>Bradi5g25740</i>	XP_003580795	<i>HX194843</i>	probable polyamine oxidase 4-like	<i>Os04g57560</i>
<i>Bradi5g25750</i>	XP_003580796	<i>FF343469</i>	uncharacterized protein	<i>Os04g57590</i>
<i>Bradi5g25760</i>	XP_003580797	<i>FF580325</i>	zinc finger CCH domain-containing protein 32-like	<i>Os04g57600</i>
<i>Bradi5g25770</i>	XP_003580798	<i>CK210581</i>	auxin response factor 12-like	<i>Os04g57610</i>
<i>Bradi5g25780</i>	XP_003579461		uncharacterized protein	<i>Os06g50180*</i>
<i>Bradi5g25790</i>	XP_003579462	<i>CJ631732</i>	phytosulfokine receptor 1-like	<i>Os04g57630</i>
<i>Bradi5g25800</i>	XP_003580799	<i>HX197537</i>	uncharacterized protein	<i>Os04g57640</i>
<i>Bradi5g25810</i>	XP_003579463	<i>DK731428</i>	uncharacterized protein	<i>Os04g57650</i>
<i>Bradi5g25820</i>	AEV41088		putative pentatricopeptide	<i>Os04g57670</i>
<i>Bradi5g25830</i>	XP_003580800	<i>DK723760</i>	peroxisome biogenesis protein 22-like	<i>Os04g57680</i>
<i>Bradi5g25840</i>	XP_003580801	<i>EG375340</i>	uncharacterized protein	<i>Os04g57690</i>
<i>Bradi5g25850</i>	XP_003580802	<i>BJ254943</i>	uncharacterized protein	<i>Os04g57700</i>
<i>Bradi5g25860</i>	XP_003579464	<i>CD934614</i>	two-component response regulator ARR5-like	<i>Os04g57720</i>
<i>Bradi5g25870</i>	XP_003580804	<i>CD893066</i>	probable NOT transcription complex subunit VIP2-like	<i>Os02g54120*</i>
<i>Bradi5g25880</i>	XP_003580805		uracil-DNA glycosylase-like	<i>Os04g57730</i>
<i>Bradi5g25890</i>	XP_003580807		early nodulin-like protein 1-like	<i>Os04g57750</i>
<i>Bradi5g25900</i>	XP_003579466		uncharacterized protein	<i>Os04g57760</i>
<i>Bradi5g25910</i>	XP_003580808	<i>DK627174</i>	uncharacterized protein	<i>Os04g57780</i>
<i>Bradi5g25920</i>	XP_003580809	<i>CD903048</i>	ubiquinone biosynthesis protein COQ4 homolog mitochondrial-like	<i>Os04g57790</i>
<i>Bradi5g25930</i>	XP_003580810	<i>CJ790419</i>	vacuolar protein sorting-associated protein 41 homolog	<i>Os04g11880*</i>
<i>Bradi5g25940</i>	XP_003579467		BTB/POZ domain-containing protein At3g19850-like	<i>Os03g61540*</i>
<i>Bradi5g25950</i>	XP_003579467	<i>BJ314745</i>	BTB/POZ domain-containing protein At3g19850-like	<i>Os04g57800</i>
<i>Bradi5g25960</i>	XP_003580811	<i>GH221070</i>	DNA-directed RNA polymerase III subunit RPC8-like	<i>Os07g29420*</i>
<i>Bradi5g25970</i>	XP_003579468	<i>HX178202</i>	anamorsin homolog 1-like	<i>Os04g57810</i>
<i>Bradi5g25980</i>	XP_003580812	<i>CJ802554</i>	probable S-acyltransferase At3g18620-like	<i>Os04g57819</i>
<i>Bradi5g25990</i>	XP_003579469	<i>HX181513</i>	probable metal-nicotianamine transporter YSL10-like	<i>Os04g57840</i>
<i>Bradi5g26000</i>	XP_003580813	<i>EG396853</i>	medium-chain-fatty-acid-CoA ligase-like	<i>Os04g57850</i>
<i>Bradi5g26010</i>	XP_003579470	<i>DK658885</i>	endoglucanase 13-like	<i>Os04g57860</i>
<i>Bradi5g26020</i>	XP_003580814	<i>DR732348</i>	Distal flanking marker	<i>Os04g57890</i>

s*, Most similar rice gene outside SrTm4 region;

#, Brachypodium genome: <http://www.modelcrop.org/>;

&, Rice genome: <http://rice.plantbiology.msu.edu/cgi-bin/gbrowse/rice/>

Supplementary Table S1: *SrTm4* colinear region in *Brachypodium*: the two flanking markers BQ461276 and DR732348 of *SrTm4* define a colinear region in *Brachypodium* that includes 29 genes.

cultivar Morocho Blanco

Synopsis

Adult plant resistance (APR) to stem rust of wheat is characterized by the apparent absence of seedling resistance and the presence of field resistance. APR is achieved by accumulating additive, partial effect resistance loci. The use of APR is thought to enhance the durability of disease resistance by conferring race non-specificity and dispersing selection for virulence across multiple loci. Strong field resistance was observed in the mid-20th century Ecuadorian bread wheat cultivar ‘Morocho Blanco’ during field testing in Njoro, Kenya from 2013-2015, despite exhibiting seedling susceptibility to the Ug99 race group. We identified and validated two quantitative trait loci (QTL), Qsr.cdl.2BS.2 and Qsr.cdl.6AS.1, located on chromosomes 6A and 2B that confer APR in ‘Morocho Blanco’. These QTL and associated SNP markers can be useful for introgressing the APR of ‘Morocho Blanco’ into breeding programs through marker-assisted selection.[†]

Introduction

Major disease resistance genes, termed R-genes, have been traditionally favored by breeders for their dominant, major-effect resistant phenotypes which facilitated easy selection and deployment in breeding programs (Boyd et al. 2013). However, it has long been noted that the use of R-genes to protect cultivars, particularly when deployed singly, resulted in human-driven ‘boom and bust’ cycles (Johnson 1961) resulting in pathogen races with virulence to one or more widely deployed R-genes. Selection for virulence has been observed on numerous occasions worldwide especially to the causal agent of stem rust of wheat, *Puccinia graminis* f. sp. *tritici*

[†] This chapter is the result of collaborative research. Collaborators include: Jordan Briggs, Matthew N. Rouse, Colin W. Hiebert, Isobel Parkin, and Sridhar Bhavani. The author contributed to designing and performing the experiments including: rating stem rust on seedling and adult plants, extracting DNA, performing KASP assays, developing the RIL population, QTL mapping, drafting the manuscript, and editing. CWH and IP developed the DH population. CWH supervised the QTL mapping and rated stem rust on adult plants. SB rated stem rust on adult plants. MNR developed the F₁ lines and the F₂ RIL population, approved the experimental design, and supervised all analyses. All collaborators reviewed, commented, and improved the manuscript. This work was submitted to *Phytopathology* in December 2015 and is under review for publication. All dissertation committee members reviewed, commented, and approved this chapter.

(*Pgt*), where the common method of disease control has been through the deployment of R-genes. In 1999 a highly virulent race of *Pgt* was identified called TTKSK, which was capable of overcoming several of the deployed R-genes including the widely utilized *Sr31*, leaving approximately 80% of global wheat susceptible to Ug99 (Pretorius et al. 2000). Deployment of a singular R-gene effective to TTKSK, *Sr24*, resulted in selection for combined virulence to *Sr31* and *Sr24* (Jin et al. 2008). More recently, wheat cultivars grown throughout Kenya and Ethiopia have utilized the resistance gene *SrTm4* to combat TTKSK and variant races. However, in 2014, cultivars with *SrTm4* experienced epidemic levels of stem rust due to selection for *SrTm4*-virulent races (Olivera et al. 2015, Patpour et al. 2015; Newcomb et al. 2016). The observed ability of *Pgt* populations to adapt to selective pressure from single R-gene based resistance has led to the targeted development of wheat lines utilizing APR which is thought to confer heightened resistance durability by enhancing race non-specificity (Sharma et al. 2013, Singh et al. 2014)

Compared to the qualitative resistance conferred by R-genes, loci contributing to APR have a subtle effect measured in the adult plant stage and often behave in a quantitative nature. Utilizing a combination of resistance QTL can lead to varieties with acceptable levels of disease resistance (Boyd 2005, 2006; Bhavani et al. 2011). APR comprised of a combination of resistance QTL is thought to enhance the durability of disease resistance through dispersing selection for virulence across multiple loci and preventing complete loss of resistance following genotypic changes in the pathogen population that result in increased virulence. Sources of APR to stem rust are limited to a few well-characterized genes in bread wheat including *Sr2*, *Sr55* (*Lr67/Yr46/Pm46*), *Sr56*, *Sr57* (*Lr34/Yr18/Pm38*), *Sr58* (*Lr46/Yr29/Pm39*), and various QTL (Yu et al. 2014). Characterizing new sources of APR and understanding interactions between known APR genes is necessary for developing lines with adequate levels of resistance, stable performance, and complementary mechanisms of resistance.

Field resistance to the Ug99 race group was observed in the mid-20th century Ecuadorian bread wheat cultivar ‘Morocho Blanco’ (PI 286545) during testing at Njoro, Kenya and in St. Paul, USA despite exhibiting a susceptible seedling response to races inoculated and naturally present in these locations (Rouse et al. 2011c). Historically, most R-genes have been detectible at the seedling stage. By possessing strong APR to *P. graminis* f. sp. *tritici* races in which it does not exhibit a seedling resistance response, ‘Morocho Blanco’ appears to carry APR. Therefore, the goals of this study were to (1) determine the genetic basis of APR in ‘Morocho Blanco’ and (2) to identify useful molecular markers for marker assisted selection of this resistance in breeding programs.

Materials and Methods

Development of mapping and verification populations

One hundred and fifty-five doubled haploid (DH) progeny were created from the cross between the Ug99 adult plant resistant ‘Morocho Blanco’ (PI 286545) and the Ug99 susceptible LMPG-6 (Knott, 1990). Both ‘Morocho Blanco’ and LMPG-6 are susceptible at the seedling stage to race TTKSK with infection types of “4” and “3+” respectively according to the Stakman infection type scale (Stakman et al. 1962). Eighty-eight progeny were genotyped with approximately 90,000 SNPs using a custom Infinium assay from Illumina (referred to as DH 90K). The remaining sixty-seven DH progeny were used to verify SNPs associated with APR (referred to as DH KASP). An additional population, referred to as RIL KASP, consisting of 73 recombinant inbred F₆ derived families was created from a cross between ‘Morocho Blanco’ and the Ug99 susceptible North Dakota variety ‘Faller’ (Mergoum et al. 2008) (PI 648350, with seedling infection type “4” to race TTKSK).

Field rating of Stem Rust

Phenotyping for stem rust severity and infection response for the populations DH 90K and DH KASP was conducted at the Kenyan Agricultural and Livestock Research Institute in Njoro, Kenya during the 2013 main season (June-October), and in the 2014 and 2015 off-seasons (January-May). Field rating of stem rust for the RIL KASP population was assessed during the 2015 off-season. Lines from each population were planted as two 70cm twin rows approximately 10 cm apart. Each line was replicated twice and planted in random order. Susceptible spreader rows were composed of lines that select for races TTKSK and TTKST (*Sr24* + *Sr31* virulence) and were sown perpendicular to the twin rows. The susceptible line 'Red Bobs' was planted every fifty entries. Inoculum for infecting the spreader rows consisted of bulked *Pgt* urediniospores collected from differential spreaders grown as urediniospore multiplication plots and was sprayed onto the spreader rows using a suspension of urediniospores in the mineral oil Soltrol 170 (Chevron Phillips Chemical Company, The Woodlands, TX).

Lines were evaluated for stem rust severity and infection response when a majority of the lines in the nursery reached anthesis. Stem rust response was rated by estimating total percent disease coverage from 0 to 100 percent following a modified Cobb Scale, in addition to recording categorical ratings describing the pustule formation (infection response, IR) as described by Roelfs et al. (1992), and recording growth stage to account for possible maturity effects on disease symptoms. To assist mapping of QTL that alter IR and growth stage, these traits were converted into numerical groups. IR categories were translated into numerical groups according to Roelfs et al. (1992). Growth stage categories were translated into numerical groups based on the scale: stem elongation = 0, boot = 1, heading = 2, anthesis = 3, watery ripe = 4, milky ripe = 5, soft dough = 6, and hard dough = 7.

DNA extraction and SNP marker assays

For use in the custom Infinium SNP assay, DNA of the DH 90K population was obtained from young leaves using the CTAB extraction method described by Kleinhofs et al. (1993). For use in KASP SNP assays, DNA of the DH KASP and RIL KASP populations were extracted using the protocol described by Edwards et al. (1991) with modifications for extraction in a 96-well plate and inclusion of a chloroform separation step. Young leaf tissue was collected in 96-well plates and incubated overnight in a RVT400 refrigerated vapor trap (ThermoSavant). Dried tissue was ground using a 'Geno Grinder 2010' (Spex SamplePrep) for 1 minute at 1400 rpm using metal beads. Following addition of the extraction buffer, chloroform was added, samples were mixed through inversion, centrifuged for 20 minutes at 3500 rpm, and the supernatant was removed. The remaining extraction process followed the protocol outlined by Edwards et al. (1991).

The DH 90K population was tested with SNP markers using the 90K Infinium wheat SNP array (Wang et al. 2014c). Only polymorphic markers with distinct bi-allelic clustering that exhibited "no-call" rates lower than 10% were used for genetic mapping. SNP markers were tested for their association with disease resistance using R/qtl. The flanking DNA sequences of SNP markers associated with disease resistance were used to develop KASP assays (KBiosciences) for QTL verification in the DH KASP and RIL KASP populations.

Allen et al. (2011) has previously shown the ability for KASP assays to validate the wheat 90K SNP array results. KASP converted 90K SNP assays were performed using the standard thermocycler protocol and reagent mixture for a 5µL total reaction volume as specified in the KASP product manual (<http://www.lgcgroup.com/LGCGroup/media/PDFs/Products/Genotyping/KASP-genotyping-chemistry-User-guide.pdf>): 1 cycle at 94⁰C 15:00 minutes; 10 cycles of 94⁰C for 20 seconds denaturing, 61-55⁰C (dropping 0.6⁰C per cycle) for 60 seconds elongating; 26 cycles 94⁰C for 20 seconds denaturing, 55⁰C for 60 seconds elongation; 30⁰C for 2 minutes to read samples. If further separation between

alleles was needed, samples were cycled for an additional 12 cycles at 94°C for 20 seconds denaturing and 55°C for 60 seconds elongation. Sequences of KASP markers used to verify QTLs are included in Supplemental Table 1. The FAM and HEX tails needed for the oligonucleotides to react with the universal FRET cassettes contained in the KASP buffer can be obtained from KBiosciences. Fluorescence was read using a StepOnePlus Real-Time PCR System and genotypes were determined using the StepOne v2.3 software (Applied Biosystems).

Constructing the genetic map and QTL mapping

10,604 SNPs were identified as polymorphic between LMPG-6 and 'Morochito Blanco' using the program GenomeStudio (GenomeStudio, v2011.1, Illumina). MSTmap (Wu et al. 2008) was used to identify segregating polymorphic markers in the DH 90K population and to identify linkage bins of co-segregating markers and develop preliminary linkage groups (cut_off_p_value = 1.0×10^{-6} , no_map_dist = 30.0, distance_function = kosambi). A single marker was chosen to represent each linkage bin for use in MapDisto (Lorieu 2012) to construct a whole genome genetic map using the Kosambi mapping algorithm (rmax = 0.3, LOD = 3). The genetic maps created in MapDisto were imported into R/qtl (Broman et al. 2003) for composite interval mapping ('cim' command; n.markercov = 4, window = 10), identification of putative QTL (LOD thresholds 4.4 (IR) and 4.5 (disease severity), highest threshold of each year defined by 100 permutations), and estimation of singular QTL effects and QTL interactions ('fitqtl' command). 'fitqtl' utilizes ANOVA to test the significance of QTL models. Tukey's Honest Significant Difference test was performed in R ('TukeyHSD' command) to determine significant differences in disease severity and IR due to QTL content. Additional interval mapping was performed using the 'scanone' command with 'addcovar' option to verify QTL loci significance and position using line maturity as a covariate. Genetic maps for chromosomes with identified QTL are displayed in Supplemental Table 2.

Results

QTL identification

Two QTL were identified in the DH 90K population that contributed to both reduced disease severity (Figure 1) and reduced IR (Figure 2) (LOD threshold 2.5). The QTL were identified on chromosome arms 2BS (*Qsr.cdl.2BS.2*) and 6AS (*Qsr.cdl.6AS.1*). In 2013-15, the additive effects of *Qsr.cdl.2BS.2* and *Qsr.cdl.6AS.1* and their interaction accounted for respectively 41.3, 48.4, and 55.8% of the observed variance for disease severity and 21.8, 31.0 and 32.5% of the observed variance for the IR. The combined effect of *Qsr.cdl.2BS.2* and *Qsr.cdl.6AS.1* corresponded to an overall reduction in disease severity of 25.8, 32.4, and 33.8% and a reduction of 0.28, 0.47, and 0.41 for the IR in 2013-2015, respectively.

Singly, each QTL elicited a greater reduction in disease severity than the expected combined effects of both QTL assuming only additivity. When in combination, a duplicate or inhibitory epistatic interaction was identified in 2013 and 2015 (p-value < 0.05) that limited the disease severity reducing effects of *Qsr.cdl.2BS.2* and *Qsr.cdl.6AS.1* (Table 1). No significant epistasis was detected between loci for the IR factor trait. Averaged over the three years *Qsr.cdl.2BS.2* and *Qsr.cdl.6AS.1* reduced stem rust severity by 18.8% and 17.5% and IR by 0.1 and 0.2 respectively. Representative DH lines with and without *Qsr.cdl.2BS.2*, *Qsr.cdl.6AS.1*, and both QTL are displayed in Figure 3.

Qsr.cdl.2BS.2 was also identified as significantly correlated with latent maturity (p-value < 0.05) in addition to reduced disease symptoms. Over 2013-2015, the average growth stage of lines with no QTL was 4.8 (watery-ripe to milk) and lines with *Qsr.cdl.6AS.1* only was 5.3 (milk to soft dough) compared to 3.4 (anthesis to watery-ripe) in the presence of *Qsr.cdl.2BS.2* and 3.8 (anthesis to watery-ripe) for both QTL. In all three populations dissociation of latent maturity and the stem

rust reducing capabilities of *Qsr.cdl.2BS.2* was observed in several recombinants lines (Table 2).

QTL validation

The RIL KASP population and 67 additional DH KASP lines also identified the *Qsr.cdl.2BS.2* and *Qsr.cdl.6AS.1* loci as significantly associated with reducing disease severity and IR (Table 3). A duplicate epistatic interaction between *Qsr.cdl.2BS.2* and *Qsr.cdl.6AS.1* was also observed in the DH KASP population for disease severity however only in the 2013 screening season (Table 4). Epistasis between *Qsr.cdl.2BS.2* and *Qsr.cdl.6AS.1* was not observed in the RIL KASP population at a 0.05 significance level however it was observed at $p\text{-value} < 0.1$ (Table 4). *Qsr.cdl.6AS.1* accounted for a much larger proportion of the observed variance for disease severity and IR factor in the RIL KASP population than *Qsr.cdl.2BS.2* when compared to the DH 90K and DH KASP populations indicating that genetic background may alter the contribution of *Qsr.cdl.2BS.2* to reducing disease resistance (Table 1 and 4). *Qsr.cdl.2BS.2* was similarly associated with latent maturity as mean maturity with both QTL (3.4; anthesis to watery) or only *Qsr.cdl.2BS.2* (3.6; anthesis to watery) were significantly different than lines with no QTL (5.3; milk to soft dough) ($p\text{-value} < 0.05$).

Discussion

The chromosome region for *Qsr.cdl.2BS.2* overlaps QTL regions recently found contributing to APR in a population derived from RB07/MN06113-8 (Bajgain et al. 2015) and ‘Thatcher’/McNeal (Rouse et al. 2014). Haplotype analysis of ‘Morocho Blanco’, MN06113-8, ‘Thatcher’, and the two susceptible lines LMPG-6 and ‘Faller’ indicate that the chromosome arm 2BS marker haplotypes are not shared between MN06113-8 and ‘Morocho Blanco’ (Table 5). However, it appears possible that the 2BS QTLs between ‘Thatcher’ and ‘Morocho Blanco’ may be similar. Additionally, a major gene for stem rust resistance, *Sr23*, has been previously reported on chromosome arm 2BS and was observed to confer a necrotic ring around *Pgt*

pustules (McIntosh et al. 1995). Three sources of *Sr23* were used to analyze haplotypes including an introgression line in ‘Thatcher’ background (*Sr23*) (Table 5). McIntosh et al. (1995) also described *Sr23* as linked to *Lr16*, which is located distally on chromosome arm 2BS. Based on map position and the haplotype of ‘Thatcher’, ‘Thatcher’ with *Sr23*, ‘Exchange’ (*Sr23*), and ‘AC Domain’ (*Sr23*), *Qsr.cdl.2BS.2* is likely not *Sr23*.

Maturity data recorded from 2013-15 was used as a covariate both in mapping the QTL and in obtaining the effects of *Qsr.cdl.2BS.2*, *Qsr.cdl.6AS.1*, and their interaction. Despite using maturity as a covariate, *Qsr.cdl.2BS.2* was associated with reduced disease severity (LOD \geq 3.0, Table 6). However, its association with IR was decreased below the 3.0 LOD threshold for QTL significance (Table 7). This suggests that the reduction in IR, but not severity, associated with *Qsr.cdl.2BS.2*, including the statistically significant correlation in 2014, may be primarily due to a closely linked maturity associated QTL. Additionally, another major QTL for maturity was identified on chromosome 5A and was not correlated with reduced disease severity (Supplemental Figure 1). Furthermore, examination of the DH 90K, DH KASP, and RIL KASP populations revealed 12 lines with *Qsr.cdl.2BS.2* that exhibit the expected level of resistance and yet retain early maturity, indicating that separation of late maturity and heightened resistance mediated by the two QTL is possible (Table 2). The identified recombinants from the DH90K, DH KASP, and RIL KASP populations exhibiting dissociation of late maturity from *Qsr.cdl.2BS.2* represent useful donors of ‘Morocho Blanco’ derived resistance for introduction into breeding programs.

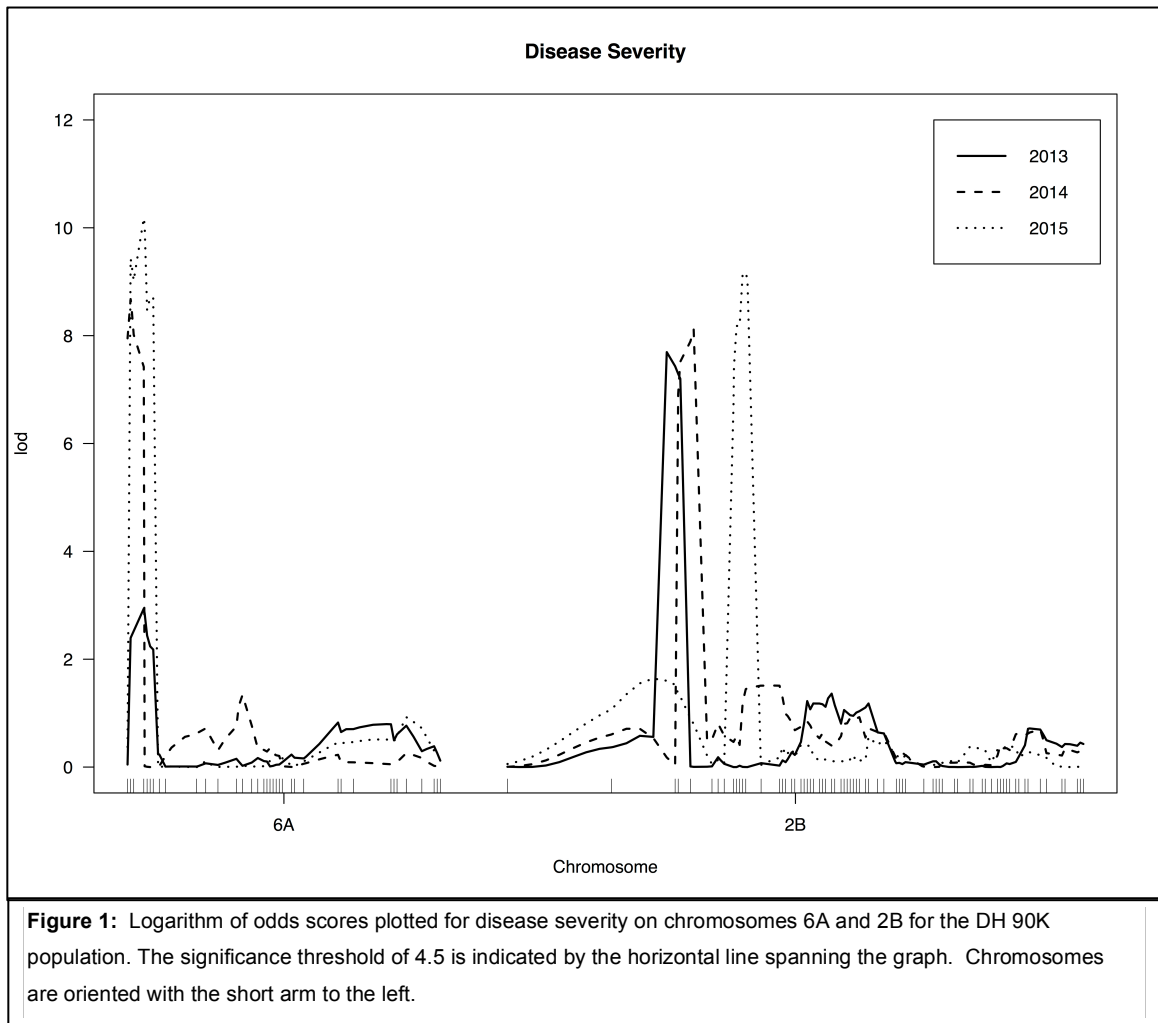
Qsr.cdl.6AS.1 provided the most consistent reduction in disease severity for each population and displayed no correlation with maturity. QTL for stem rust resistance was previously identified on 6AS by Yu et al. (2011) and more recently in a CIMMYT mapping population developed from ‘PBW343’/‘Kenya Swara’ (Yu et al. 2014). The associated SNP markers for the 6AS QTL identified in the ‘PBW343’/‘Kenya Swara’ population correspond to the 6AS QTL region found in this study. Haplotype

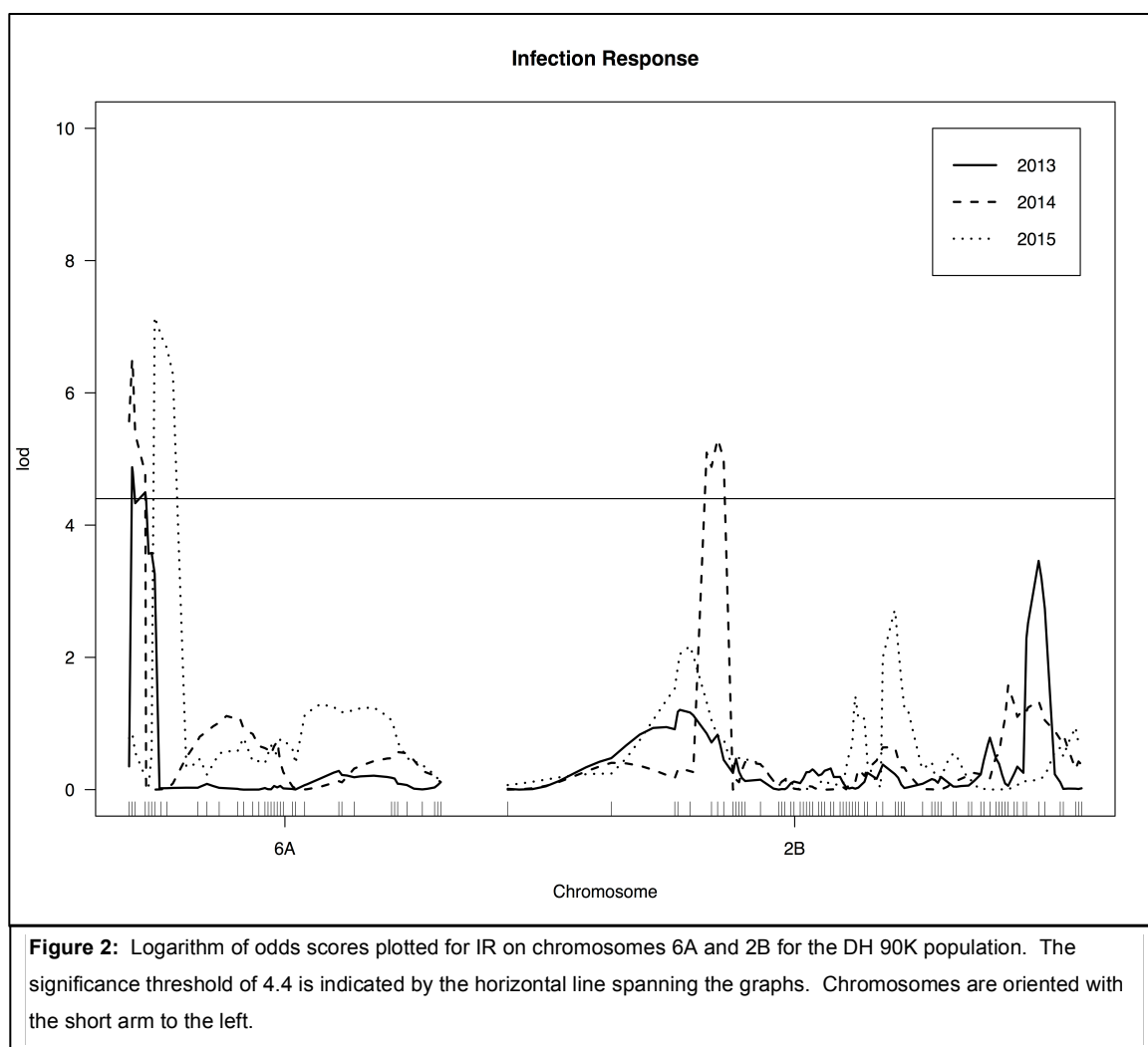
analyses using the SNP markers identified in this study indicate that the resistance QTL of 'Kenya Swara' and 'Morochito Blanco' may be the same (Table 8). The 6AS region in which *Qsr.cdl.6AS.1* was identified coincides with a Ug99 effective APR QTL, *Qsr.abr-6AS*, found by Babiker et al. (2016), a companion article to this report. Four of seven SNP markers linked to *Qsr.cdl.6AS.1* were shared with markers linked to *Qsr.abr-6AS*: BobWhite_c16182_53 (IWB882), BobWhite_c3073_1156 (IWB2392), BobWhite_rep_c52979_181 (IWB5029), and BS00023192_51 (IWB7466). Beyond having similar location, the estimated additive effect conferred by *Qsr.abr-6AS* and *Qsr.cdl.6AS.1* share similar magnitudes. In addition, KASP assays have identified that the shared SNP markers have the same allelic states indicating that the resistance loci *Qsr.cdl.6AS.1* and *Qsr.abr-6AS* may be derived from the same source. Interestingly, another group, Guerrero-Chavez et al. (2015), mapped a qualitative stem rust resistance gene in the elite hard red spring wheat line SD4279 which maps within a linkage block between the 6AS SNP markers BobWhite_c3073_1156 and BobWhite_c16182_53. Guerrero-Chavez and colleagues reasoned that this locus was *Sr8a*. Additionally, Zhang et al. (2014) mapped a qualitative stem rust resistance locus in North American winter wheat germplasm to a similar region on 6AS. Zhang et al. (2014) indicated that although the SSR marker *Xgwm334* associated with the 6AS resistance locus maps near *Sr8a*, the race specific phenotypes were inconsistent with *Sr8a* and provided resistance to the North American Pgt races QTHJC and QFCSC. Our data and recent studies identifying stem rust resistance QTL on chromosome arm 6AS suggest the presence of genes or alleles in addition to *Sr8* that confer resistance, at least at the adult-plant stage, to virulent *Pgt* races such as TTKSK. Additional studies are needed to dissect the genetic relationships between the APR identified and *Sr8*.

Separately and in combination the two QTL identified in this study were shown to significantly reduce stem rust severity in Njoro, Kenya during three growing seasons in two biparental populations. The two loci and linked SNP markers can be useful for breeding programs seeking APR as the primary method for

controlling *Pgt* infection. The SNP markers associated with stem rust resistance in this study could be used for the introgression of resistance from 'Morochó Blanco' into regionally adapted cultivars.

Tables and Figures





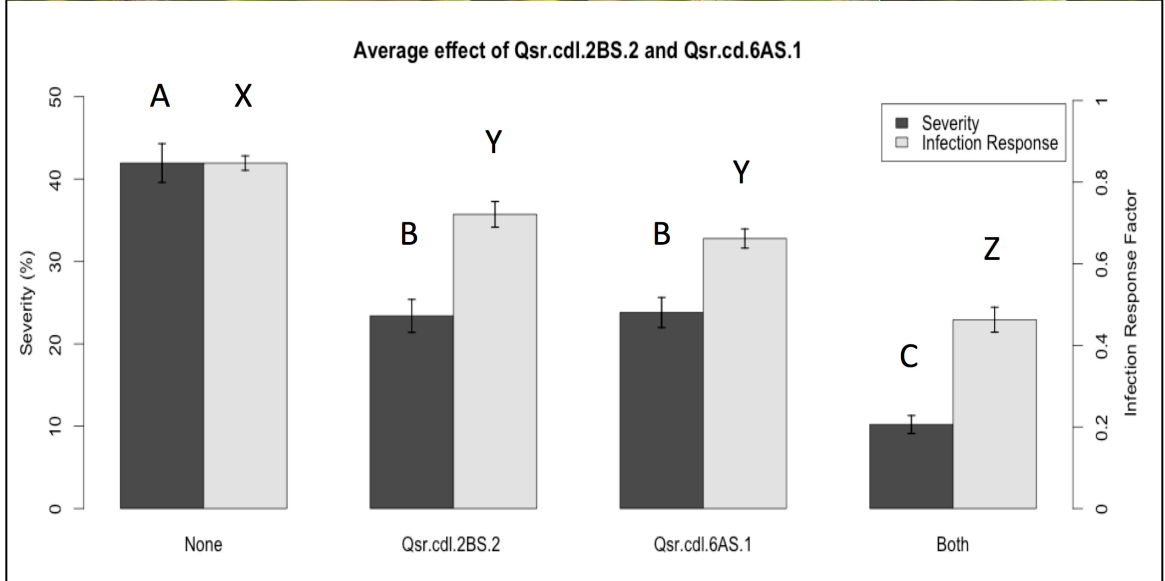
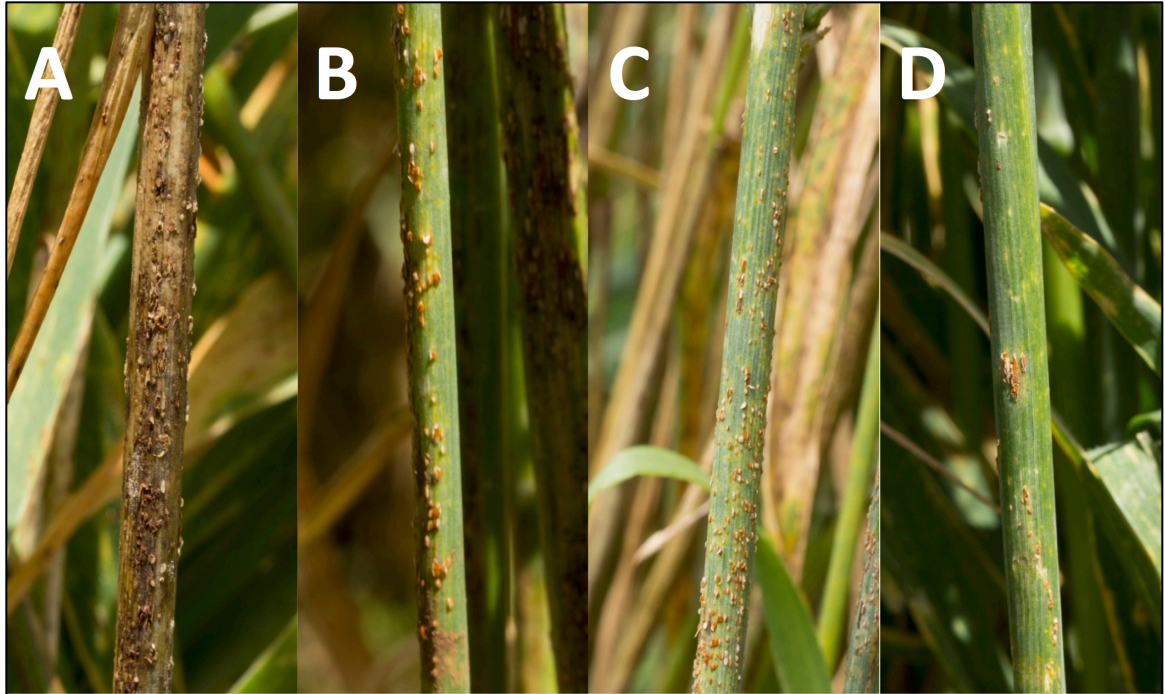


Figure 3: Effect of QTL in the LMPG-6/'Morochito Blanco' DH population. Top: lines representative of QTL presence/absence; (A) no QTL, (B) *Qsr.cdl.2BS.2* only, (C) *Qsr.cim.6AS.1* only, and (D) both QTL. Bottom: numerical representation of QTL effects for disease severity and IR including standard error bars and designation of significant differences for severity (A, B, C) and IR (X, Y, Z).

QTL	Population	2013			2014			2015		
		Effect	%Variance	P-value	Effect	%Variance	P-value	Effect	%Variance	P-value
<i>Qsr.cdl.2BS.2</i>	DH 90K	-0.11	6.16	0.04	-0.18	8.32	8.02E-03	-0.15	8.14	0.02
	DH KASP	-0.32	35.13	1.94E-07	-0.20	15.93	5.25E-04	-0.14	5.31	0.15
	RIL KASP							-0.07	4.35	0.11
<i>Qsr.cdl.6AS.1</i>	DH 90K	-0.17	15.64	4.79E-04	-0.29	22.71	5.84E-06	-0.26	24.38	2.47E-05
	DH KASP	-0.19	13.28	1.16E-03	-0.28	29.15	3.09E-06	-0.19	10.26	0.03
	RIL KASP							-0.24	31.30	1.48E-06
QTL Interaction	DH 90K	0.04	0.64	0.41	-0.02	0.17	0.65	0.03	0.32	0.57
	DH KASP	-0.08	2.13	0.12	-0.04	0.55	0.45	0.00	0.01	0.94
	RIL KASP							0.05	1.31	0.25

Table 1: Percentage of variation and additive effects conferred by *Qsr.cdl.2BS.2* and *Qsr.cdl.6AS.1* on stem rust IR factor in the three populations across three years.

Cross	Line	Severity (%)	IR Factor	Maturity	QTL content
Full DH Population	Population Average	42.0	0.85	4.8	None
DH 90K	Z04N*B0411	10.0	0.5	5.0	<i>Qsr.cdl.6AS.1</i> and <i>Qsr.cdl.2BS.2</i>
DH 90K	Z04N*B0568	7.5	0.65	6.5	<i>Qsr.cdl.6AS.1</i> and <i>Qsr.cdl.2BS.2</i>
DH KASP	Z04N*D0261	13.3	0.6	5.0	<i>Qsr.cdl.6AS.1</i> and <i>Qsr.cdl.2BS.2</i>
DH KASP	Z04N*E0112	10.0	0.45	5.0	<i>Qsr.cdl.6AS.1</i> and <i>Qsr.cdl.2BS.2</i>
DH 90K	Z04N*A0120	21.7	0.69	5.1	<i>Qsr.cdl.2BS.2</i>
DH KASP	Z04N*A0123	21.7	0.72	5.8	<i>Qsr.cdl.2BS.2</i>
DH 90K	Z04N*B0056	10.0	0.45	5.8	<i>Qsr.cdl.2BS.2</i>
DH 90K	Z04N*B0234	7.0	0.37	5.1	<i>Qsr.cdl.2BS.2</i>
DH KASP	Z04N*E0473	8.3	0.67	6.0	<i>Qsr.cdl.2BS.2</i>
RIL KASP	Population Average	34.6	0.82	5.3	None
RIL KASP	1-1E6	1.0	0.8	6.0	<i>Qsr.cdl.6AS.1</i> and <i>Qsr.cdl.2BS.2</i>
RIL KASP	1-1H3	5.0	0.4	6.0	<i>Qsr.cdl.6AS.1</i> and <i>Qsr.cdl.2BS.2</i>
RIL KASP	1-2E3	10.0	0.6	5.0	<i>Qsr.cdl.6AS.1</i> and <i>Qsr.cdl.2BS.2</i>

Table 2: Recombinant lines from the DH 90K, DH KASP, and RIL KASP populations that retain a high level of resistance consistent with *Qsr.cdl.2BS.2* and retain a maturity similar or earlier than the average populations members without *Qsr.cdl.2BS.2*. Severity and IR factor ratings are a three-year, two-replicate average for members of DH 90K and DH KASP lines and a two replicate average in 2015 for members of RIL KASP. Highlighted lines are the ratings for members of the populations with no QTL. QTL content was determined by marker haplotype.

QTL	SNP ID	LMPG6/Morocho Blanco						Faller/Morocho Blanco	
		2013 Severity	2013 IR	2014 Severity	2014 IR	2015 Severity	2015 IR	2015 Severity	2015 IR
<i>Qsr.cdl.2BS.2</i>	Kukri_c53810_315	1.52E-03	2.51E-03	2.11E-03	0.01	3.70E-03	0.05	0.67	0.98
	Excalibur_c11491_1147	5.27E-04	9.62E-04	2.23E-04	9.62E-04	1.89E-03	0.01	0.76	0.87
	Kukri_c53810_137	1.07E-03	1.62E-03	1.45E-03	0.01	3.02E-03	0.04	0.43	0.42
	BS00064658_51	3.93E-04	3.39E-07	3.10E-03	0.01	2.01E-03	8.60E-03	0.02	0.23
	Tdurum_contig42153_1190	7.92E-04	1.82E-05	8.14E-04	8.72E-03	4.61E-04	1.50E-03	0.03	0.14
<i>Qsr.cdl.6AS.1</i>	BS00066615_51	0.07	0.01	5.71E-03	3.80E-03	0.22	0.37	Monomorphic	Monomorphic
	BS00074487_51	0.03	0.04	3.03E-04	2.22E-03	0.07	0.16	Monomorphic	Monomorphic
	BS00023192_51	0.01	4.18E-03	3.30E-05	2.74E-04	0.10	0.47	1.85E-03	4.85E-04
	Kukri_c16030_181	0.18	0.07	3.57E-05	2.94E-04	0.02	0.07	Monomorphic	Monomorphic
	BobWhite_c16182_53	0.02	6.65E-03	5.13E-06	8.32E-05	0.02	0.07	Monomorphic	Monomorphic
	BobWhite_c3073_1156	0.02	0.01	6.54E-07	1.41E-05	0.01	0.04	7.02E-09	4.29E-07
	BobWhite_rep_c52979_181	0.02	0.01	6.54E-07	1.41E-05	0.01	0.04	1.60E-08	2.13E-05

Table 3: P-values for single marker ANOVA of *Qsr.cdl.2BS.2* and *Qsr.cdl.6AS.1* associated SNP markers for severity and IR phenotypes in the 2013-2015 Kenyan screening seasons. SNP genotypes were determined via KASP assays. Highlighted SNP markers were significantly associated with resistance for all three screening seasons and in all populations (DH 90K, DH KASP, and RIL KASP). "2013 IR" indicates the 2013 screening season infection response phenotype.

QTL	Population	2013			2014			2015		
		Effect	%Variance	P-value	Effect	%Variance	P-value	Effect	%Variance	P-value
<i>Qsr.cdl.2BS.2</i>	DH 90K	-21.3	29.9	5.29E-08	-16.7	20.9	6.05E-07	-18.4	23.4	4.90E-07
	DH KASP	-11.0	25.2	4.24E-05	-16.0	21.8	5.24E-06	-13.0	15.3	2.25E-03
	RIL KASP							-9.5	9.1	4.60E-03
<i>Qsr.cdl.6AS.1</i>	DH 90K	-11.7	11.4	7.66E-04	-19.0	27.5	1.49E-08	-21.7	32.4	6.87E-09
	DH KASP	-7.3	14.5	2.09E-03	-21.1	37.5	7.51E-09	-13.1	16.1	1.71E-03
	RIL KASP							-22.5	39.8	5.33E-09
QTL Interaction	DH 90K	7.2	3.1	0.04	3.7	1.0	0.20	6.3	2.5	0.05
	DH KASP	5.6	5.4	0.03	4.4	1.6	0.14	3.4	1.0	0.35
	RIL KASP							6.0	2.6	0.07

Table 4: Percentage of variation and additive effects conferred by *Qsr.cdl.2BS.2* and *Qsr.cdl.6AS.1* on stem rust disease severity in the three populations across three years.

Variety	<i>Qsr.cdl.2BS.2</i> associated SNP alleles				
	Kukri_c53810_315	Excalibur_c11491_1147	Kukri_c53810_137	BS00064658_51	Tdurum_contig42153_1190
'Morocho Blanco'	T	A	C	T	G
LMPG-6	C	G	T	G	A
MN06113-8	C	G	T	G	A
'Thatcher'	C	G	T	T	G
'Thatcher' (Sr23)	C	G	T	T	G
'Exchange' (Sr23)	C	G	T	T	G
'AcDomain' (Sr23)	C	G	C	T	G

Table 5: Haplotype analysis of SNPs associated with *Qsr.cdl.2BS.2*. Highlighted markers indicated the same allelic state as 'Morocho Blanco'.

SNP ID	2013	2013 corrected	2014	2014 corrected	2015	2015 corrected
Kukri_c53810_315	3.46	3.07	2.93	1.73	1.86	1.12
Excalibur_c11491_1147	6.19	5.72	4.52	3.23	4.03	3.70
Kukri_c53810_137	5.99	5.39	4.45	3.05	4.03	3.21
BS00064658_51	3.51	3.01	4.56	2.60	4.49	2.72
Tdurum_contig42153_1190	3.83	3.19	4.85	2.51	5.61	3.26

Table 6: Interval mapping logarithm of odds (LOD) scores for *Qsr.cdl.2BS.2* associated SNP markers and their correlation with disease severity in the DH 90K population. "2013 corrected" indicates 2013 interval mapping results where the maturity trait was used as a covariate for severity.

SNP ID	2013	2013 corrected	2014	2014 corrected	2015	2015 corrected
Kukri_c53810_315	0.59	0.34	1.07	0.27	0.60	0.28
Excalibur_c11491_1147	1.15	0.74	1.74	0.81	1.70	1.46
Kukri_c53810_137	1.31	0.85	1.99	0.94	1.79	1.52
BS00064658_51	1.16	0.67	2.75	1.22	1.37	1.01
Tdurum_contig42153_1190	1.16	0.60	3.24	1.36	1.37	0.98

Table 7: Interval mapping logarithm of odds (LOD) scores for *Qsr.cdl.2BS.2* associated SNP markers and their correlation with IR in the DH 90K population. "2013 corrected" indicates 2013 interval mapping results where the maturity trait was used as a covariate for IR.

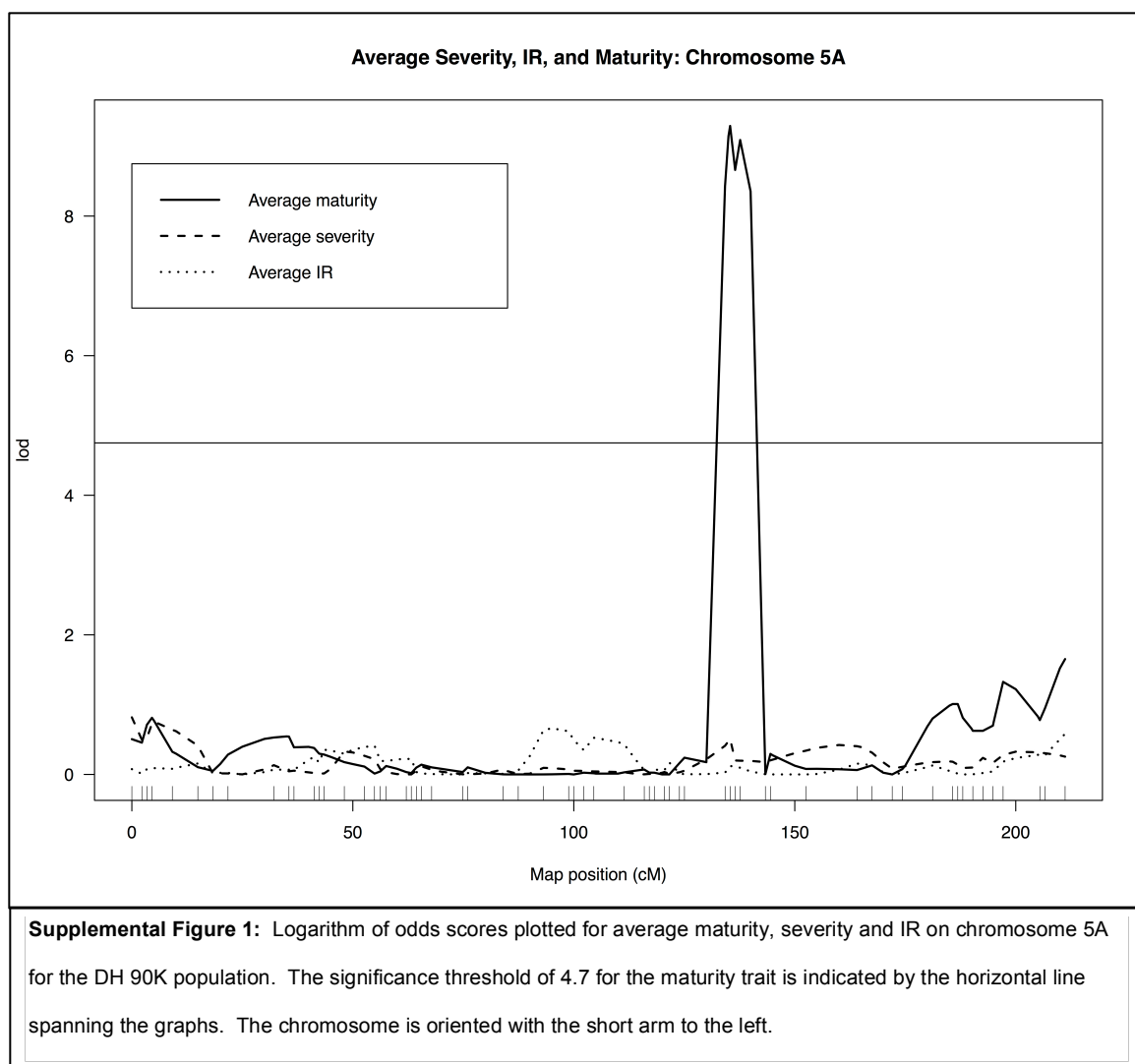
Variety	<i>Qsr.cdl.6AS.1</i> associated SNP alleles						
	BS00066615_51	BS00074487_51	BS00023192_51	Kukri_c16030_181	BobWhite_c16182_53	BobWhite_c3073_1156	BobWhite_rep_c52979_181
'Morochito Blanco'	A	G	A	T	G	A	C
LMPG-6	G	A	C	C	T	G	T
'Faller'	A	G	C	T	G	G	T
'Kenya Swara'	A	A	A	T	G	A	C
'PBW343'	A	A	A	T	T	G	T

Table 8: Haplotype analysis of SNPs associated with *Qsr.cim.6AS.1*. Highlighted markers indicate the same allelic state as 'Morochito Blanco'.

QTL	SNP ID	KASP Marker Sequences		
		Allele 1	Allele 2	Common Reverse
<i>Qsr.cim.6AS.1</i>	BS00066615_51	CATCTCTGGCATGAGCGGT	CTCATCTCTGGCATGAGCGGC	AGGAACTGTGTACGCCGCCA
	BS00074487_51	CAGTTTGTACTGCTGAACACAGCT	AGTTTGTACTGCTGAACACAGCC	AGATGTAACCGCAAGGCAGTCACTA
	BS00023192_51	CAATGCCTTGTAGATTTCTACGATGAT	AATGCCTTGTAGATTTCTACGATGAG	AAATTACTGGCGAAAAAATCTCCAGATT
	Kukri_c16030_181	GCGACCTGGCTACATCGC	GGCGACCTGGCTACATCGT	TCGTCGTCCACCGGCCGA
	BobWhite_c16182_53	GTCAAGTCTTCCATGATGTTCTC	GTGTCAAGTCTTCCATGATGTTCTA	CAAAACAGGAATGGAATCACCAGCTGAT
	BobWhite_c3073_1156	CCCTGGCCTGGAGAGGAT	CCCTGGCCTGGAGAGGAC	CCCAGGCCGTCTCGTCGCT
	BobWhite_rep_c52979_181	AAGCTCCGGCTCTACTCCATC	CAAGCTCCGGCTCTACTCCATT	AGTCCCCAGCGCGCTGCT
<i>Qsr.cim.2BS.1</i>	Kukri_c53810_315	AATTGGGGAGCATTCCATGTCAC	CTAATTGGGGAGCATTCCATGTCAT	CCAGCTGGCCTTCTATTAACAGAGAA
	Excalibur_c11491_1147	AACTCTGCAACCATACTCTGACCA	CTCTGCAACCATACTCTGACCG	CAGTTAGCAGATAAACTCAATGGCCATAT
	Kukri_c53810_137	ATTGGGCTAGGAGTCGTAGGGC	TGGCTAGGAGTCGTAGGGT	CAGACACTGCCGGGCAAAGTAT
	BS00064658_51	CAAACTGTTCAAGTTGAAGAACACGG	CAAACTGTTCAAGTTGAAGAACACGT	CAACAACACACAAAGCGAAAGGATTT
	Tdurum_contig42153_1190	CCTTGATGGGAACATGAGTTCTGATA	CTTGATGGGAACATGAGTTCTGATG	GAAAAGTCACTGATCCACCATGTTGTAT

Supplemental Table 1: DNA sequences for SNP markers associated with 'Morochito Blanco' resistance loci. Highlighted markers indicate markers that were associated with resistance in all populations and in all years.

Genetic map chromosome 2B		Genetic map chromosome 6A	
SNP marker	cM	SNP marker	cM
Ex_c19516_1139	0.0	BobWhite_rep_c52979_181	0.0
Kukri_c53810_315	38.6	BobWhite_c3073_1156	1.1
Excalibur_c11491_1147	62.4	BobWhite_c16182_53	2.3
<i>Qsrcll.2BS.2</i>	63.5	Kukri_c16030_181	6.0
Kukri_c53810_137	63.5	<i>Qsrcll.64S.1</i>	6.0
GENE-0592_352	68.1	BS00023192_51	7.3



Race specific analysis of adult plant resistance

Synopsis

Adult plant resistance to stem rust of wheat has become a target for plant breeders seeking to enhance durability of stem rust resistance. Adult plant resistance to stem rust of wheat is often presumed to be race non-specific due to the examples of *Sr2*, *Lr34* and *Lr67*. These resistance genes are effective at the adult plant stage and remain effective to all assayed stem rust pathogen races despite wide deployment in agriculture. However race specific adult plant resistance genes have been identified in other wheat rust systems including: leaf rust (*Lr22a*) and stripe rust (*Yr49*). The Ecuadorian bread wheat cultivar 'Morochito Blanco' was previously identified as having two adult plant resistance loci, *Qsr.cdl.2BS.2* and *Qsr.cdl.6AS.1*, effective to stem rust races TTKSK and TTKST. This study compared the efficacy of these loci over changes in race and environment. *Qsr.cdl.2BS.2* and *Qsr.cdl.6AS.1* were not effective outside of Kenya, indicating either environment or race specificity. Additionally, in the absence of these QTL and in the absence of major genes effective to the races TPMKC and RCRSC, Morochito Blanco exhibited a genotype x race interaction affecting disease severity and infection response. These results indicate that both major disease resistance QTL and small-effect, unmapped loci, can exhibit interactions with both pathogen race and environment indicating the need to test sources of resistance in their target environments.[‡]

Introduction

[‡] This chapter is the result of collaborative research. Co-Authors include: Jordan Briggs, Matthew N. Rouse, Colin W. Hiebert, and Sridhar Bhavani. The author contributed to designing and performing the experiments including: planting U.S.A. field plots, inoculating U.S.A. field plots, rating stem rust on adult plants in all locations, rating stem rust on seedlings, extracting DNA, performing KASP assays, QTL mapping, and performing all statistical analyses. CWH supervised the QTL mapping. SB rated stem rust on adult plants. MNR developed all F₁ lines, approved the experimental design, and supervised all analyses. All dissertation committee members reviewed, commented, and approved this chapter.

Quantitative disease resistance is characterized as host plant resistance that results in the reduction, rather than absence of disease (Young 1996, Poland et al. 2009). Quantitative Trait Loci (QTL) have become a target of plant breeders in numerous host-pathogen systems for the presumed race non-specificity and therefore durability in genetically variable pathogen populations (Parlevliet 2002). Following the emergence of the Ug99 race group of *Puccinia graminis* f. sp. *tritici*, the causal agent of stem rust, and continued selection for races virulent to deployed resistance genes (R-genes) (Pretorius et al. 2000, Jin et al. 2008, Jin et al. 2009, Olivera et al. 2015, Patpour et al. 2016), QTL to stem rust of wheat have become a target of breeders for their presumed race non-specificity and stability of resistance in response to genetically variable pathogen populations (Rutkowski et al. 2014, Ellis et al. 2014). The molecular mechanisms of quantitative disease resistance are unknown. Current hypotheses state that QTL results from morphological or developmental barriers in the host in response to the pathogen, mutations or alleles at genes for basal defenses, altered production of chemical defenses, changes in defense related signal transduction, weak or defeated resistance genes (R-genes), or genes with yet unidentified functions (Young 1996, Poland et al. 2009).

Regardless of the molecular mechanisms responsible for QTL, if race non-specificity truly is characteristic of QTL then careful consideration and testing must be performed before releasing varieties using QTL as the sole source of resistance. Numerous studies have indicated that although QTL are often considered race non-specific, QTL do indeed exhibit interactions with pathogen races. Carlisle et al. (2002) identified that *Phytophthora infestans* isolates exhibited significant variation in disease parameters such as latent period, infection frequency, area under the lesion expansion curve, and sporulation capacity when inoculated on potato lines identified as having varying levels of race non-specific resistance. Calenge and colleagues (2004) identified QTL in apple to *Venturia inaequalis* isolates that exhibited both broad-spectrum responses and clear isolate specific interactions. Azzimonti et al. (2013) showed that significant genotype x isolate interactions

existed for assayed measures of pathogenicity (infection efficiency, latent period, lesion size, spore production per lesion, and spore production per unit of sporulating tissue) of *Puccinia triticina* when inoculated on 86 wheat lines with varying levels of quantitative resistance. Marcel and colleagues (2008) identified three QTL in the cultivar 'Vada' effective to *Puccinia hordei*, the causal agent of barley leaf rust, which exhibited both isolate specific interactions and growth stage specific interactions and were not associated with hypersensitive interactions at either stage. Li et al. (2006) measured the specificity of QTL for two rice populations to 10 different isolates of *Xanthomonas oryzae* pv. *oryzae*, the causal agent of bacterial blight of rice. They identified that the observed QTL were as isolate specific as the loci of known major resistance genes. Barba et al. (2015) characterized quantitative resistance to *Erysiphe necator*, the causal agent of powdery mildew in grapevine, in *Vitis rupestris* line 'B38'. The resistance derived from 'B38' resulted in reduced penetration by arresting further growth of *E. necator* following formation of appresoria. The efficacy of 'B38' derived resistance was however significantly dependent on the isolate of *E. necator*. Lastly, Chen et al. (2003) Identified 12 QTL in rice and 12 QTL in barley effective to *Pyricularia grisea*. The majority of the QTL, 10 of 12 in rice and 11 of 12 in barley, lacked broad-spectrum efficacy and were only effective to one or two of the tested isolates.

If race non-specificity is the exception and not the rule with QTL then relying solely on the presence of QTL-mediated resistance may result in the selection of resistant lines that harbor weakly acting race-specific resistance instead of major resistance genes. In addition, QTL to stem rust of wheat are often defined by the lack of an apparent seedling resistance response with the presence of visible field resistance. If this field resistance is also race specific then the sources of QTL acting in the field may not only be less effective than typical major resistance genes but also more limited in their expression during the lifetime of the cultivar. Recently, highly effective QTL to stem rust of wheat were identified in the mid-20th century Ecuadorian spring wheat cultivar 'Morochito Blanco' to *Pgt* races TTKSK and

TTKST (Chapter 2). Two QTL were found to contribute to the majority of the variation in the observed response to stem rust phenotype. However, the ability for *Pgt* populations to adapt to selective pressure from race-specific resistance genes necessitates testing the resistance identified in 'Morocho Blanco' for possible race specificity. The goal of the study is to compare 'Morocho Blanco' sourced QTL in Kenya, Ethiopia, and USA to determine the effect of variable *Pgt* races and environment on the efficacy of the QTL.

Materials and Methods

Development of the mapping population:

Eighty-eight doubled haploid (DH) progeny were created from the cross between the Ug99 field-resistant line 'Morocho Blanco' (PI 286545) and the Ug99 susceptible line LMPG-6 (Knott, 1990). Both 'Morocho Blanco' and LMPG-6 are susceptible at the seedling stage to race Ug99 with infection types of "4" and "3+" respectively according to the Stakman infection type scale (Stakman et al. 1962). The eighty-eight progeny were genotyped with 81,587 SNPs using a custom Infinium assay from Illumina (referred to as DH 90K).

SNP marker assays and statistical analysis:

DNA of the DH 90K population was obtained from young leaves using the CTAB extraction method described by Kleinhoffs et al. (1993). The DH 90K population was tested with SNP markers using the 90K Infinium wheat SNP array (Wang et al. 2014c). Only polymorphic markers with distinct bi-allelic clustering that exhibited "no-call" rates lower than 10% were used for genetic mapping.

Statistical analyses were performed in 'R'. QTL mapping was performed using the 'qtl' package and the 'cim()' command (window = 10, n.marcover = 4). The threshold for QTL significant was determined based on 100 'cim()' permutations. Best linear unbiased predictions (BLUPs) were determined using the 'lme4' package. The 'lmer()' command was used for linear modeling of disease

severity and infection response. The 'ranef()' command was used to create BLUP values for each doubled haploid line.

Field rating of disease:

Field layout and inoculation of *Puccinia graminis* f. sp. *tritici* in Kenya:

Phenotyping for stem rust severity and infection response for the DH 90K population was conducted at the Kenyan Agricultural and Livestock Research Institute in Njoro, Kenya during the 2013 main season (June-October), and in the 2014 and 2015 off-seasons (January-May). Lines were planted as two 70cm twin rows approximately 10 cm apart. Each line was replicated twice and planted in random order in two blocks. Susceptible spreader rows were composed of wheat varieties that select for races TTKSK and TTKST (Sr24 + Sr31 virulence) and were sown perpendicular to the twin rows. The susceptible line 'Red Bobs' was planted every fifty entries. Inoculum for infecting the spreader rows consisted of bulked Pgt urediniospores collected from differential spreaders grown as multiplication plots for the season and were sprayed onto the spreader rows using a suspension of urediniospores in the mineral oil Soltrol 170 (Chevron Phillips Chemical Company, The Woodlands, TX).

Field layout and inoculation of *Puccinia graminis* f. sp. *tritici* in Ethiopia:

Phenotyping for stem rust severity and infection response for the DH 90K population was conducted at the Ethiopian Institute of Agricultural Research (EIAR) Debre Zeit Agricultural Research Center in Debre Zeit, Ethiopia in the 2015 and 2016 off-season. Each line was replicated twice in two blocks and planted as 100cm long twin rows approximately 30cm apart. Susceptible spreader rows were planted perpendicular to the lines and flanking the blocks. The spreader rows were artificially inoculated by spraying with a mixed suspension of urediniospores of the stem rust pathogen races TTKSK, TKTTF, TRTTF, JRCQC, and locally collected bulked field isolates. Races TTKSK, TKTTF, TRTTF, and JRCQC (isolates P14ETH02-1,

Digelu 1/1 Assasa, #33 Wonchi-1, and PETH01DZ-2) were increased in isolation at the EIAR Ambo Plant Protection Center in Ambo, Ethiopia urediniospores were suspended in the mineral oil Soltrol 170. Single race nurseries using the same planting methods as the bulked race nursery were planted at the EIAR Kulumsa Agricultural Research Center in Kulumsa, Ethiopia. The single race nurseries were inoculated with races TTKSK, TKTTT, TRTTT, and JRCQC and utilized the same source of spores as the bulked stem rust nursery in Debre Zeit, Ethiopia. The spreader rows of the single race nurseries were chosen to select for the respective stem rust races: TTKSK ('PBW343'), TKTTT ('Digalu'), TRTTT ('Laketch'), and JRCQC ('St464').

Field layout and inoculation of *Puccinia graminis* f. sp. *tritici* in USA:

Phenotyping for stem rust severity and infection response for the DH 90K population was conducted at the University of Minnesota Agricultural Research Station in Rosemount, MN during the summer seasons of 2014-2016 Each line was replicated twice per field and planted as 100cm single rows approximated 30cm apart. Spreader rows were planted perpendicular to the lines every two blocks of lines. Each population was planted in four replicated fields inoculated with singular stem rust pathogen races of TPMKC (74MN1049), RCRSC (95MN1080), QFCSC (00MN99C), and QTHJC (69MN399). The replicated fields were planted a minimum distance of 0.5 km apart. Urediniospores were suspended in Soltrol 170 and inoculated by spraying using four different sprayers designated for each field. No one entered more than one field in a day until disease was rated.

Evaluation of field disease:

Lines were evaluated for stem rust severity and infection response when a majority of lines in the nursery reached anthesis. The nurseries were evaluated twice per year per location and were evaluated between 5-7 days apart. The second evaluation was used for QTL mapping and linear modeling. Stem rust response was rated by estimating total percent disease coverage from 0 to 100 percent

following a modified Cobb Scale, in addition to recording categorical ratings describing the pustule formation (infection response, IR) as described by Roelfs et al. (1992), and recording growth stage to account for possible maturity effects on disease symptoms. To assist mapping of QTL that alter IR and growth stage, these traits were converted into numerical groups. IR categories were translated into numerical groups according to Roelfs et al. (1992). Growth stage categories were translated into numerical groups based on the scale: stem elongation = 0, boot = 1, heading = 2, anthesis = 3, watery = 4, milk = 5, soft dough = 6, and hard dough = 7.

Evaluation of seedling infection response:

Morocho Blanco and LMPG-6 were assessed for phenotypic differences in their seedling infection responses to stem rust pathogen races TTKSK (04KEN156/04), TTKST (06KEN19v3), TRTTF (06YEM34-1), TKTTF (13ETH18-1), JRCQC (09ETH8-3), TPMKC (74MN1049), RCRSC (95MN1080), QFCSC (00MN99C), QTHJC (69MN399), and BCCBC (09CA115-2). The DH 90K population was assessed for seedling responses to races that elicited differential seedling phenotypes between the mapping parents; QFCSC, QTHJC, and BCCBC. Seedling evaluations were conducted at the Cereal Disease Laboratory in St. Paul, MN. Inoculations were performed as previously described by Rouse et al. (2011) under greenhouse conditions (18-23C, 16hr day length) supplemented by 1000W HPS lamps.

Results

Field screening:

The QTL originally reported by Briggs et al. (Chapter 2) effective to stem rust in Kenya on chromosome arms 6AS and 2BS did not significantly reduce infection response in the Ethiopian bulked stem rust nursery or Rosemount, USA nurseries (Figure 1). One significant QTL peak was identified in 2014 in the TPMKC single race nursery on chromosome 4A, however this peak was not detected in 2015 or 2016. A chromosome 4A QTL peak was also identified in the QTHJC single race nursery.

This locus is near the location identified as containing a major resistance gene from 'Morocho Blanco' effective to races QTHJC and QFCSC at the seedling stage (Table 1).

Similarly, the 6AS QTL identified as consistently reducing disease severity was not replicated in the Ethiopian bulked stem rust nursery or the Rosemount, USA single race nurseries (Figure 2). The 2B QTL appeared to be verified in 2016 RCRSC and TPMKC nurseries however this trend did not occur in the 2014 or 2015 seasons. No additional QTL were consistently identified throughout years and between race/environments (Table 3 and 4). However, a QTL on chromosome arm 1BL was identified in the QFCSC and TPMKC single race nurseries in 2015 and in QTHJC, RCRSC, and TPMKC in 2016. A comprehensive list of significant QTL identified in all race/environments between 2013-2016 can be found in Table 2.

Seedling Screening:

No variation in the seedling response phenotype was observed between LMPG-6 and 'Morocho Blanco' for races TPMKC, RCRSC, TTKSK, TTKST, JRCQC, TRTTF, and TKTTF. Infection types of both parents to these races were recorded as susceptible. 'Morocho Blanco' was determined to have moderate seedling resistance (infection type '2+') to race QTHJC and QFCSC and displayed a resistant response to race BCCBC (infection type ';'). The infection types of the mapping population indicate that the QTHJC and QFCSC seedling resistance is conferred by a single resistance gene located on chromosome 4A (P-value 0.93; Table 3). Inoculation of the DH 90K population with race BCCBC resulted in segregation of multiple infection types indicating the presence of more than one effective gene. We were not able to identify races capable of selecting for singularly effective genes that contributed to the BCCBC seedling resistance phenotype. Therefore, to proceed with mapping of the BCCBC seedling response, seedling infection types were converted to a 0-9 numerical scale using the PERL script published by Gao et al. (2016). Mapping the quantitative scores using standard procedures identified that the resistance observed to BCCBC is likely due in part to loci on chromosomes 6A, 2B (Figure

3). A Chi-square analysis of the combined proportion of resistant to susceptible lines of the DH 90K populations indicate however that three dominant loci are likely segregating for BCCBC resistance (P-value 0.6). Using the expected ratio for two dominant segregating resistance loci results in a P-value of 1.6×10^{-3} indicating that the 6A and 2B resistance loci are unlikely to comprise the entirety of the observed BCCBC seedling resistance. The 6A seedling resistance locus co-locates with the 6A APR QTL identified in Kenya. The 2B seedling resistance locus and the 2B APR locus do not co-locate. No other significant QTL peaks were observed (pvalue < 0.05) however a weaker correlation (pvalue < 0.15) was observed on chromosome 4A at a similar locus as the QTL peak for infection response to race QFCSC observed in 2015.

Correlation analyses:

Comparing the predicted performance rank for DH 90K lines based on BLUP values for disease severity indicates that changes in performance rank only significantly differ between race RCRSC and the Ethiopian screening environment (Table 3). Comparing the rank of BLUP values for the infection response trait indicate that no significant change between race environments was observed (Table 4). Despite the observed correlation of line performance in the DH 90K population between race/environments significant differences were observed between population phenotypic distributions between race/environments (Figure 4 and 5). Within the location of Rosemount, RCRSC average phenotypes were observed to be significantly higher than that of race TPMKC (Figures 4 and 5). Linear modeling of disease severity and IR to races RCRSC and TPMKC indicate a significant genotype x race interaction is partially responsible for the differences observed in disease phenotypes (Tables 6 and 7). No seedling resistance was observed to either races of RCRSC and TPMKC indicating that this observed differences in APR efficacy is likely due to a genotype x race interaction for APR related genes.

Discussion

The QTL identified by Briggs et al. 2016 (Chapter 2) were not observed to significantly reduce disease severity or infection response to all race/environments tested at the adult plant stage in this study. It is important to note that the BLUP performance rank of lines for the disease severity trait generally did not significantly change with changes in race/environment with the exception of race RCRSC when compared to the Ethiopian screening environment. BLUP performance rank for the infection response trait was not observed to significantly change with changing race/environment indicating that the population tends to perform similarly across race environments much like the disease severity trait.

Clear significant differences between race/environments are discernable when consideration is taken for the performance of the population as a whole across race/environments. Race RCRSC elicits significantly higher disease severities than all other race/environments and significantly higher infection responses than the Kenyan, Ethiopian, QTHJC, and QFCSC race/environments, indicating that although the source of resistance is APR, and generally considered to be race non-specific, this race in particular is more fit for infecting the DH 90K population than all other tested race/environments. Conversely, the DH 90K population shows a clear resistance advantage in the Kenyan and Ethiopian race environments as the disease severity distributions of the population is significantly lower in these locations compared to all other race/environments. The inability to dissociate the presence of specific stem rust races with the environment in which they are found (ex. TKTTF and Ethiopia) confounds the ability to separate environmental effects from race effects on disease severity and IR. However, using only the Rosemount, MN location for linear modeling and ANOVA create the ability to separate environment effects from race effects. Using only the Rosemount screening location it was possible to identify that the disease severity phenotypic distributions of the 90K population were significantly different for race RCRSC and TPMKC (Figure 4). Additionally, ANOVA of the linear model components for disease severity and IR both indicate genotype x race interactions as a significant determinant of disease severity

and IR phenotypes (Tables 6 and 7)

Briggs et al. 2016 (Chapter 2) reported the maximum variance accounted for by the 6A and 2B locus in Kenya was 55.8%. If the two main QTL providing resistance in Kenya were not effective in all other environments and the best performing lines tended to perform the best in all other environments then it would follow that additional mechanisms of resistance were consistently functional in all locations. In consideration that the 6A and 2B loci did not provide detectable levels of disease resistance, it may be possible that the remaining variance truly results from a large number of small effect loci that are undetectable in the current doubled haploid population when using standard mapping procedures. The significant correlation of line performance across environments coupled with the significant differences in overall population performance indicates that although these putative small effect loci are contributing to disease resistance, it may be possible that their levels of contribution vary to each race/environment.

Seedling screening for disease resistance responses indicated that no apparent seedling resistance gene exists for all races tested in the field other than QTHJC, and QFCSC. Race BCCBC was screened at the seedling stage because of its strong avirulence profile to identify the presence of additional seedling resistance genes other than the 4A locus effective to QTHJC and QFCSC. A quantitative analysis of BCCBC seedling resistance indicated that the 6A locus is effective at the seedling stage and induces visually distinct changes in seedling phenotypes. The behavior of 6A to BCCBC is characteristic of a seedling resistance gene. Scoring at the seedling stage is used to highlight changes in infection response due to the presence or absence of seedling genes in the relative absence of systemic acquired resistance that is observed more strongly at the adult stage (Pretorius et al. 1988, Panter and Jones 2002, Kock and Mew 1991). Based on the lack of the 6A locus expression outside of Kenya and the presence of a 6A locus response at the seedling stage, it appears that the 6A locus is less likely involved in a broad-spectrum resistance

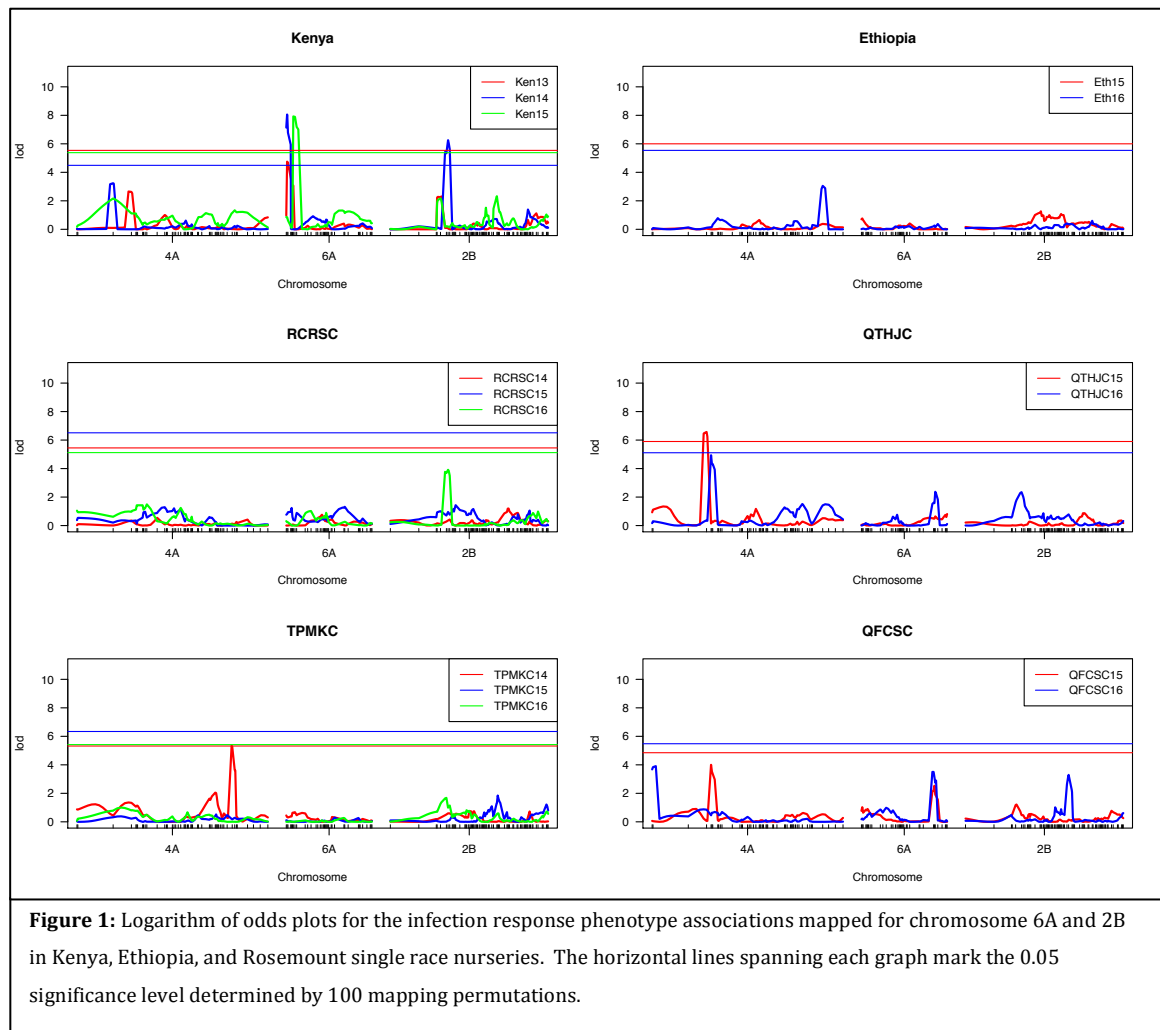
response pathway and is more likely involved in race-specific interactions. It is impossible in the current study to completely discern whether the 6A or 2B locus are truly race-specific as they were not expressed outside of the Kenyan screening environment and the 6A locus was only associated with resistance at the seedling stage to one race. However the 6A region that contributed to disease resistance in Kenya and seedling resistance to BCCBC co-locates with previously identified seedling resistance genes (Guerrero-Chavez et al. 2015, Zhang et al. 2014). These correlations provide evidence that the 6A locus may not be a race non-specific APR gene and instead a race-specific resistance locus primarily effective at the adult plant stage. A similar trend was observed by Hiebert et al. 2016 with the *Sr12* seedling resistance gene found in ‘Thatcher’ wheat. *Sr12* was mapped to a coincident location as the APR locus effective to race TTKSK (Hiebert et al. 2016, Rouse et al. 2014). Separation of the seedling resistance and APR phenotypes has so far been unsuccessful.

One year of screening has been performed with ‘Morocho Blanco’ in 2016 using single race nurseries in Kulumsa, Ethiopia with races TTKSK, TKTTF, TRTTF, and JRCQC. Morocho Blanco does not exhibit a seedling response to the four races tested in Kulumsa and exhibits a low disease severity phenotype at the adult stage to TTKSK in Kenya. The results for disease severity indicate that possible race-specificity exists for ‘Morocho Blanco’ based APR and that the 6A and 2B loci effective to TTKSK and TTKST may vary in effectiveness as changes in race occur (Table 5). Although this data was resultant from a single year of screening, it supports and emphasizes the impact of the genotype x race interaction for APR observed in the Rosemount single race nurseries. The results of the single race nurseries in Rosemount, MN and Kulumsa, Ethiopia, the field trials in Debre Zeit, Ethiopia and Njoro, Kenya and the seedling screening with BCCBC indicate that ‘Morocho Blanco’ based APR likely has a race specific component. The implications of race specificity for quantitative disease resistance identified using standard procedures in the wheat community indicate that our current definition of APR

is too broad and assumes too much about the interaction of pathogen races and quantitative resistance. Based on this study, APR derived from 'Morochito Blanco' could select for virulent races in a similar fashion to seedling resistance genes. Additionally, 'Morochito Blanco' based resistance is not effective in the United States indicating that selection for APR characteristics must occur in the region in which that resistance will be deployed.

Based on the current study, line performance relative to the population in which it was made can be predicted from one location to another. Comparison of BLUP ranks across each location indicates significant correlations between environments for both disease severity and infection response (Tables 3 and 4). However, the effectiveness of those lines in reference to total disease severity cannot be predicted accurately. Phenotypic distributions of disease severity even within the same location were found to differ significantly (Figure 4). Linear modeling and ANOVA of the disease phenotypes also identified the genotype x race interaction as significantly ($P\text{-value} < 0.05$) contributing to disease severity (Table 6 and 7). Therefore, this study identifies that APR and subsequently agronomic performance under disease pressure cannot be predicted accurately using singular environments to test APR.

Tables and Figures



Locus	Postion (cM)
BS00036649_51	0.0
wsnp_Ex_c5231_9256869	1.2
Kukri_c11770_148	49.1
QTHJ-QFCSC-Major gene	73.9
RFL_Contig4435_2881	80.1
RAC875_c55173_65	81.2
BobWhite_c3259_96	82.3
BS00039811_51	89.2
IAAV2388	90.3
Kukri_c46302_194	92.6
BobWhite_c10583_352	94.9
Ku_c24957_677	108.9
Kukri_c17417_291	119.2
BobWhite_c10610_1096	121.5
BobWhite_c19497_606	122.7
RFL_Contig4336_184	129.6
Kukri_c77040_87	131.8
Excalibur_rep_c74900_73	134.1
BS00065444_51	137.5
Kukri_c63460_739	140.9
RAC875_c20429_903	145.5
BS00020778_51	146.6
BobWhite_c15406_510	147.8
BS00064563_51	150.1
BobWhite_c35402_66	151.3
wsnp_Ex_c24474_33721784	154.7
RAC875_c25124_182	155.8
BobWhite_c12128_187	156.9
BS00023151_51	163.8
Ex_c66324_1151	164.9
BobWhite_c19919_301	169.5
BobWhite_c20909_243	179.9
BS00077716_51	181.0
IAAV8200	183.3
BobWhite_rep_c50869_1676	187.8
BobWhite_c3266_501	189.0
BobWhite_c13322_215	190.2
RAC875_c4629_1344	191.3
BobWhite_c17999_112	192.4
GENE-2354_155	194.7
RAC875_c49255_1313	197.1
BS00077633_51	199.4
BobWhite_c5633_59	204.0
CAP12_c2677_138	210.8
Tdurum_contig8061_56	214.3
BS00017267_51	216.5
Ex_c883_2618	217.7
BS00092244_51	231.7
BS00043286_51	239.7
BS00021716_51	248.9
Excalibur_c31175_162	259.2

Table 1: The genetic map for chromosome 4A of the DH 90K population. The seedling resistance gene effective to QTHJC and QFCSC is highlighted in red.

Race/Environment	Year	Marker	Chromosome	Location (cM)	LOD	Trait
QFCSC	2015	BobWhite_c39901_338	1BL	2.3	5.08	S
QTHJC	2016	BobWhite_c16824_151	1BL	12.6	6.23	S
TPMKC	2015	BobWhite_c16824_151	1BL	12.6	10.3	S
TPMKC	2016	BobWhite_c16824_151	1BL	12.6	8.63	S
RCRSC	2016	BobWhite_c12960_168	1BL	13.7	11.1	S
Kenya	2013	c2B.loc155	2B	59.3	9.1	S
Kenya	2014	c2B.loc145	2B	69.28	7.95	S
Kenya	2014	Tdurum_contig42153_1190	2B	78.37	6.26	IR
Kenya	2015	BobWhite_c44986_217	2B	88.65	10.2	S
RCRSC	2016	BobWhite_c44986_217	2B	88.7	6.9	S
TPMKC	2016	Kukri_c29600_68	2B	109.2	6.01	S
QTHJC	2015	4A Major Gene	4A	73.9	6.57	IR
TPMKC	2014	c4A.loc210	4A	210	5.33	IR
RCRSC	2014	BobWhite_c10385_374	5A	137.64	5.12	S
TPMKC	2014	BobWhite_c10385_374	5A	138	8.69	S
Kenya	2014	BobWhite_c3073_1156	6A	1.14	10.3	S
Kenya	2014	BobWhite_c3073_1156	6A	1.14	8.06	IR
Kenya	2015	Kukri_c16030_181	6A	6.04	10.8	S
Kenya	2015	BS0006615_51	6A	9.55	7.92	IR
RCRSC	2014	BobWhite_c7090_2001	6DS	2.27	5.27	S
TPMKC	2015	BobWhite_c7090_2001	6DS	2.27	6.41	IR
QFCSC	2015	c7D.loc15	7D	15	4.88	S

Table 2: Significant QTL (pvalue <0.05) for all race/environments.

Traits S= disease severity, IR= infection response.

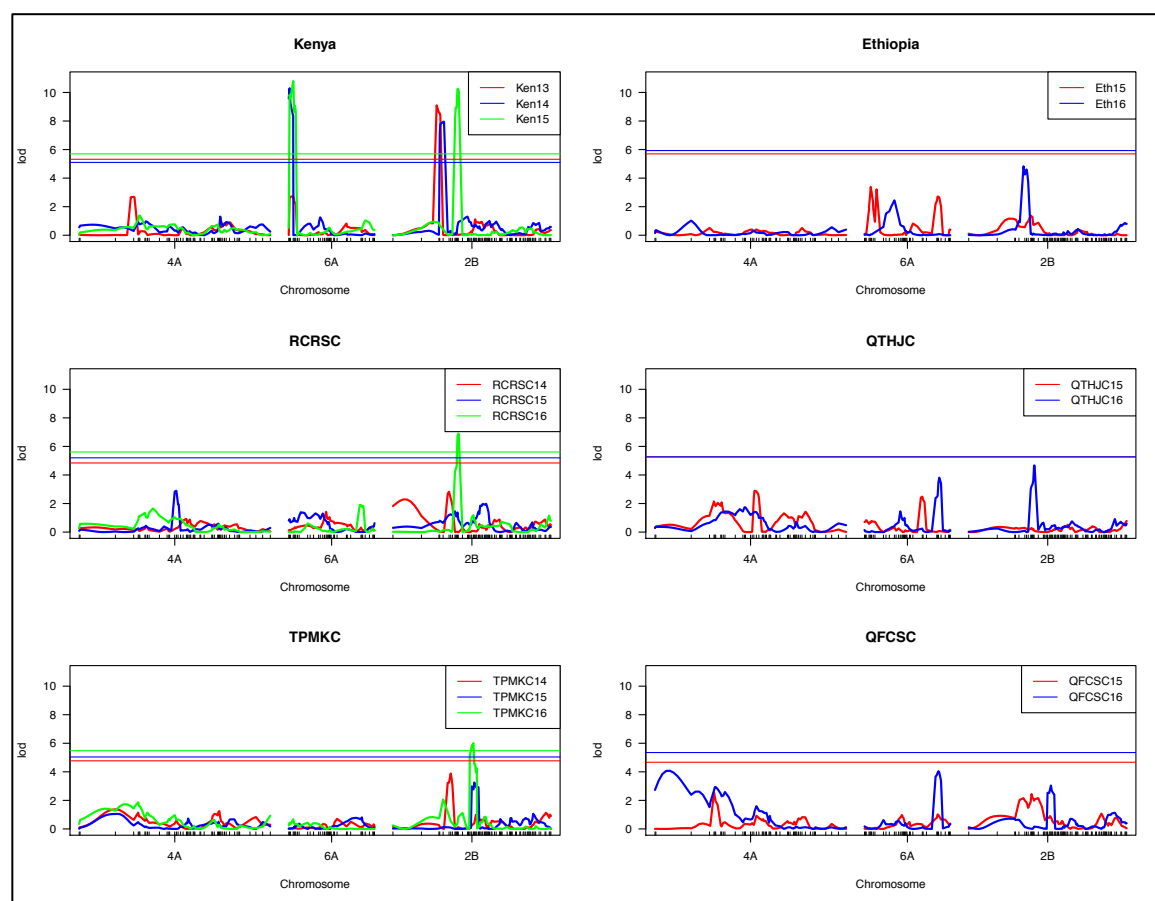


Figure 2: Logarithm of odds plots for the severity phenotype associations mapped for chromosome 6A and 2B in Kenya, Ethiopia, and Rosemount single race nurseries. The horizontal lines spanning each graph mark the 0.05 significance level determined by 100 mapping permutations.

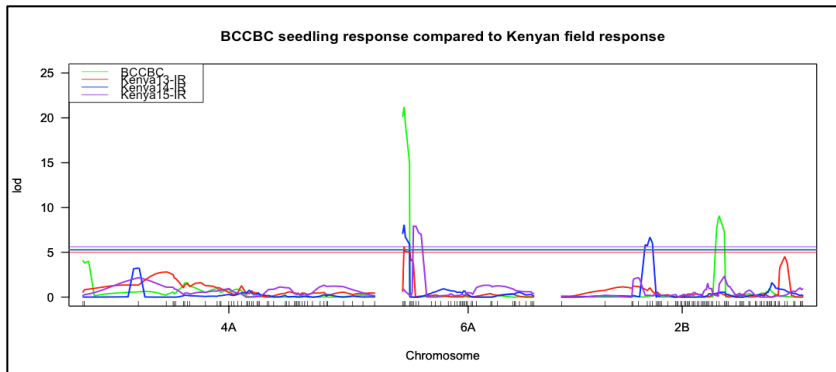


Figure 3: BCCBC seedling infection types were converted to a 0-9 numerical score and compared to the 2013-2015 Kenyan infection response field data. Horizontal lines spanning the graph indicate the 0.05 significance thresholds for each trait.

Race/Enviroment	Ethiopia	Kenya	TPMKC	RCRSC	QTHJC	QFCSC
Ethiopia	1					
Kenya	0.3889852	1				
TPMKC	0.2628314	0.3263657	1			
RCRSC	0.1959942	0.3590475	0.553255	1		
QTHJC	0.3640881	0.4630204	0.5453518	0.6804256	1	
QFCSC	0.3984687	0.3936004	0.4987569	0.6195341	0.7386862	1

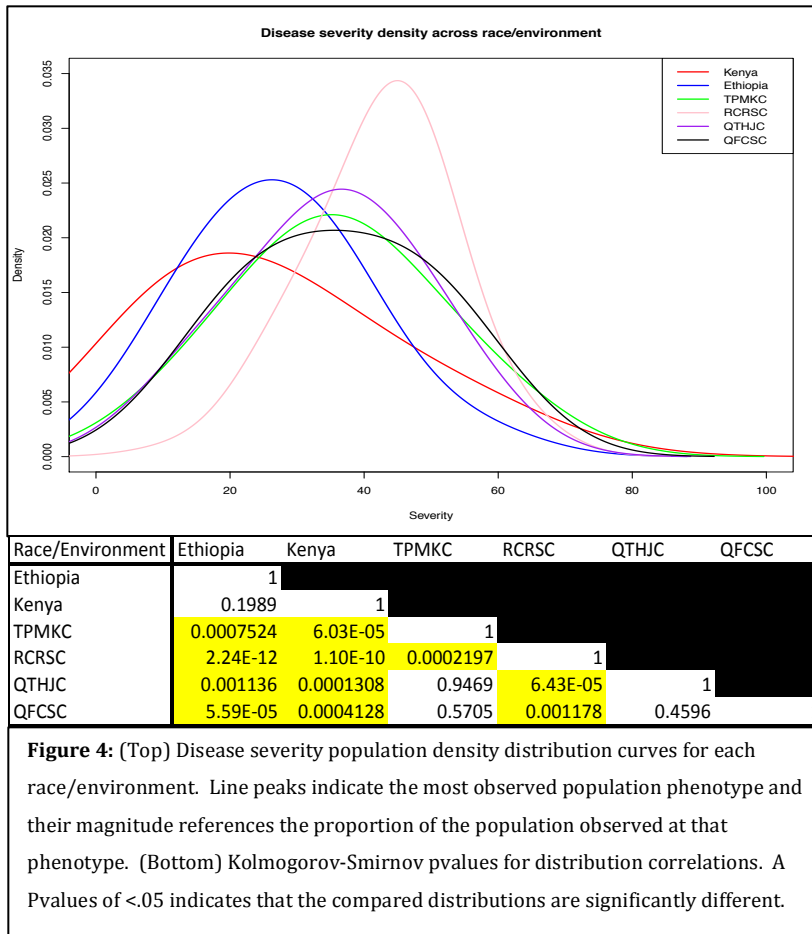
Table 3: Correlation values of BLUP performance rank for the disease severity phenotype. Highlighted boxes indicated a p-value of <0.05 indicating no significant correlation.

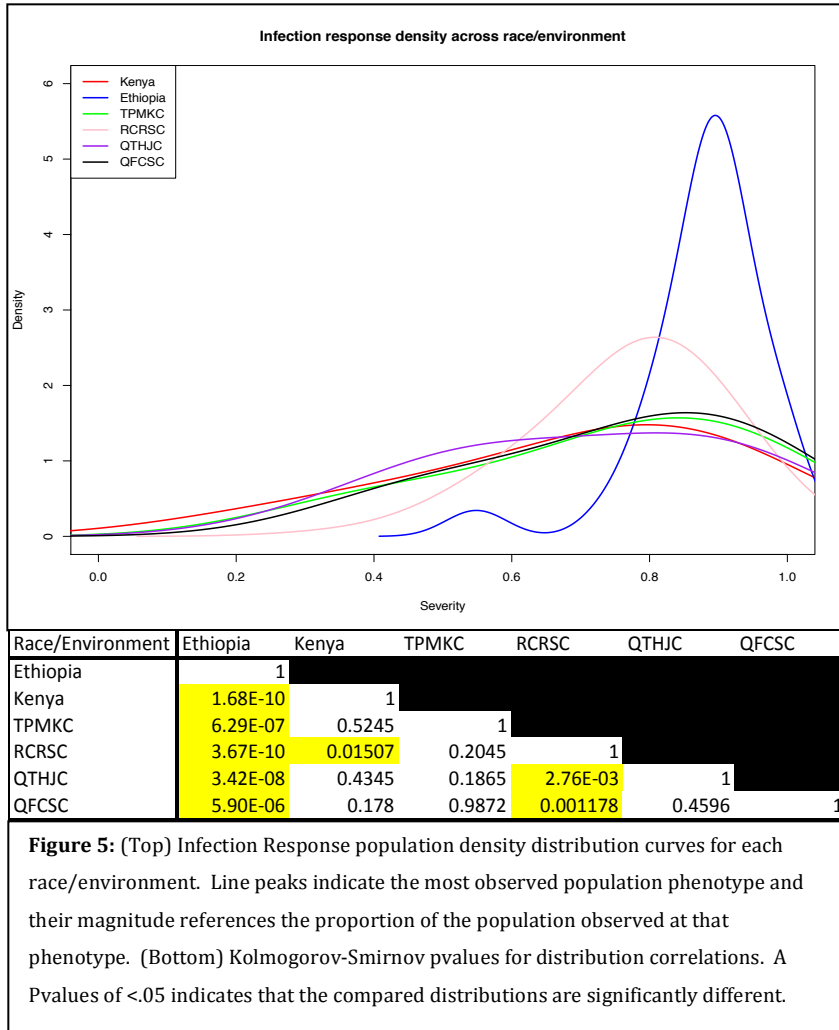
Race/Enviroment	Ethiopia	Kenya	TPMKC	RCRSC	QTHJC	QFCSC
Ethiopia	1					
Kenya	0.3680919	1				
TPMKC	0.2803177	0.4402454	1			
RCRSC	0.2542661	0.3496316	0.5508907	1		
QTHJC	0.4082698	0.5539621	0.4340846	0.4615329	1	
QFCSC	0.3259744	0.3693481	0.3819813	0.4752175	0.5037657	1

Table 4: Correlation values of BLUP performance rank for the infection response phenotype. Significant differences (p-value <0.05.) were not observed.

Race	Severity (%)	Infection Response	Growth Stage
TTKSK	Trace	Susceptible	Dry
TKTTF	30	Moderately Susceptible	Hard Dough
TRTTF	Trace	Resistant	Milk
JRCQC	15	Moderately Susceptible	Milk

Table 5: Disease severity and Infection response exhibited by 'Morocho Blanco' in the Kulumsa, Ethiopia in single race nurseries of TTKSK, TKTTF, TRTTF, and JRCQC.





Component	Df	Sum Sq	Mean Sq	F value	Pr(>F)	% Variance
Genotype	155	184053	1187	17.198	2E-16	41.0
Race	1	522	522	7.555	6.18E-03	0.1
Rep	1	1744	1744	25.261	6.76E-07	0.4
Year	2	58536	29268	423.899	2E-16	13.0
Genotype:Race	155	29414	190	2.748	2E-16	6.5
Genotype:Year	276	48883	177	2.565	2E-16	10.9
Race:Year	2	63964	31982	463.203	2E-16	14.2
Genotype:Year:Race	240	23480	98	1.417	5.32E-04	5.2
Residuals	558	38527	69			8.6

Table 6: ANOVA analysis of the linear model for disease severity in Rosemount, MN to stem rust races RCRSC and TPMKC.

Component	Df	Sum Sq	Mean Sq	F value	Pr(>F)	% Variance
Genotype	155	28.346	0.183	7.976	2E-16	37.9
Race	1	0.371	0.371	16.197	6.50E-05	0.5
Rep	1	0.064	0.064	2.788	0.09556	0.1
Year	2	1.505	0.753	32.829	3.32E-14	2.0
Genotype:Race	155	7.843	0.051	2.207	1.95E-11	10.5
Genotype:Year	276	8.354	0.03	1.32	3.30E-03	11.2
Race:Year	2	8.246	4.123	179.821	2E-16	11.0
Genotype:Year:Race	240	7.344	0.031	1.335	3.42E-03	9.8
Residuals	558	12.794	0.023			17.1

Table 7: ANOVA analysis of the linear model for IR in Rosemount, MN to stem rust races RCRSC and TPMKC.

Comparative differential expression of compatible rust infections

Synopsis

The ability for a plant pathogen to infect a host relies on the capability to surpass host defenses. Pathogens have previously been shown to use host topological features, host-derived proteins, and altered gene expression to facilitate the infection process and elicit disease symptoms. Host genes and gene products used to facilitate the infection process are referred to as susceptibility genes. Interrupting susceptibility gene production or function can reduce the susceptibility of the host and enhance the innate resistance response. This study identifies three host derived nitrate transporters from barley (MLOC_57296), maize (GRMZM5G865298), and soybean (GLYMA01G04830) that are upregulated in compatible interactions. T-DNA mutation of a homologous gene, *BRADI1G34610*, in the model grass species *Brachypodium distachyon* (accession Bd21-3) alters host susceptibility to *Puccinia graminis* f. sp. *avenae* and increases disease resistance relative to the non-mutagenized Bd21-3. Mutant lines also exhibited enlarged leaves and later maturity indicated possible pleiotropic effects of mutating *BRADI1G34610*.[§]

Introduction

Plants have developed numerous methods for resisting pathogen infection including passive barriers, constitutive production of protective compounds, and induced defense responses. The ability for a pathogen to exploit a host necessitates the capability to overcome such defenses. Examples of pathogen adaptation to host defenses include degradation of cell walls (Edwards and Bonde 2011, Huckelhoven

[§] This chapter is the result of collaborative research. Collaborators include: Jordan Briggs, Matthew N. Rouse, John Garbe, and James Kurle. The author of this dissertation contributed to designing and performing the experiments including: inoculating plants with rust pathogens, extracting RNA, performing the RNA-seq analysis, identifying *Brachypodium distachyon* mutants, and screening the mutant for changes in the host-pathogen interaction. MNR and JG approved the experimental design. JG supervised the RNA-seq analysis. JK provided the soybean germplasm and *Phakopsora pachyrhizi* spores. MNR approved the experimental design and supervised the analyses. All dissertation committee members reviewed, commented, and approved this chapter.

2007), detoxification of constitutively produced protective compounds (Morrissey and Osbourn 1999, Mueller et al. 2013), and suppression of induced defenses (Sun et al. 2006, Truman et al. 2006, Houterman et al. 2008, van Esse et al. 2008).

Pathogens are able to suppress induced host defenses through enhancing expression of negative regulators of defense responses (Veronese et al. 2006, Oh et al. 2008, Day et al. 2005, Gao et al. 2009), utilizing thigmotropic and chemical cues to coordinate infection (Bolton et al. 2008, Uppalapati et al. 2012), and commandeer host metabolic pathways for their own growth and proliferation (Diaz-Pendon et al. 2004, Caillaud et al. 2008, Gaspar et al. 2004, Hewezi et al. 2008). Host gene products used by pathogens to coordinate the infection process or enhance susceptibility of the host have been referred to as susceptibility factors and susceptibility genes (Eckardt 2002, Pavan et al. 2010). Susceptibility genes are characterized by their involvement in negatively regulating the defense responses of the host. Susceptibility factors are plant gene products that are required or aid in the establishment of basic compatibility between the pathogen and specific hosts. Mutation of either susceptibility genes or factors can alter the host pathogen interaction and result in enhanced disease resistance. Susceptibility genes have been identified in a range of host pathogen systems including those involving pathogenic fungi, bacteria, viruses, oomycetes, and nematodes and typically behave in a dominant manner (Pavan et al. 2010).

Previous examples of susceptibility genes have shown that mutant homologues of susceptibility genes in different species can provide similar resistance to their respective adapted pathogens. The *mlo* locus in barley has long been shown to provide race non-specific resistance to the powdery mildew pathogen *Blumeria graminis* f. sp. *hordei*. Mutation of *mlo* homologues in pea (Humphry et al. 2011; Pavan et al., 2011), wheat (Wang et al. 2014a), tomato (Bai et al., 2008, Zheng et al. 2013), and pepper (Zheng et al. 2013) result in similar *mlo*-type powdery mildew resistance. Similarly, isoforms in components of the translation initiation

complex such as eIF4E and eIF4G have been shown to enhance resistance to viral infection of TuMV, LMV, TEV, and CMV, in *Arabidopsis thaliana* (Duprat et al. 2002, Lellis et al. 2002, Whitham et al. 1999, Yoshii et al. 1998 and 2004, Sato et al. 2005), TYMV in rice (Albar et al. 2006), LMV in lettuce (Candresse et al. 2002; Nicaise et al. 2003), PVY in pepper (Ruffel et al. 2002), and ZYMV in watermelon (Ling et al. 2009).

Rust pathogens have proven to be a destructive force in agriculture. Rust diseases of high value U.S. crops are able to greatly affect yield potential in susceptible varieties: Southern corn rust can cause up to 45% losses (Rodriguez-Ardon et al. 1980), Asian soybean rust up to 70% (King et al. 2016), wheat stem rust can cause greater than 50% losses (Roelfs 1978), wheat stripe rust as high as 70% losses (Chen 2005), wheat leaf rust up to 33% losses (Green et al. 2014), and common corn rust up to 24% losses (Hooker 1962, Russell 1965).

Little is known of the presence of susceptibility gene involvement in host-rust pathogen interactions. Previous studies seeking to identify pathogen targets in the host have used expression analyses to identify upregulated host derived genes that may result in reduced defense capabilities (Yang et al. 2006, Goellner et al. 2001, Fung et al. 2008, Tremblay et al. 2010). Most studies focus on a singular host-pathogen interaction that likely result in observable changes specific to not only the pathogen but also the genetic composition of the pathogen (e.g. isolate). This study seeks to identify putative susceptibility genes through a comparative transcriptome analysis approach between three host-pathogen systems: barley and *Puccinia graminis* f. sp. *tritici* (*Pgt*); maize and *Puccinia sorghi* (*Ps*); and soybean and *Phakopsora pachyrhizi* (*Ps*). The use of three host-pathogen systems will provide the ability to shift away from host and pathogen specific interactions to analyzing more conserved changes that rust pathogens elicit in the host to create a more conducive environment for infection.

Materials and Methods

Plant and pathogen materials

The plant species and varieties used in this study were the barley cultivar 'Morex', the maize inbred 'B73', and the soybean cultivar 'Williams 82'. Each variety was chosen based on their compatible response to their respective adapted pathogens in addition to each having a sequenced genome and annotated transcriptome. *Pgt* race TTKSK (isolate 04KEN156/04) was chosen as a compatible isolate for the barley cultivar 'Morex'. Previous experiments indicate 'Morex' as being susceptible as a seedling to race TTKSK and exhibiting an infection type of 3 on the Stakman scale (Steffenson et al. 2013, Stakman et al. 1962) in addition to high field susceptibility. Bulk *Pp* spores were collected from Kudzu in Northern Florida and used to inoculate 'Williams 82'. 'Williams 82' is considered a universal susceptible variety for *Pp* and was tested for susceptibility to the bulked *Pp* spores. 'Williams 82' showed susceptible infections as described previously (Pham et al. 2009). The maize line 'B73' was inoculated with an isolate of *Ps* derived from a collection of common corn rust from St. Paul, Minnesota in 2012. The isolate was determined to elicit a compatible reaction with 'B73' as no apparent resistance response was observed based on pustule size, color, and the color of plant tissue around the infection.

Barley and soybean plants were grown in a walk-in growth chamber set to a 14-hour day length and 70% constant humidity. Temperatures were set to 24°C during the day and 20°C at night. Lighting consisted of 18 400W metal halide lamps and 12 90W incandescent lamps. Maize plants were grown in a greenhouse under a 16-hour day length and were supplemented with 1000W high-pressure sodium lamps. Temperatures were set to a range of 74-78°C during the day and 66-70°C at night.

Brachypodium T-DNA insertion lines

T-DNA insertion lines of putative susceptibility gene homologues identified in this study were ordered from the *Brachypodium* T-DNA collection of the Joint Genome Institute (Bragg et al. 2012). For the T-DNA lines received all seeds were planted, selfed, and treated as separate families for further DNA and phenotypic analyses. The *Brachypodium* line Bd21-3 was used to create the T-DNA insertion population and was used as a control line for the effect of T-DNA insertions on host-pathogen interactions.

Pathogen inoculation for RNA-seq

‘Morex’ barley plants were inoculated at the heading stage by carefully peeling away the flag leaf and sheath from the stem and painting a mixture of *Pgt* and soltrol 170 (Chevron Phillips Chemical Company) on the stems. The inoculum mixture was at a concentration of 5mg *Pgt* spores/800µL of Soltrol 170. Mock inoculations were performed using only Soltrol 170. ‘B73’ maize plants were inoculated when four fully expanded leaves were formed. The inoculum was applied by painting a mixture of *Ps* spores and Soltrol 170 on the leaves. The inoculum mixture was at a concentration of 5mg *Ps* spores/800µL of soltrol 170. Mock inoculations were performed using only soltrol 170. ‘Williams 82’ soybean plants were inoculated after three fully expanded trifoliate leaves had formed by painting a *Pp* spore and Talc mixture on trifoliate leaves. The inoculum mixture was 1mg *Pp* spores / 29mg Talc. Mock inoculations were performed using only Talc. Following inoculation using soltrol 170 plants were air-dried for 30 minutes. Plants inoculated with Talc were placed directly into the dew chamber. Inoculated plants were incubated in a dew chamber maintaining near 100% for approximately 16 hours. One 600W high-pressure sodium lamp provided light after 12 hours of incubation.

Tissue was collected at 6, 12, 24, and 72 hours post inoculation (hpi). The time of inoculation was considered 0 hpi when inoculated plants were placed into the dew chamber for incubation. A total of 5 biological replicates were used per time-

point and bulked for RNA extraction. Two sets of inoculations were performed per host-pathogen system approximately 14 days apart to create two experimental replicates.

RNA extraction and organic cleanup

Total RNA was extracted using the following protocol: 1) approximately 1.0g of tissue was ground with a motor and pestle in liquid nitrogen, 2) ground tissue was added to 10mL of TRIzol Reagent (Life Technologies) in a 50mL conical tube and mixed by partial inversion, 3) samples were incubated in a water bath at 60°C for 15 minutes, 4) samples were centrifuged for 20 minutes at 4300 rpm at 4°C, 5) the upper aqueous layer was transferred to a new 50mL conical tube containing 2.0 mL of chloroform and mixed by partial inversion, 6) samples were incubated at room temperature for 10-15 minutes, 7) samples were centrifuged for 20 minutes at 4300 rpm at 4°C, 8) the upper aqueous layer was transferred to a new 50mL conical tube and 2.5 mL of isopropanol and 2.5 mL of 0.8M Na-Citrate/1.2M NaCl was added, 9) samples were incubated at -20°C for 20 minutes and then centrifuged for 20 minutes at 4300 rpm at 4°C, 10) RNA pellets were washed with 10mL 75% ethanol and centrifuged for 10 minutes at 4300 rpm at 4°C, 11) RNA pellets were air-dried for 10 minutes by inversion on a clean Kimwipe (Kimberly-Clark), 12) RNA pellets were resuspended in 500 µL DEPC-treated H₂O (Life Technologies) by repeated pipetting, 13) 2.0 µL SUPERase-In RNAase inhibitor (Life Technologies) was added and samples were incubated in a water bath at 60°C until the pellets were dissolved.

To remove organic chemical residues, samples were cleaned a Qiagen RNeasy Plant Midi Kit following a modified cleanup protocol: 1) 2.0 mL of RLT buffer and 1.4 mL of 100% ethanol were added to the 500 µL of the RNA extraction and mixed by pipetting, 2) samples were applied to a Midi column placed in a 15 mL centrifuge tube and centrifuged at 4300 rpm for 5.0 minutes at room temperature, 3) after discarding the flow through, 2.5 mL of RPE buffer was added to the column and

incubated at room temperature for 3.0 minutes, 4) columns were centrifuged at 4300 rpm for 2.0 minutes at room temperature and the flow through was discarded, 5) another 2.5 mL of RPE buffer was added to the column, columns were incubated for 3.0 minutes at room temperature and centrifuged for 5.0 minutes at 4300 rpm at room temperature, 6) the flow through was discarded and the columns were centrifuged again for 3.0 minutes at 4300 rpm at room temperature to dry the column membrane, 7) the columns were transferred to a new 15 mL tube and 150 μ L of RNase-free water was added directly to the membrane, 8) columns were incubated for 1.0 minute at room temperature and centrifuged for 4.0 minutes at 4300 rpm at room temperature, 9) the flow through was pipetted back onto the membrane, columns were incubated for 1 minute at room temperature, and then centrifuged for 4 minutes at 4300 rpm at room temperature. RNA extracts were stored at -80°C.

Pathogen inoculation of *Brachypodium distachyon* seedlings

B. distachyon lines were planted in covered trays containing vermiculite (Sun Gro Horticulture, Bellevue, WA) saturated with water for three days at 4°C. After three days the trays were uncovered and grown in a growth chamber at a 16-hour day length with a temperature schedule of 20°C/18°C (day/night). Approximately nine days after incubation at 4°C the *B. distachyon* lines were inoculated with *Puccinia graminis* f. sp. *avenae* (*Pga*) race DBL (05ID107) following the protocol outline by Rouse et al. (2011).

Expression analyses and homologue identification

RNA extracts were sequenced using Illumina's HiSeq 2000 platform at 20 million, 100 bp, paired-end reads per time-point and treatment condition. The Tuxedo Suite (Illumina) was used to analyze RNA sequences obtained from sequencing. Read qualities were assessed using FastQC. Sequence reads were aligned using TopHat2. TopHat2 was used again to map paired-end reads using a corrected average interval length. The genomes used for mapping paired reads were obtained from

Ensembl Genomes (plants.ensembl.org) and were the following versions: maize (Zea_mays.APGv3.22), barley (Hordeum_vulgare030312v2), and soybean (Gmax_109). Cufflinks was used to develop an experimental transcriptome for each time-point using the annotated transcriptome as a guide. The annotated transcriptomes were also obtained from Ensembl Genomes and were versions: maize (Zea_mays.AGPv3.22), barley (Hordeum_vulgare.030312v2.20), and soybean (Glycine_max.V1.0.20). Cuffmerge was used to create a singular transcriptome for expression analysis that combined all time-points and all conditions. Differential expression was determined with CuffDiff at a false discovery rate of <0.05. A BLAST database was created for each host species using the nucleotide sequences of the combined transcriptomes from all time-points of both the experimental and mock conditions. To identify differentially expressed homologues between all host species, TBLASTX (evalue <0.001) were performed using the differentially expressed transcript sequences. Soybean was used as the hub parent for which the significant TBLASTX results from barley and maize sequences would be compared.

DNA extraction and T-DNA verification

DNA of the putative T-DNA insertion mutants were extracted using the protocol described by Edwards et al. (1991) with modifications for extraction in a 96-well plate and inclusion of a chloroform separation step. PCR primers were designed to flank the putative T-DNA insertion site and result in an approximately 1000 bp product. Primer sequences can be found in Table 1. The PCR protocol conditions were: 1 cycle of 94°C for 30 seconds; 40 cycles of 94°C for 15 sec, 51°C for 15 sec, 72°C for 30 sec; and 1 cycle of 72°C for 2 min.

Results

Differential Expression

Genes differentially expressed for barley and soybean interactions with *Pgt* and *Pp* respectively appeared to follow a biphasic pattern (Table 2). No differential expression in barley was observed at 6 hpi and low differential expression was

observed 24 hpi relative to 12 and 72 hpi. Differential expression was characterized by a predominance of upregulation compared to downregulation. Unlike barley, no differential expression was observed at 24 hpi in soybean and a much larger number of downregulated genes were observed at 12 and 72 hpi. Few genes were identified as differentially expressed in maize. At 6 hpi only 34 genes were differentially expressed with a predominance of downregulated genes. At 24 hpi significant upregulation occurred followed by no significant differential expression at 24 and 72 hpi.

Homologous and Differentially Expressed Genes

A non-redundant list of differentially expressed gene models was identified for each host and compared to the total assessed gene models (Table 3). The number of non-redundant differentially expressed gene models composed a small proportion of the total experimental transcriptome for each species. Barley was observed to have 3.01% of its transcriptome differentially expressed while soybean and maize were observed to have 1.43% and 0.64% respectively. The proportion of non-redundant and differentially expressed homologues was observed to comprise less than 1% of each transcriptome however the homologues contributed to a significant proportion of the total amount of differentially expressed genes (Table 3). Overrepresented gene ontology categories consisted of those typical for stress responses and included genes with predicted function for: regulation of transcription; protein phosphorylation; carbohydrate metabolism; oxidation reduction; and peptidase inhibition.

Only one trio of homologous and differentially expressed genes showed a similar change in regulation between all three host-pathogen interactions. The three genes: MLOC_57296 (barley), GLYMA01G04830 (soybean), and GRMZM5G865298 (Maize) exhibited gene ontologies to transmembrane nitrate transporters and were all significantly upregulated between 6 and 12 hpi (Figure 1). No other set of homologues with similar differential expression represented all host species.

However four homologous gene sets representing genes from barley and soybean were significantly differentially expressed at 72 hpi (Figure 2). Three of the homologous gene sets exhibited gene ontologies characteristic of transcription factors and were identified as affecting processes involved with response to heat stress, response to osmotic stress, and regulation of metabolic processes including nitrogen metabolism. One set of homologues exhibited gene ontologies involved in defense responses to pathogenic bacterium, protein serine/threonine phosphatase activity, and localization to the plasma membrane and mitochondria (Table 4). No other pairs of homologues were differentially expressed at similar time-points when comparing only maize and barley.

Mutant Analysis

T-DNA insertion mutant homologues of the nitrate transporters identified in this study were found in the grass species, *Brachypodium distachyon*, (Table 5) in the *Brachypodium* T-DNA collection of the Joint Genome Institute (Bragg et al. 2012). Only one set of homologues was found to contain possible insertions within the gene of interest and were available in multiple genetic backgrounds. T-DNA insertion events were assessed using PCR with genic and T-DNA specific primers. The seeds obtained for the JJ18123 mutant lines were identified as having a fixed T-DNA insertion using primers designed for *BRADI3G28410* (Figure 3). Results of PCR screening indicate that the insertion could not be identified in a homozygous state as wild-type PCR products were always observed. The JJ18123 mutants were in the T₄ generation indicating that any insertion should be homozygous. Tiled PCR reactions were designed with 2-3 redundant overlaps and covered approximately 2000bp before and after the putative *BRADI3G28410* T-DNA insertion site. These reactions only resulted in wild-type PCR products (data not shown). Cloning and sequencing of PCR products resulting from the 18123-F1 and T3 T-DNA LB (T-DNA specific) primers identified that the insertion was not in the *BRADI3G28410* gene and instead was located near *BRADI1G34610* (Figure 4). Much like *BRADI3G28410*, *BRADI1G34610* also has gene ontology to membrane bound proton-dependent oligopeptide transporters with possible nitrate transportation function. The similarity in sequence between *BRADI3G28410* and *BRADI1G34610* likely created confusion with initial identification of T-DNA insertions from flanking

sequence tags.

Inoculation of the control line Bd21-3 and the eight replicated lines of the JJ18123 mutant stock with the *Puccinia graminis* f. sp. *avenae* (race DBL) resulted in an altered host response to the pathogen (Figure 5). *B. distachyon* line Bd21-3 exhibited a moderately susceptible phenotype to race DBL characterized by small circular pustules. The JJ18123-derived lines did not show pustule formation however necrotic spots were observed. Although the JJ18123 stock exhibited heightened resistance to *Pga*, these lines were also observed to have enlarged leaves, later maturity, and more prolific tillering (Figure 6). Bragg et al. (2012) identified the mutant stocks JJ18133 and JJ18143 presumably containing the same insertion as JJ18123. These lines however did not have the same resistant response to *Pga* race DBL as JJ18123 (Figure 5) and exhibited pustule types similar to Bd21-3 (Figure 5 and 7). Screening with T-DNA specific primers determined that these lines did not have a T-DNA insertion near the *BRADI1G34610* gene. Additionally, JJ18113, JJ18133, and JJ18143 grew similarly to Bd21-3 and did not exhibit the later maturity, enlarged leaves and prolific tillering observed in JJ18123 lines.

Discussion

In the current study three homologous nitrate transporters were differentially expressed at 12 hpi in all compatible host-pathogen interactions. A similar study performed by Choi et al. (2008) identified a soybean nitrate transporter (*NTR1-5*) that was upregulated at 6 and 12 hpi in response to *Pp* inoculation. Similarly, Pike and colleagues (2014) identified the grapevine nitrate transporter *VvNPF3.2* was upregulated during a susceptible interaction with the powdery mildew pathogen *Erysiphe necator* but in a resistant one. La Mantia et al. (2013) found that resistance in poplar to the poplar leaf rust pathogen *Melampsora x columbiana* was significantly associated with knockdown mutants in two closely linked nitrate transporters *PtNRT2.1* and *PtNRT2.4*. Similar to La Mantia and colleagues (2013), Camañes et al. (2012) found the mutant *Arabidopsis* line *nrt2*, which is deficient in two linked nitrate transporters *NRT2.1* and *NRT2.2*, exhibited reduced susceptibility to *Pseudomonas syringae* pv *tomato* DC3000. *NRT2.1* and *NRT2.2* from *Arabidopsis* are orthologous to *PtNRT2.1* and *PtNRT2.4* in poplar. In this study a T-DNA

insertion mutant in a *B. distachyon* nitrate transporter (*BRADI3G28410*) homologous to the three nitrate transporters in this study induced heightened cell death in response to pathogen inoculation.

This study observed differential expression for soybean that exhibited a characteristic biphasic pattern similar to that observed by van de Mortel et al. (2007) and Schneider et al. (2011). van de Mortel and colleagues reported that the initial peak in differential expression began at approximately 6 hpi and ended at 36 hpi, followed by a reduction in differential expression from 24 to 72 hpi, and then another peak in differential expression from 72 to 168 hpi. Schneider and colleagues found that the early differential expression was observed within the first 12 h regardless of the presence of effective resistance genes, only one gene was differentially expressed at 24 hpi, and the second peak in differential expression was observed to begin at 72 hpi and increase in magnitude as the fungal colonies established and grew in size. The peaks in differential expression were observed to coincide with penetration into the leaf interior and establishment of haustorium while the timing of reduced differential expression coincided with intercellular growth. The infection cycle of *Pgt* and the pattern of differential gene expression observed in barley follow a similar pattern to that found in soybean. Germination of the urediniospores and formation of appressoria occur within 6-12 hpi. Penetration into the leaf interior, formation of haustoria mother cells, and haustoria occur between 24-72 hpi. The establishment of the fungal colony through the formation of multiple haustoria can be observed by 72 hpi (Figueroa et al. 2013). The reduced differential expression at 24 hpi observed in barley overlaps with the stage of infection in which intercellular growth is occurring. The infection cycle for *Ps* occurs along a similar schedule as *Pgt* and *Pp*. Early scanning electron studies by Hughes and Rijkenberg (1985) showed that by 6 hpi germination of the urediniospores, formation of appressoria, and development of the substomatal vesicles will have occurred. By 12 hpi the primary hyphae will develop and within 24 hpi the first haustorial mother cells and haustorial will have formed from

the primary hyphae. By 72 hpi the infection is fully established and secondary hyphae have begun to proliferate and develop into the intercellular mycelium. Interestingly, the differential expression patterns observed in maize did not correlate similarly to developmental changes of *Ps* much like that observed in soybean to *Pp* and barley to *Pgt*. The lack of differential expression in maize at 72 hpi is seemingly unusual because this is the time-point at which the largest proportion of host tissue is interacting with *Pp*.

The timing of differential expression for the nitrate transporters observed in the current study and those performed by Choi et al. (2008) and Pike et al. (2014) occurred before and into the early haustorial development phase. In addition, each study identified that differential expression was not maintained after colony establishment. These results indicate that nitrate movement is likely not due to the pathogen altering nutrient movement or obtaining nutrients. Additionally, genomic studies and EST sequencing of the sequenced obligate biotrophic pathogens *Blumeria graminis*, *Puccinia graminis*, *Melampsora larici-populina*, *Hyaloperonospora arabidopsidis*, *Albugo laibachii*, and *Puccinia striiformis* have identified that no obligate biotrophic genome and EST libraries contain genes coding for nitrate uptake and assimilation (Spanu 2012, Garnica et al. 2013). It is possible that early host-pathogen interactions at the leaf surface may direct the host to a more resistant or susceptible response.

Nitric oxide (NO) has been previously identified as a mediator of abiotic and biotic stress responses including inducing the hypersensitive response and initiating systemic acquired resistance (Delledonne et al. 1998, Durner et al. 1998, Delledonne et al. 2001, Zago et al. 2006, Wang et al. 2014b). The relationship between NO and triggering plant defense responses has however been shown to be concentration dependent, where too much or too little NO reduces the plants ability to induce resistance responses (Wang et al. 2014b). The metabolic mechanisms that alter the concentration of NO in plants is poorly understood: however at least seven

possible NO producing pathways have been described that utilize reduction, oxidation, and scavenging methods (Gupta et al. 2011). One of the most well described pathways for NO production involves reduction of nitrite to NO through the enzyme nitrate reductase (Rockel et al. 2002). Nitrate reductase has been implicated in elicitor induced production of NO for both necrotrophic and biotrophic pathogens (Rasul et al. 2012, Shi and Li 2008, Yamamoto-Katou et al. 2006, Asai et al. 2010, Perchevied et al. 2010, Modolo et al. 2006, Oliveira et al. 2009). However, Rockel and colleagues (2002) identified that production of NO through reduction of nitrite is competitively inhibited by local concentrations of nitrate. The current trend of pathogen-induced nitrate transporters implicates upregulation in compatible interactions (the current study, Pike et al. 2014, Choi et al. 2008), and downregulation with heightened resistance responses (Camañes et al. 2012, La Mantia et al. 2013). The enhanced resistance observed in line JJ18123 in the current study, and the attenuated hypersensitive response observed in *A. thaliana* lines deficient in nitrate reductase (Modolo et al. 2006; Oliveira et al. 2009) indicate a possible mechanism for diminishing plant resistance responses by increasing local nitrate concentrations to inhibit NO production. Another hypothesis may be that the loss of nitrate transporters reduces the plants ability to regulate NO concentrations resulting in an early NO burst and increased hypersensitive response instead of a controlled SAR response. The apparent increase in resistance of JJ18123 T-DNA lines indicates that the resistance response to *Pga* is possibly greater in magnitude or is initiated faster.

Verification of the correlated mutant phenotype and putative T-DNA insertion observed in JJ18123 is necessary. JJ18123 exhibited consistent resistant-like responses in all lines derived from the original mutant stock and in all experiments following inoculation with *Pga* race DBL. The background in which the *BRADI1G34610* was assayed contains at least one and likely more fixed T-DNA insertions. Creating a segregating F₂ population between Bd21-3 and a representative JJ18123 line would enable discernment if the T-DNA insertion

near *BRADI1G34610* is the causal mutation for the resistance-like response and altered growth patterns. A segregating F₂ population would also identify if the mutation functions in a dominant, recessive, or additive manner. Additional lines that may contain the *BRADI3G28410*(*BRADI1G34610*) T-DNA insertion can be found in the *B. distachyon* mutant population and represent useful tools in verifying the effect of a *BRADI1G34610* mutant (Table 3). Additionally, mutation using CRISPR/Cas9 targeted mutagenesis is both a method to test the effects of the current insertion near *BRADI1G34610* and also to test the effect of the original target *BRADI3G28410* on host-pathogen interactions. Creating double-stranded breaks flanking the candidate genes creates the ability to remove candidates from transformed lines.

Tables and Figures

Oligo ID	Sequence
18123-F1	CTAGTCTCTCCCAGAGGTCA
18123-R1	GGATTGCTTTCAGGTTAGA
T3 T-DNA LB	AGCTGTTTCCTGTGTGAAATTG

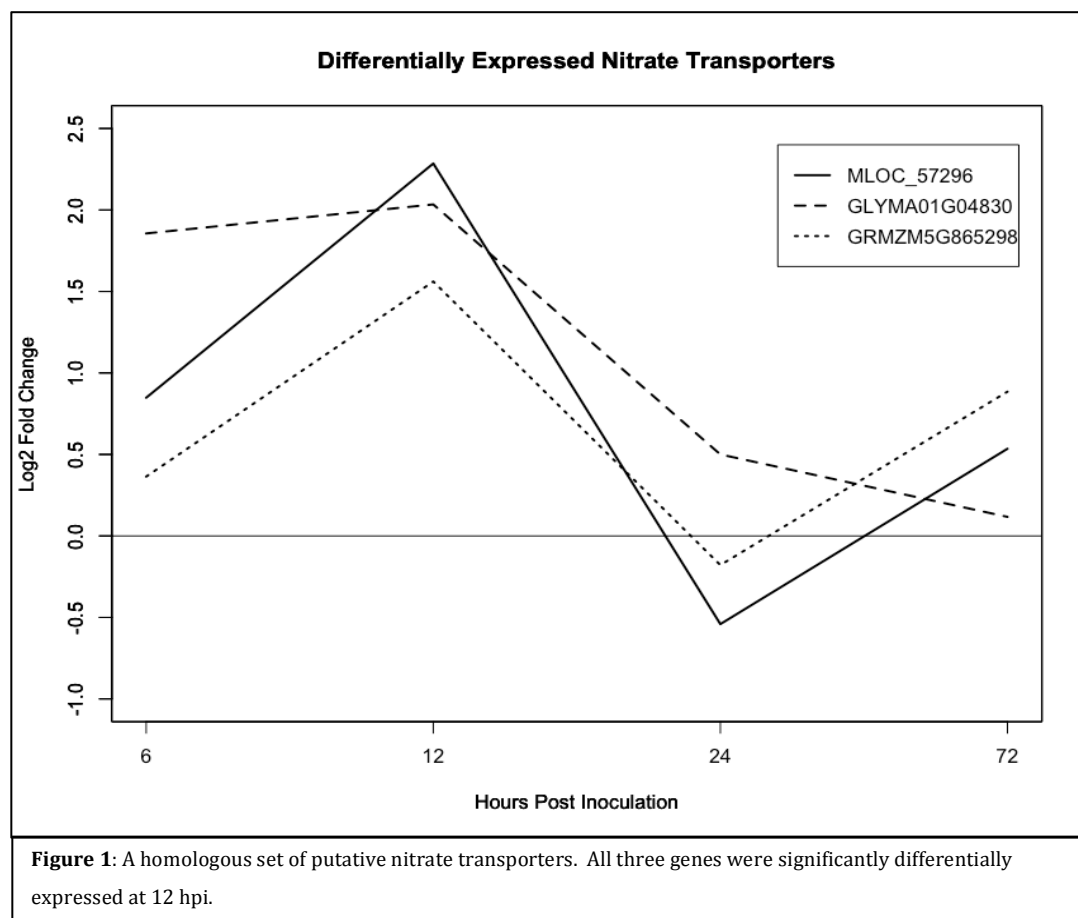
Table 1: Primers used to verify the presence of the T-DNA insertion in *BRADI3G28410*.

Host	Change in Expression	Hours Post Inoculation			
		6	12	24	72
Barley	Upregulated	0	270	40	1100
	Downregulated	0	80	57	97
Soybean	Upregulated	214	100	0	52
	Downregulated	157	226	0	146
Maize	Upregulated	2	246	0	0
	Downregulated	32	8	0	0

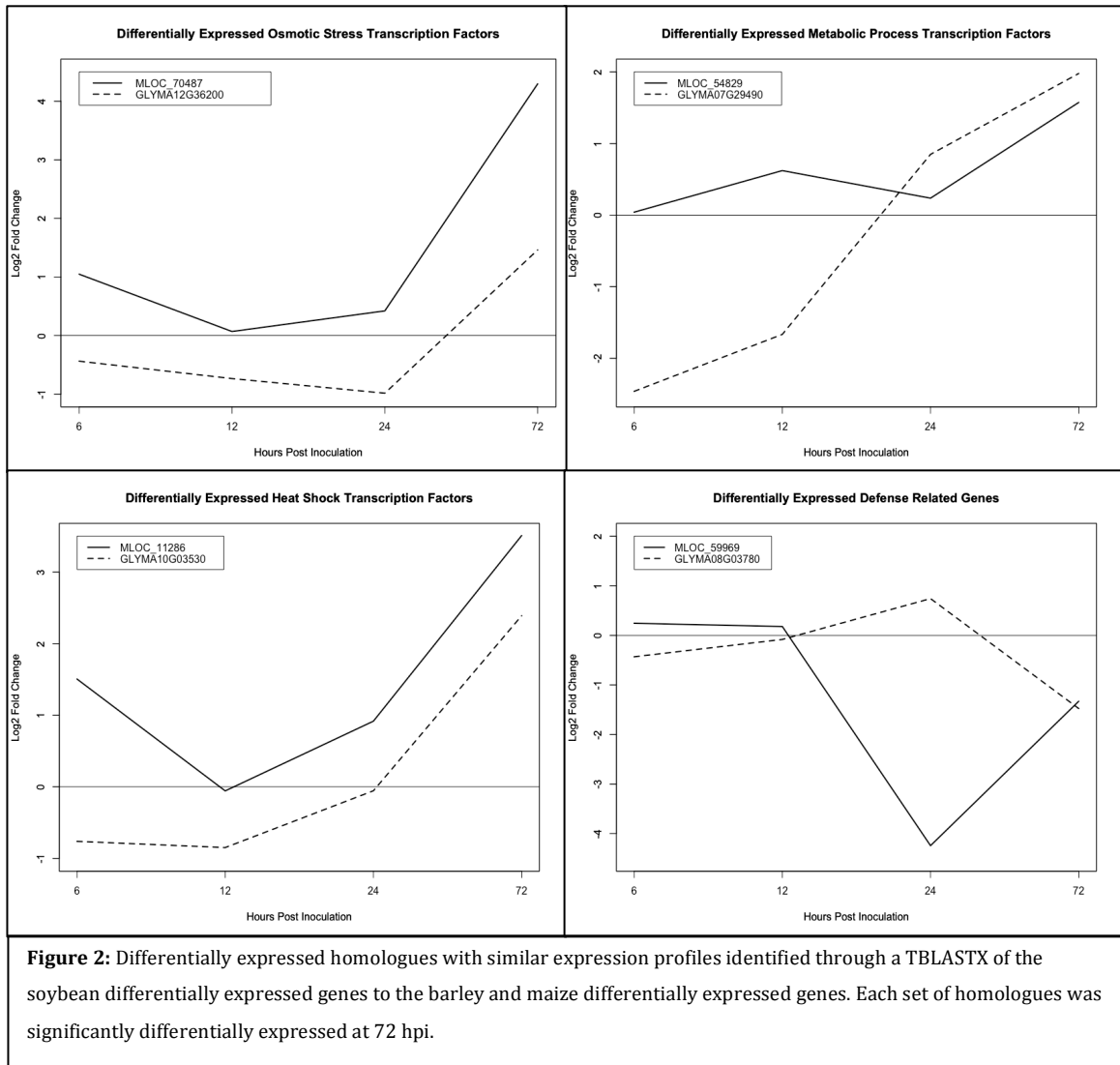
Table 2: The total number of differentially expressed genes per time-point and change in regulation for each host; barley, soybean, and maize.

Host	Total Assessed Gene Models	Non-Redundant DEGs	% DE Gene Models	Non-Redundant Homologous DEGs	% Homologous DE Gene Models
Barley	46899	1410	3.01	334	0.71
Soybean	54780	783	1.43	436	0.80
Maize	44616	286	0.64	214	0.48

Table 3: The total non-redundant differentially expressed genes that are homologous to at least one other host expressed as a proportion of the total number of gene models assessed in this study.



IV Function	Time of DE
porter activity; 12	
porter activity;	
	72
	72
	72
	72



Host	Host Gene	Brachypodium Homologue	Locatino of the Insertion	T-DNA stock with the Insertion
Maize	GRMZM5G865298	BRADI3G28410	Insertion in exon	JJ18103, JJ18113, JJ18123, JJ18133, JJ18143, JJ18153, JJ18163,
Maize	GRMZM5G865298	BRADI3G28417	Insertion near gene	JJ13767, JJ13807, JJ13793, JJ13779, JJ13818, JJ13830
Barley	MLOC_57296	BRADI3G52096	Insertion in exon	JJ12235

Table 5: Three putative nitrate transporter homologues were identified in *B. distachyon* using TBLASTX to compare the maize, soybean, and barley nitrate transporter gene models to the *B. distachyon* genome. Two *B. distachyon* homologues were found to have insertions within exonic sequences and only one homologue could be found in multiple T-DNA stock

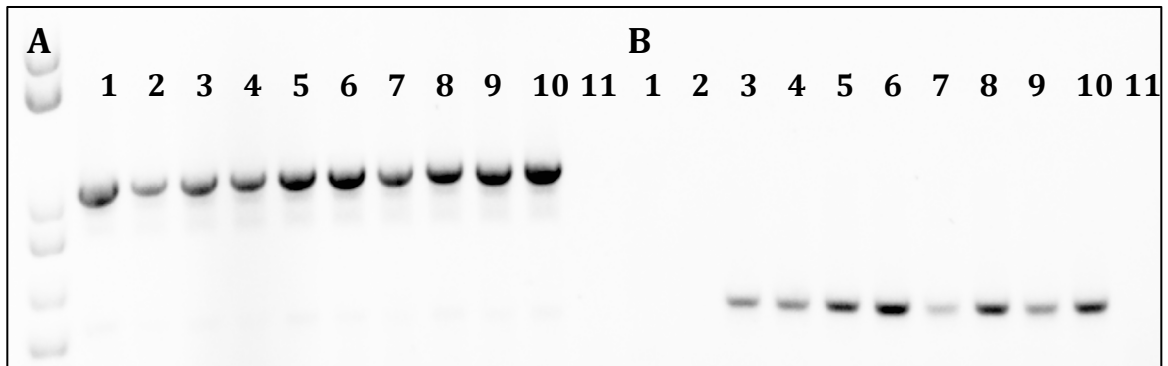


Figure 3: A) Line Bd21-3 and the mutant families 18123-1 through 18123-8 were screened with primers targeting the T-DNA insertion site for *BRAD13G28410*. **B)** The forward primer from **(A)** was used with the transposon specific T3 primer described by Bragg et al. (2012). Both replicates of Bd21-3 did not amplify when the T3 primer was used. 1= Bd21-3; 2= Bd21-3; 3= 18123-1; 4= 18123-2; 5= 18123-3 6= 18123-4; 7= 18123-5; 8= 18123-6; 9= 18123-7; 10= 18123-8; 11= No template negative control.

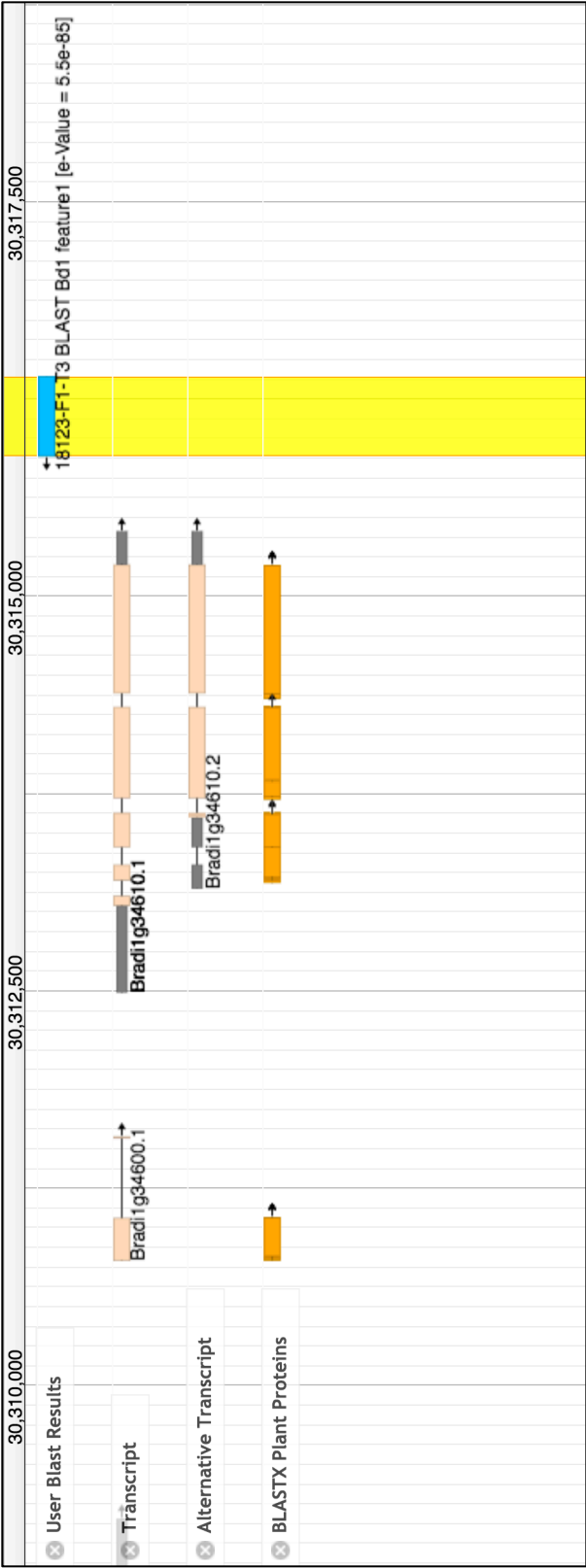


Figure 4: The most significant BLAST alignment of the PCR product resulting from the 18123-F1 and T3 primer pair to the Bd21-3 genome sequence (V3.1, phytozome.jgi.doe.gov). The highlighted region indicates the genomic alignment of the PCR product. Transcript and alternative transcript tracks indicate the nearest *Brachypodium* genes. The BLASTX Plant Proteins track provides added evidence for proteins of similar sequence in *Oryza sativa* (rice).

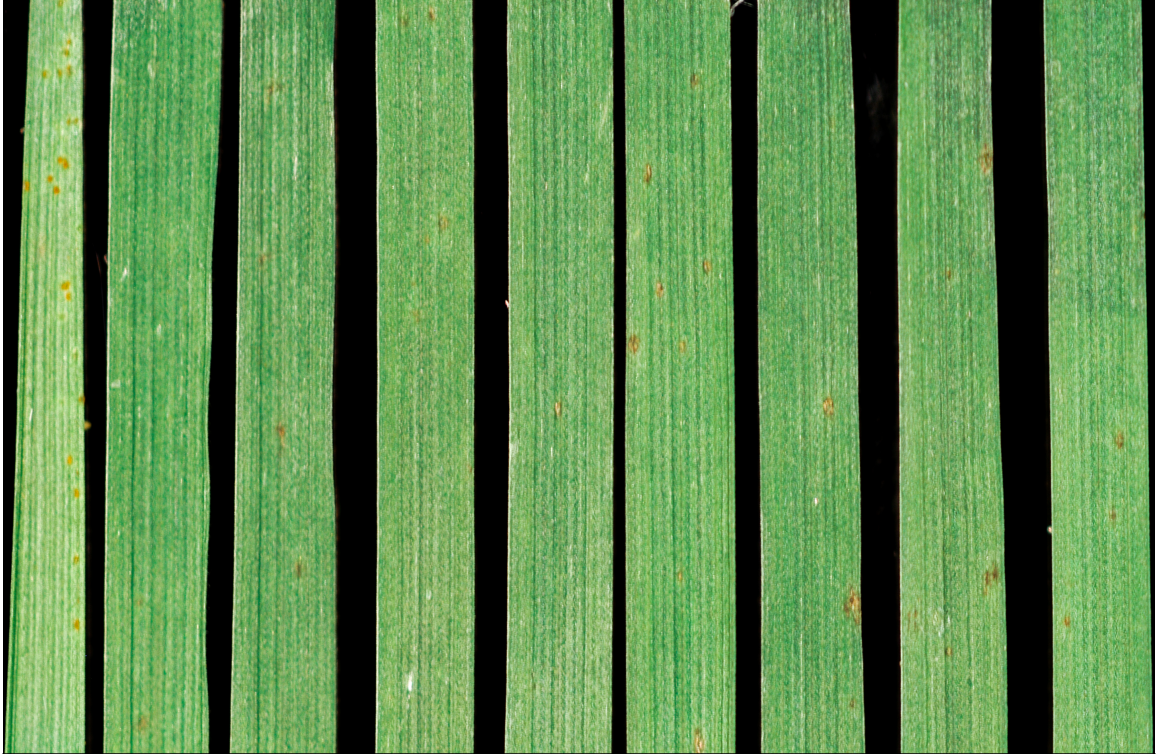
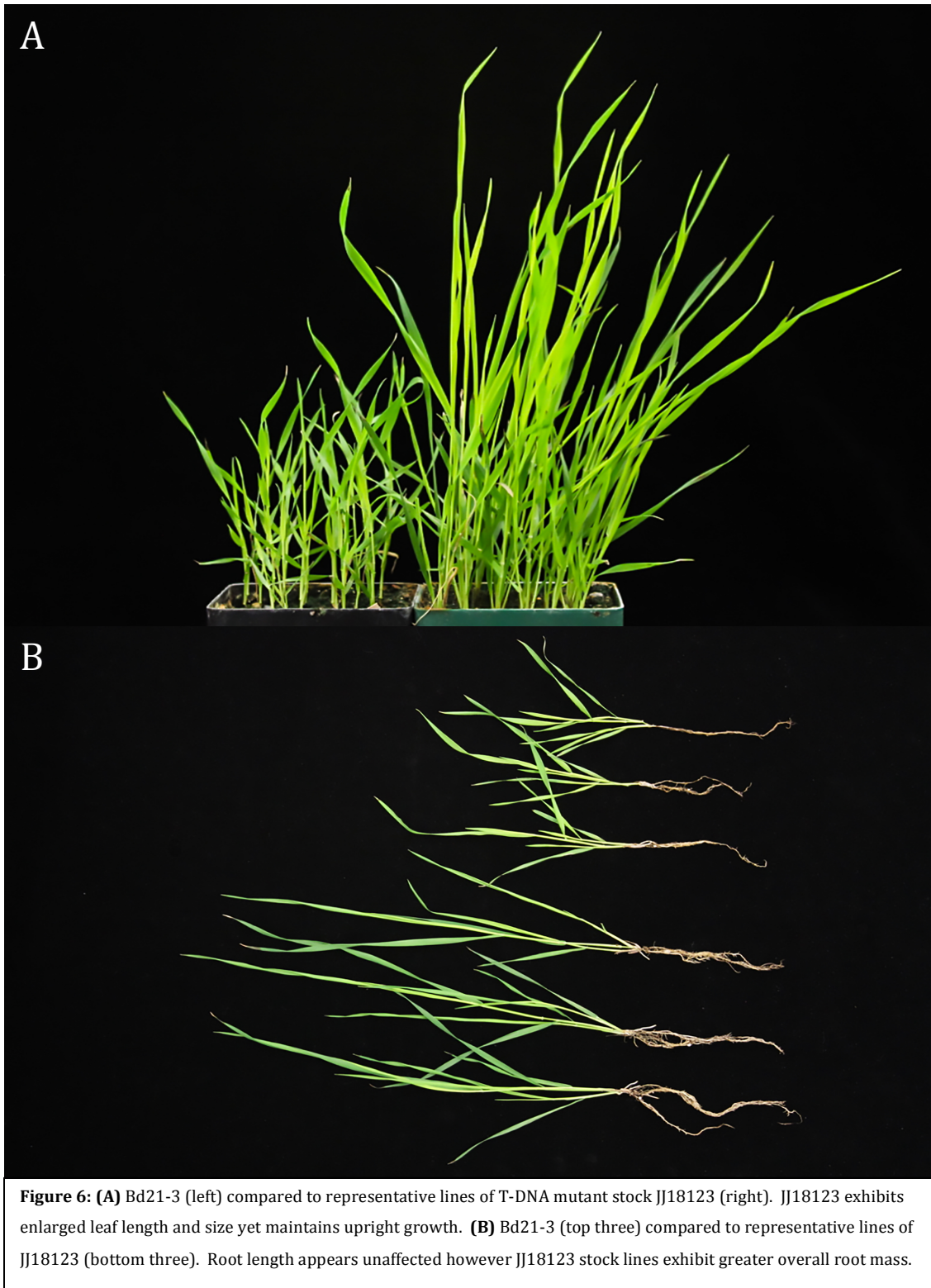


Figure 5: *B. distachyon* line Bd21-3 and the JJ18123 mutant families inoculated with *Pga* race DBL. From left to right: Bd21-3; 18123-1; 18123-2; 18123-3; 18123-4; 18123-5; 18123-6; 18123-7; and 18123-8.



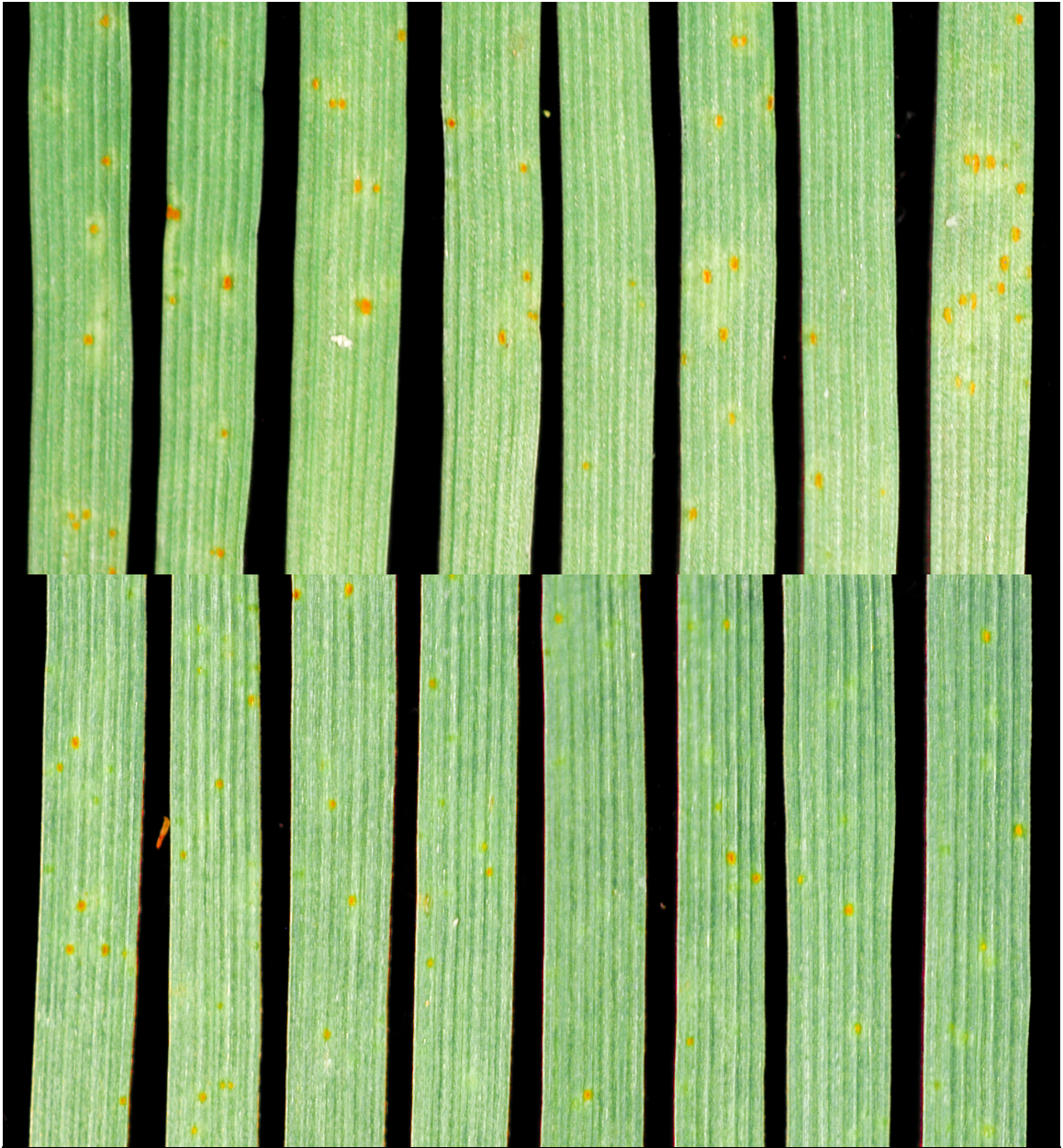


Figure 7: Pustule formation on T-DNA stock lines **(Top)** JJ18133 and **(Bottom)** JJ18143.

Creation of *Sr12* mutants derived from ‘Thatcher’ wheat

Synopsis

‘Thatcher’ wheat is one of the first spring wheat cultivars specifically bred for stem rust resistance and combined the stem rust resistance of ‘Kanred’ bread wheat and ‘Iumillo’ durum wheat. Stem rust resistance in ‘Thatcher’ has been consistently identified as complex and includes numerous seedling resistance genes and adult plant resistance loci. The seedling resistance gene *Sr12* is one of the sources of ‘Thatcher’ stem rust resistance. Additionally, *Sr12* coincides with an adult plant resistance locus effective to stem rust pathogen races virulent to *Sr12* at the seedling stage. This study identifies 13 putative *Sr12* mutants created through chemical mutagenesis using sodium azide (NaN₃) and ethyl methanesulfonate (EMS). The mutants created in this study can be used to decipher the relationship between *Sr12* and the coinciding adult plant resistance locus.**

Introduction

The hard red spring wheat cultivar ‘Thatcher’ was one of the first spring wheat cultivars specifically bred for stem rust resistance (Hayes et al. 1936). It combined the agronomic qualities and bread making characteristics of ‘Marquis’ with the stem rust resistance of ‘Kanred’ and ‘Iumillo’ durum wheat. Due to its combination of stem rust resistance and end use quality, ‘Thatcher’ was widely grown throughout the United States and Canada from its release in 1935 to the 1960s. Subsequently, ‘Thatcher’ was used as a recurrent parent in wheat breeding programs in both

** This chapter is the result of collaborative research. Collaborators include: Jordan Briggs, Matthew N. Rouse, Colin W. Hiebert, Wolfgang Spielmeyer, and Samuel Stoxen. The author of this dissertation contributed to designing and performing the experiments including: rating stem rust infection on the mutagenesis populations, testing inbred mutant progeny for infection types, parsing and analyzing DNA marker data, and drafting this chapter. WS and SS developed the mutagenesis populations. CWH provided the NB-LRR3 marker to screen for *Sr12*. MNR approved the experiment design and supervised the analyses. All dissertation committee members reviewed, commented, and approved this chapter.

Canada and the United States resulting in widespread use of ‘Thatcher’ derived stem rust resistance in North America (Kolmer et al. 2011).

The inheritance of stem rust resistance in ‘Thatcher’ wheat has been shown to be complex and include at least four known seedling resistance genes (*Sr5*, *Sr9g*, *Sr12*, and *Sr16*), an additional undescribed seedling resistance gene (*SrTc*), and multiple adult plant resistance loci (Knott 2000, Knott 2001, Nazareno and Roelfs 1981, Rouse et al. 2014). Despite exhibiting susceptible seedling phenotypes to the Ug99 race group, ‘Thatcher’ displays moderate field resistance to the same races. Recent efforts to map the causal loci contributing to adult plant resistance to Ug99 have identified a QTL co-locating with the ‘defeated’ seedling resistance gene *Sr12* as a central component of the observed resistance (Rouse et al. 2014, Hiebert et al. 2016). This locus was observed to interact with multiple adult plant resistance loci and be required for expression of the field resistant phenotype of ‘Thatcher’. Vanegas et al. (2008) and Nazareno and Roelfs (1981) also correlated *Sr12* with heightened field resistance, however no definitive link between *Sr12* and field resistance to *Sr12* virulent races have been made.

Previous correlations between adult plant resistance and the presence of R-genes absent of an observable hypersensitive response have been previously identified. Rietman et al. (2012) found a quantitative disease resistance locus, *Rpi-Smira2*, to *Phytophthora infestans* in the potato variety ‘Sarpö Mira’ that correlated with a response to the cloned avirulence protein (PITG_07558). *P. infestans* isolates that did not elicit a hypersensitive response in detached leaf assays showed reduced pathogenicity during field conditions in lines carrying *Rpi-Smira2*. Chantret et al. (1999) found that the powdery mildew resistance gene *MIRE* has residual dominant effects on adult plant resistance to *MIRE* races virulent at the seedling stage. Additionally, Li et al. (1998) identified a ‘defeated’ rice resistance gene *Xa4* that acts as a recessive QTL against *Xa4* virulent races of the rice blast pathogen, *Xanthomonas oryzae* pv. *oryzae*. Similar to *Xa4*, the *Sr12* locus also functions in

a recessive manner (Mcintosh 1967, Sheen 1964) and co-locates with adult plant resistance (APR) QTL to *Pgt* races virulent at the seedling stage (Rouse et al. 2014, Hiebert et al. 2016).

The consistent correlation between *Sr12* and heightened field resistance in addition to similar observations in other pathosystems indicate that further analysis into the molecular function of *Sr12* could provide insight into the link between standard NBLRR resistance pathways and field resistance. In addition, if *Sr12* is truly the causal gene behind heightened field resistance it represents a useful tool in developing wheat lines with improved resistance stability due to its qualitative and quantitative action in addition to its apparent ability for epistatic enhancement of additional stem rust resistance QTL (Rouse et al. 2014).

Development of the RenSeq workflow has created a pipeline for relatively quick and efficient cloning of R-genes compared to standard mapping procedures. (Jupe et al. 2013). RenSeq is able to combine next-gen sequencing with mutagenesis to identified causal genes and therefore is not affected by dissimilarities in chromatin structure or inhibition of recombination due to the centromere. Recently, the RenSeq workflow has been established for cloning R-genes in the wheat stem rust pathosystem. Steuernagel et al. (2016) reported re-cloning of *Sr33* as a proof of concept and further cloning of *Sr22* and *Sr45* using only knockout mutants. RenSeq therefore shows promise for distinguishing the link between *Sr12* and observed field resistance in ‘Thatcher’ wheat. Using chemical mutagens to knockout *Sr12* offers the dual function of providing material for RenSeq based cloning as well as creating ‘Thatcher’ germplasm deficient in *Sr12* to discern the effects of *Sr12* on field resistance without generating the confounding effects of closely linked genes that are observed in standard mapping studies.

This study seeks to develop several mutation events of *Sr12* for later fulfillment of two objectives: 1) To develop a source of germplasm to use in the RenSeq workflow for cloning *Sr12* and 2) to develop ‘Thatcher’ lines deficient in only *Sr12* to

assess the effect of a knockout allele on the field resistant phenotype of ‘Thatcher’.

Materials and Methods

Mutagenesis of ‘Thatcher’

Mutagenized M₂ families were obtained from Dr. Wolfgang Spielmeier. ‘Thatcher’ seeds were mutated with 1mM sodium azide (NaN₃) as previously described (Chandler and Harding 2013). The M₁ plants were planted in the field to produce M₂ seed. Single spikes were collected from each surviving plant to screen M₂ families for segregating *Sr12* mutations using *Pgt* race SCCSC (09ID73-2). 600 M₂ families were developed through NaN₃ mutagenesis.

Mutagenesis of ‘TcMn83’

The population ‘Thatcher’ x ‘McNeal’ has been previously used to map causal loci for ‘Thatcher’-derived field resistance and its interaction with the stem rust APR gene *Lr34/Sr57* (Rouse et al. 2014). A recombinant inbred line derived from this population, ‘TcMn83’ (GSTR 10285), was determined to have all QTL associated with APR including *Sr12* and was used as the parental line for the ethyl methanesulfonate (EMS) mutagenesis population. The concentration of EMS in which 50% lethality was observed was 0.5%. 400 seeds per 250mL flask were soaked in 100mL ddH₂O for 7 hours. During imbibition seeds were shaken gently using an orbital shaker (Bellco Biotechnology). Following imbibition the seeds were rinsed three times with 250 mL ddH₂O. 75mL of 0.5% EMS was added to the flasks and the seeds were soaked for 16 hours. The EMS was removed and 50mL ddH₂O was used to rinse seeds. Flasks were covered and rinsed under running water for 2 hours. Seeds were germinated on paper towel in petri dishes and transplanted for propagation. 1600 M₂ families were developed from ‘TcMn83’ and screened for *Sr12* mutant phenotypes.

Screening mutagenesis populations for *Sr12* mutants

SCCSC has been previously identified as avirulent on *Sr12* and *Sr16* (data unpublished). In response to *Sr12* and *Sr16*, SCCSC elicits a 0; to ;1 and a 2+ infection type (IT) respectively on the Stakman scale (Stakman 1962) in greenhouse conditions (18-23 °C, 16 hour day length supplemented with 1000 W HPS lamps). 600 M₂ segregating families were screened in 38 cm x 61 cm x 9 cm metal trays. 5 cm of steamed soil was added to the bottom of the trays and covered with 3 cm of vermiculite. Approximately 20-25 seeds were sown in 16 cm headrows with 2.5 cm spacing between each row. SCCSC was inoculated 7-9 days after planting when the first leaf was fully expanded. Seedlings were scored according the Stakman scale (Stakman 1962) at 14 days post inoculation. All families exhibiting segregating infection responses greater than the control lines ‘Thatcher’, ‘TcMn83’, and ‘Prelude’ (+*Sr12*) were retained for progeny testing.

Verification of mutants

Progeny verification of the *Sr12* mutant phenotype

1-2 putative *Sr12* M₂ mutant lines were collected from each segregating family and advanced one generation for progeny testing. At least 10 M_{1:2} seedling progeny were inoculated and screened with SCCSC for stem rust infection responses as previously described (Rouse et al. 2011c).

Screening with *Pgt* for *Sr5* and *Sr16*

Mutant progeny were screened with *Pgt* pathogen races avirulent to additional seedling resistance genes in ‘Thatcher’ (*Sr5* and *Sr16*). Using *Pgt* races to screen for additional resistance genes in ‘Thatcher’ can provide added evidence for mutant derivation from ‘Thatcher’. SCCSC elicits a 2+ infection response in the presence of *Sr16* (Figure 1). The *Pgt* race BFBJC (78MNBB463) can be used in ‘Thatcher’ to identify the presence of *Sr5* as it is avirulent to *Sr5* (IT 0 to 0;) and virulent on the remaining ‘Thatcher’ seedling genes; *Sr9g*, *Sr12*, and *Sr16* (Figure 2).

Molecular markers

Sr12 was recently shown by Hiebert et al. (2016) to be closely linked to the SNP marker NB-LRR3. Putative mutants were screened with NB-LRR3 for the SNP allele consistent with the presence of *Sr12* to discern possible contaminants from true mutants in M₁ families. KASP assays were performed using the standard thermocycler protocol and reagent mixture for a 5µL total reaction volume as specified in the KASP product manual

(<http://www.lgcgroup.com/LGCGroup/media/PDFs/Products/Genotyping/KASP-genotyping-chemistry-User-guide.pdf>): 1 cycle at 94°C 15:00 minutes; 10 cycles of 94°C for 20 seconds denaturing, 61-55°C (dropping 0.6°C per cycle) for 60 seconds elongating; 26 cycles 94°C for 20 seconds denaturing, 55°C for 60 seconds elongation; 30°C for 2 minutes to read samples. If further separation between alleles was needed, samples were cycled for an additional 12 cycles at 94°C for 20 seconds denaturing and 55°C for 60 seconds elongation. Fluorescence was read using a StepOnePlus Real-Time PCR System and genotypes were analyzed using StepOne v2.3 software (Applied Biosystems).

Mutants that exhibited an NB-LRR3 allelic state consistent with ‘Thatcher’ and the presence of *Sr12* were tested with additional SNP markers using the wheat 90K Infinium SNP array from Illumina. 1497 SNP markers were used to compare allelic states of each putative *Sr12* mutant and ‘Thatcher’ to one another as an additional measure of mutant similarity. Any mutant exhibiting lower than 95% similarity to ‘Thatcher’ was removed from further analysis. Comparisons of marker similarity were performed in GenomeStudio (GenomeStudio v2011.1, Illumina).

DNA extraction

DNA of the mutant lines were extracted using the protocol described by Edwards et al. (1991) with inclusion of a chloroform separation step: 1) young leaf tissue was collected in 1.5mL microfuge tubes, 2) the tissue was frozen using liquid nitrogen and ground with a pestle. 3) 500 µL of extraction buffer was added to each

tube, the samples were mixed by inversion and spun for 10 minutes at 10,000 rpm, 4) 200 μ L of chloroform was added to each tube, the samples were mixed by inversion and spun for 10 minutes at 10,000 rpm, 5) 300 μ L of the upper aqueous phase was removed, an equal volume of isopropanol was added, and the samples were incubated at room temperature for 5 minutes, 6) the supernatant was removed and 400 μ L of 75% ethanol was added to the pellets, 7) the supernatant was removed and pellets were dried at room temperature by inversion on a Kimwipe (Kimberly-Clark).

Allelism assays

Mutant lines that had been progeny tested and had shown a high degree of genetic similarity to 'Thatcher' wheat were intercrossed to identify allelic groups. 5-10 resulting F_1 progeny were screened at the seedling stage with SCCSC for phenotypes consistent with an *Sr12* knockout. At least 30 F_2 progeny from two F_1 seedlings of each cross were screened for phenotypes consistent with an *Sr12* knockout. *Sr12* has been previously identified as recessive (Mcintosh 1967, Sheen 1964). If *Sr12* is recessive then screening at the F_1 stage can only result in phenotypes consistent with homozygous wild-type *Sr12* if both mutant phenotypes were resultant from different mutations in the *Sr12* resistance response pathway and complementation through hybridization formed a functional metabolic pathway or if both lines used for crossing were heterozygous. Only F_2 allelism testing would truly determine if both mutants are allelic.

Results

SCCSC screening of M_2 families

Of the 600 M_2 families created using NaN_3 and screened with SCCSC, 14 families showed the presence of the stem rust IT 2+, consistent with a knockout mutation in *Sr12*. Of the 1600 M_2 families created with EMS only one family was identified that exhibited a 2+ infection type. No family from either mutagenesis population exhibited the predicted segregation pattern of a knockout mutant in a

recessive gene. In a family segregating for an *Sr12* loss of function allele, the expected segregation of susceptible to resistant lines would be 3:1 susceptible:resistant. However, in only one family the predominant phenotype was IT 2+. Furthermore, family 580-1 only exhibited ITs of 2+ and 3 indicating that this family was likely derived from a contaminant seed planted along with the NaN₃ mutated 'Thatcher' seeds (Table 1).

Progeny verification

The M_{2:3} mutant progeny screened with SCCSC were identified as either heterogeneous or fixed for *Sr12* loss of function (Table 2). IT 3 was not expected for the mutant progeny and no M₁ families with the exception of family 580 segregated for 2 and 3 infection types (Figure 3). The occurrence of the 2+ IT in mutant progeny also indicates the presence of *Sr16*, providing added evidence for derivation from a 'Thatcher' genetic background.

BFBJC screening of mutant progeny

Seedling assays of the mutant progeny using *Pgt* race BFBJC indicated the putative *Sr12* mutants identified through SCCSC screening likely carried the seedling resistance gene *Sr5*. Mutant progeny exhibited a near immune response characteristic of the *Sr5* gene (Figure 4). One mutant line, 179-1, exhibited segregation of susceptible phenotypes of 3 to ;1 indicating a possible mutation of *Sr5*.

NB-LRR3 marker analysis

All mutants with the exception of mutant 580-1 exhibited NB-LRR3 alleles consistent with those observed in 'Thatcher' wheat. In addition, the 580 M₁ family exhibited segregating ITs to SCCSC of 2+ and 3. Such phenotypes could only exist following a homozygous knockout of *Sr12* and heterozygous knockout of *Sr16*. The absence of the proper NBR-LLR3 allele in addition to the unlikely probability that a knockout point mutation would occur simultaneously in two 'Thatcher'

seedling genes was cause for the 580-1 mutant to be removed from further analyses. Line 60-1 exhibited a heterozygous state indicative of either a mutation directly in the KASP oligo binding sequence or possible incursion of foreign pollen during field growth of the M₁ mutants. 60-1 was retained for analysis on the 90K array to definitively identify if cross-pollination had occurred. (Table 3)

Wheat 90K SNP array analysis

Mutants exhibiting SNP alleles consistent with *Sr12* were genotyped using Illumina's 90K Infinium wheat SNP array. Based on SNP alleles, most of the identified mutants shared greater than or equal to 95% similarity to their respective mutagenesis parents: 'Thatcher' and 'TcMn83'. Only mutant 60-1 did not appear to be of the correct genetic background and exhibited only 66 % marker similarity to 'Thatcher' (Table 4). 60-1 was removed from further analyses due to the observed divergence in genetic similarity with 'Thatcher'.

Allelism assays

F₁ allelism assays indicated that *Sr12* behaved in a recessive manner. Control crosses of two mutants to 'Thatcher' using the mutants as the pollen donor resulted in all F₁ progeny exhibiting a 2+ IT (Table 5). Heterozygosity likely exists among the 447-1, 250-1, 31-1, and or 83-1 mutants used to develop the F₁ lines because they resulted in progeny exhibiting 0; resistant IT's. No F₁ progeny were consistently identified as having a resistant phenotype indicating that at least one of the lines used in each cross contained an *Sr12* knockout allele. If no lines used in the crosses possessed an *Sr12* knockout allele and instead carried a mutation in the *Sr12* resistance pathway then complementation would be expected.

F₂ allelism assays also indicated that heterozygosity still remains in the crosses 447-1/250-1, 447-1/35-1, and 31-1/83-1. Chi-squared analyses indicated that they

did not deviate significantly from the ratios of expected susceptible to resistant lines in a population segregating for recessive resistance (Table 6). The cross 150-1/234-1 had one F₂ progeny that exhibited a resistant phenotype. Given the amount of susceptible lines, the singular resistant phenotype likely represents a contaminant seed. Similarly, the cross 179-1/272-1 was observed to have a small amount of resistant F₂ progeny. However, at least 7 resistant lines were observed in the 179-1/272-1 cross, indicating that at least one of the lines in the cross has exhibited heterozygosity despite the statistically significant deviation from the expected segregation ratios for disease resistance. The crosses 'Thatcher'/150-1 and 35-1/234-1 exhibited highly unusual segregation ratios of 0.53 and 0.30 susceptible to resistant lines instead of the expected ratio of 3 susceptible to 1 resistant. This type of segregation is not expected, yet was observed in replicated crosses.

Discussion

15 putative *Sr12* knockout mutants derived from NaN₃ and EMS mutagenesis were identified following screening 600 M₂ 'Thatcher' families and 1600 M₂ 'TcMn83' families based on the presence of a 2+ IT. The number of susceptible lines observed per segregating family were less than the predicted ratio of 3:1 susceptible to resistant lines indicative of a recessive resistance as previously noted for *Sr12* (Mcintosh 1967, Sheen 1964). Two mutant lines, 60-1 and 580-1, were removed from further consideration due to significant deviation of SNP marker similarity to 'Thatcher' (line 60-1) and segregation of IT's inconsistent with a hemizygous *Sr12* knockout or wild-type *Sr16* (line 580-1). The remaining 13 mutants exhibited IT's consistent with a knockout *Sr12* and wild-type *Sr16*.

Progeny testing of the harvested mutants indicate that 8 of 13 mutants may be heterozygous for the recessive wild-type *Sr12* however statistical deviation from the 3:1 ratio of susceptible to resistant lines predicted for a recessive resistance was again observed (P-value < 0.05). Although segregation of mutant progeny phenotypes deviating from predicted ratios were observed, crossing mutants

150-1 and 132-1 to 'Thatcher' using the mutants as a pollen donor resulted in loss of the *Sr12* resistance phenotype indicating a recessive gene action.

F₁ allelism testing also indicated that the identified mutants were heterozygous based on the presence of resistant phenotypes in the 447-1/250-1 and 31-1/83-1 crosses. The resulting F₂ progeny from the crosses 447-1/250-1, 447-1/35-1, 31-1/83-1, 132-1/'Thatcher' also indicated heterozygosity of the mutant lines used for crossing because the resulting progeny followed a segregation ratio indicative of a recessive resistance gene. The cross 150-1/234-1 exhibited no segregation indicating both allelism and homozygosity of the F₁ cross. 'Thatcher'/150-1, 35-1/234-1 however exhibited unexpected ratios of susceptible to resistant lines that are more indicative of a partially dominant or additive gene action. The presence of remaining heterozygosity impairs the ability to differentiate putative loss of function *Sr12* alleles from possible mutations involved in resistance pathways associated with *Sr12*. Further inbreeding of the mutants with recurrent selection for susceptible phenotypes is a necessity to ensure homozygosity of the mutations. All further techniques regarding sequencing and cloning of the mutants requires homozygosity to identify sequence differences between the susceptible mutant allele and the resistant wild type allele.

Future directions

RenSeq will be used in future cloning efforts to identify *Sr12* candidate genes. The RenSeq workflow is able to complement the current mapping of *Sr12* (Rouse et al. 2014, Hiebert et al. 2016) and mutants identified in this study. Hiebert and colleagues (2016) mapped *Sr12* to a 27 Mb region according the 'Chinese Spring' physical map. At least one partial NB-LRR gene was identified within this region according to the draft genome and may be homologous to a candidate gene for *Sr12* in 'Thatcher'. However, partial sequencing of this NB-LRR gene fragment has yet to identify genetic dissimilarities between wild-type *Sr12* and the *Sr12* mutants (data not shown). Steuernagel and colleagues (2016) reported that as the number of

sequenced mutants had increased, the number of shared NB-LRR contigs with mutations had decreased: 39-142 NB-LRR mutations were identified for each mutant, 31 mutations were found in shared contigs when comparing 2 pooled mutants, 2 mutations in shared contigs with 3 mutants, and 2 mutations in shared contigs with 4 mutants with the two shared contigs containing deleterious mutations belonging to the causal gene for their target resistance phenotypes. The current study has identified 12 putative *Sr12* mutants through NaN_3 mutagenesis of 'Thatcher' and one putative *Sr12* mutant through EMS mutagenesis of 'TcMn83'. If *Sr12* has the sequence characteristics of an NB-LRR gene, mutagenesis-assisted RenSeq in conjunction with the mapping populations will allow quick identification and verification of the *Sr12* gene. However, this approach requires *Sr12* to be a NB-LRR gene with a sequence homologous to known genes within the hybridization array. Winfield et al. (2012) report the development of a whole exome capture array for enriched next-gen sequencing that could provide an alternative approach that does not require *Sr12* to be of a specific gene class but does require that it retains homology to known gene space. If the current genome build does not contain the *Sr12* gene then the exome capture array would fail to identify mutant gene candidates. Another tactic may be the MutChromSeq approach of Sánchez-Martín et al. (2016). The MutChromSeq approach uses chromosome flow sorting and high throughput sequencing to sequence a complete chromosome containing your mutation of interest. Comparing the mutant sequence to the wild type creates resolution and confidence similar to that of the RenSeq approach. The requirement is that the chromosome that contains the mutation is known. Both the chromosome and chromosome region is known for *Sr12* based on the results recent mapping experiments (Rouse et al. 2014, Hiebert et al. 2016). Therefore, the MutChromSeq approach proves to be a strong candidate method for cloning *Sr12* because it functions in a manner less consistent with standard resistance genes.

Tables and Figures

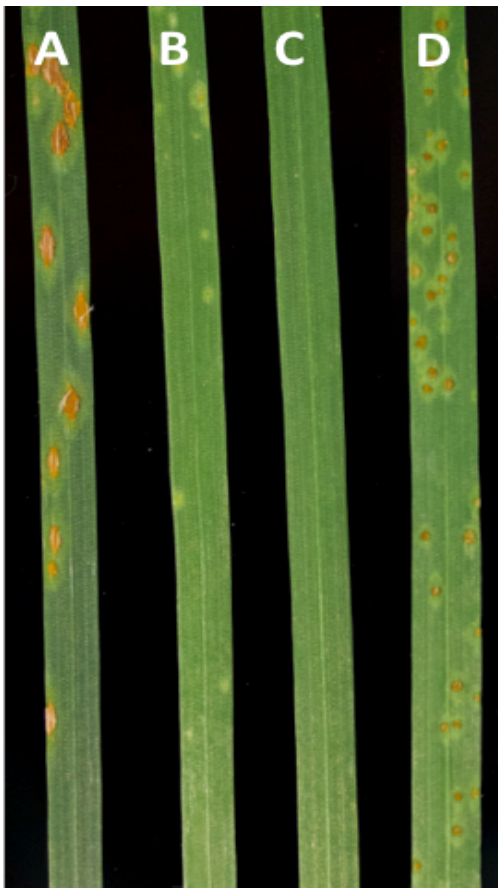


Figure 1: SCCSC infection response for **A)** 'Prelude', **B)** 'Prelude' (+Sr12), **C)** 'Thatcher', and **D)** *Sr16* (ISr-Sr16).



Figure 2: BFBJC infection response for **A)** 'Thatcher', **B)** 'Prelude', **C)** 'Prelude' (+Sr12), **D)** IS-Sr9g, **E)** IS-Sr16, and **F)** IS-Sr5.

Mutagenesis population	Mutant family	# of 2+ IT's per headrow
NaN3	31	1
	35	1
	50	1
	60	2
	83	1
	132	1
	150	4
	179	2
	234	1
	250	2
	272	1
	447	1
	520	2
	580	8
EMS	547	2

Table 1: 'Thatcher' M1 families exhibiting lines indicative of a *Sr12* knockout and the number of observed mutant lines per headrow. Approximately 20 plants were rated for infection type per headrow .



Figure 3: SCCSC infection response on *Sr12* mutants. From left to right; 'Thatcher', 31-1, 35-1, 50-1, 83-1, 132-1, 150-1, 179-1, 234-1, 250-1, 272-1, 447-1, 520-1, and 547-1.

Mutant Line	2+	0;
31-1	19	0
35-1	12	8
50-1	9	2
83-1	20	4
132-1	16	4
150-1	30	1
179-1	25	0
234-1	37	0
250-1	15	2
272-1	19	0
447-1	10	4
520-1	16	2
547-1	20	0

Table 2: Observed IT's to SCCSC for progeny of mutant lines.

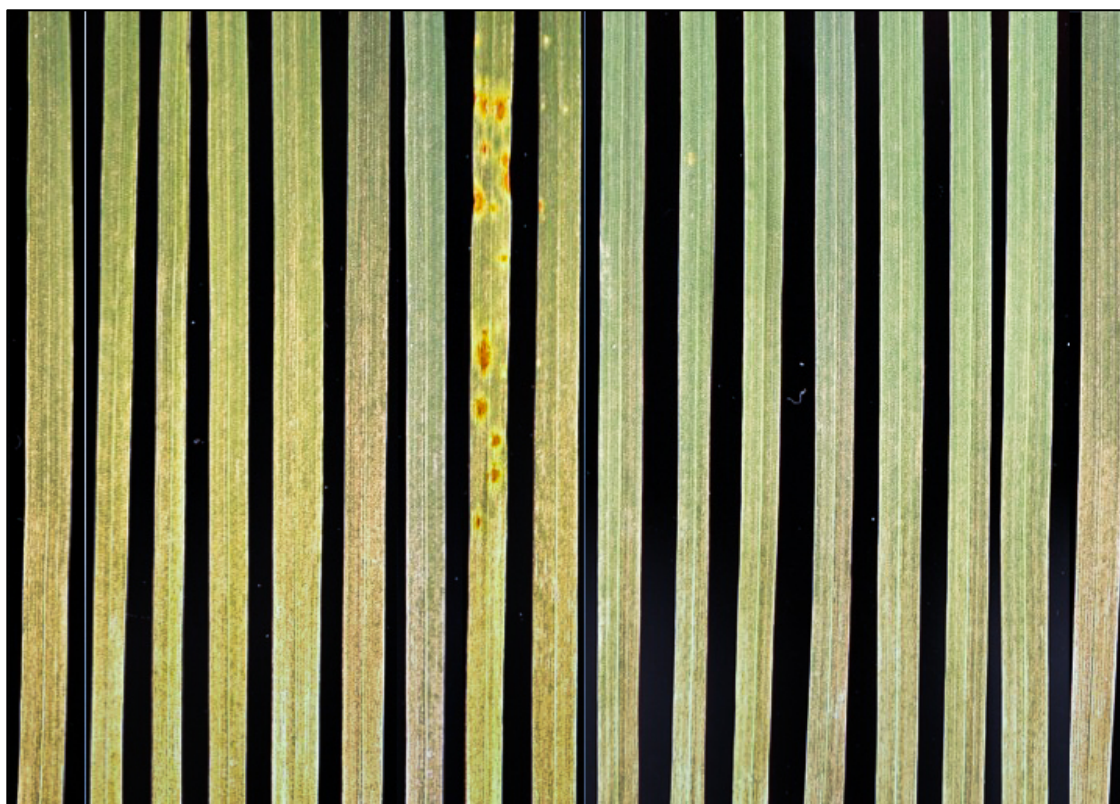


Figure 4: BFBJC infection response on Sr12 mutants. From left to right; 'Thatcher', 31-1, 35-1, 50-1, 83-1, 132-1, 150-1, 179-1 (IT 3), 179-1 (IT ;1), 234-1, 250-1, 272-1, 447-1, 520-1, and 547-1.

<i>Sr12</i> mutant lines	Genetic background	NBLRR3 allele
31-1	'Thatcher'	T/T
35-1	'Thatcher'	T/T
50-1	'Thatcher'	T/T
60-1	'Thatcher'	T/C
83-1	'Thatcher'	T/T
132-1	'Thatcher'	T/T
150-1	'Thatcher'	T/T
179-1	'Thatcher'	T/T
234-1	'Thatcher'	T/T
250-1	'Thatcher'	T/T
272-1	'Thatcher'	T/T
447-1	'Thatcher'	T/T
520-1	'Thatcher'	T/T
580-1	'Thatcher'	C/C
547-1	'TcMn83'	T/T
Parental line		
'Thatcher'	'Thatcher'	T/T
'TcMn83'	'TcMn83'	T/T
'McNeal'	'McNeal'	C/C

Table 3: Results of the NB-LRR3 KASP assay. Allelic state 'T' is consistent with 'Thatcher' and *Sr12*. Allelic state 'C' is consistent with non-*Sr12* lines. Shaded results indicate lines that did not exhibit complete similarity to 'Thatcher' allelic

Parental line	Mutant Line	% similarity to parental line
'Thatcher'	31-1	97.4
	35-1	97.8
	50-1	97.8
	60-1	66.3
	83-1	96.7
	132-1	96.3
	150-1	97.9
	179-1	98.0
	234-1	97.9
	250-1	97.1
	272-1	98.3
	447-1	98.1
	520-1	98.2
'TcMn83'	547-1	100.0

Table 4: Percent similarity of *Sr12* mutants to parental lines based on SNP marker alleles.

F1 Cross	2+	0;
447-1/35-1	8	
447-1/250-1	6	1
31-1/83-1	7	1
179-1/272-1	9	
150-1/234-1	6	
35-1/234-1	9	
Cross (control)		
'Thatcher'/132-1	2	
'Thatcher'/150-1	27	

Table 5: F₁ allelism assay of M₂ *Sr12* mutant crosses. IT 2+ is the expected phenotype for *Sr12* knockout mutants. Segregation of phenotypes indicates possible heterozygosity in *Sr12* mutants.

F2 crosses	Observed IT's		Expected IT's			Chi2 Test
	2+	0;	Total Plants	2+	0;	
447-1/250-1	30	6	36	27	9	0.25
447-1/35-1	60	14	74	55.5	18.5	0.23
35-1/234-1	16	53	69	51.75	17.25	2.81E-23
179-1/272-1	66	7	73	54.75	18.25	2.35E-03
31-1/83-1	53	10	63	47.25	15.75	0.09
150-1/234-1	39	1	40	30	10	1.02E-03
Thatcher/150-1	54	102	156	117	39	2.33E-31
132-1/Thatcher	28	8	36	27	9	0.7

Table 6: Proportion of susceptible (IT 2+) to resistant (IT 0;) progeny of F1 *Sr12* mutant crosses. Chi-squared Tests were used to identify significant deviation from 3:1 susceptible to resistant segregation.

Bibliography

Albar L., Bangratz-Reyser M., Hébrard E., Ndjiondjop M. N., Jones M., Ghesquière A. (2006). Mutations in the *eIF(iso)4G* translation initiation factor confer high resistance of rice to *Rice yellow mottle virus*. *Plant J.*, 47(3): 417-26.

Allen A. M., Barker G. L.A., Berry S. T., Coghill J. A., Gwilliam R., Kirby S., Robinson P., Brenchley R. C., D'Amore R., McKenzie N., Waite D., Hall A., Bevan M., Hall N. and Edwards K. J. (2011). Transcript-specific, single-nucleotide polymorphism discovery and linkage analysis in hexaploid bread wheat (*Triticum aestivum* L.). *Plant Biotech. J.*, 9: 1086–99. doi:10.1111/j.1467-7652.2011.00628.x

Asai S., Mase K., and Yoshioka H. (2010). Role of nitric oxide and reactive oxygen species in disease resistance to necrotrophic pathogens. *Plant Signal. Behav.*, 5: 872-74.

Azzimonti G., Lannou C., Sache I., Goyeau H. (2013). Components of quantitative resistance to leaf rust in wheat cultivars: diversity, variability and specificity. *Plant Pathology*, 62(5): 970-81.

Babiker E. M., Gordon T. C., Chao S., Rouse M. N., Jin Y., Newcomb M., Wanyera R., Bhavani S., and Bonman J. M., (2016). Genetic loci conditioning adult plant resistance to the Ug99 race group and seedling resistance to races TRTTF and TTTTF of the stem rust pathogen in wheat landrace Cltr 15026. *Plant Dis*, XX: XXX-XX. DOI 10.1094/PDIS-10-16-1447-RE

Bai Y., Pavan S., Zheng Z., Zappel N. F., Reinstädler A., Lotti C., De Giovanni C., Ricciardi L., Lindhout P., Visser R., Theres K., and Panstruga R. (2008). Naturally occurring broad-spectrum powdery mildew resistance in a Central American tomato accession is caused by loss of *Mlo* function. *Mol. Plant Microbe Interact.* 21: 30–39.

Bajgain P., Rouse M. N., Bhavani S., and Anderson J. A., (2015). QTL mapping of adult plant resistance to Ug99 stem rust in the spring wheat population RB07/MN06113-8. *Mol. Breeding*, 35: 170. DOI 10.1007/s11032-015-0362-x

Bansal, U. K., Bossolini, E., Miah, H., Keller, B., Park, R. F., and Bariana, H. S. (2008). Genetic mapping of seedling and adult plant stem rust resistance in two European winter wheat cultivars. *Euphytica* 164: 821-28.

Bansal, U. K., Hayden, M. J., Keller, B., Wellings, C. R., Park, R. F., and Bariana, H. S. (2009). Relationship between wheat rust resistance genes Yr1 and Sr48 and a microsatellite marker. *Plant Pathol.* 58: 1039-43.

Barba P., Cadle-Davidson L., Galarneau E., and Reisch B. (2015). *Vitis rupestris* 101

B38 confers isolate-specific quantitative resistance to penetration by *Erysiphe necator*.

Phytopathology, 105: 1097–103.

Bhavani S., Singh R. P., Argillier O., Huerta-Espino J., Singh S., Njau P., Brun S., Lacam S., and Desmouceaux N., (2011). Mapping durable adult plant stem rust resistance to the race Ug99 group in six CIMMYT wheats. *2011 BGRI Technical Workshop*, pp. 43–53.

Bolton M. D., Kolmer J. A., Garvin D. F. (2008). Wheat leaf rust caused by *Puccinia triticina*. *Mol. Plant Pathol.*, 9: 563–75.

Boyd L. A., (2005). Can Robigus defeat an old enemy? – Yellow rust of wheat, *J. Agric. Sci.*, 143(4): 233–43. doi: 10.1017/S0021859605005095.

Boyd L. A., (2006). Can the durability of resistance be predicted? *J. Sci. Food Agric.*, 86: 2523–26. doi:10.1002/jsfa.2648

Boyd L. A., Ridout C., O'Sullivan D. M., Leach J. E., and Leung H., (2012). Plant-pathogen interactions: disease resistance in modern agriculture. *Trends Genet.*, 29(4): 233-40.

Bragg J. N., Wu J., Gordon S. P., Guttman M. E., Thilmony R., Lazo G. R., Gu Y. Q., and Vogel J. P. (2012). Generation and Characterization of the Western Regional Research Center Brachypodium T-DNA Insertional Mutant Collection. *PLoS ONE*, 7(9): e41916. doi:10.1371/journal.pone.0041916.

Broman K. W., Wu H., Sen Ś., and Churchill G.A. (2003) R/qtl: QTL mapping in experimental crosses. *Bioinformatics*, 19: 889-90.

Caillaud M.-C., Lecomte P., Jammes F., Quentin M., Pagnotta S., Andrio Em., de Almeida-Engler J., Marfaing N., Gounon P., Abad P. and Favery B. (2008). MAP65-3 Microtubule-Associated Protein Is Essential for Nematode-Induced Giant Cell Ontogenesis in Arabidopsis. *Plant Cell*, 20(2): 423-37. doi:10.1105/tpc.107.057422.

Camañes G., Pastor V., Cerezo M., García-Andrade J., Vicedo B., García-Agustín P., and Flors V. (2012). A Deletion in NRT2.1 Attenuates *Pseudomonas syringae*-Induced Hormonal Perturbation, Resulting in Primed Plant Defenses. *Plant Physiol.*, 158(2): 1054-66. doi:10.1104/pp.111.184424.

Candresse T., Le Gall O., Maisonneuve B., German-Retana S., Redondo E. (2002). The use of green fluorescent protein-tagged recombinant viruses greatly simplifies *Lettuce mosaic virus* resistance testing in lettuce. *Phytopathology*, 92: 169–76.

Chen X. M. (2005). Epidemiology and control of stripe rust [*Puccinia striiformis* f. sp. *tritici*] on wheat. *Can. J. Plant Pathol.* 27: 314–37.

Calenge F., Faure A., Goerre M., Gebhardt C., Van de Weg W. E., Parisi L., and Durel C.-E. (2004). Quantitative trait loci (QTL) analysis reveals both broad-spectrum and isolate-specific QTL for scab resistance in an apple progeny challenged with eight isolates of *Venturia inaequalis*. *Phytopathology*, 94: 370-79.

Carlisle D. J., Cooke L. R., Watson S., and Brown A. E. (2002). Foliar aggressiveness of Northern Ireland isolates of *Phytophthora infestans* on detached leaflets of three potato cultivars. *Plant Pathol.*, 51: 424-34.

Chandler P. M and Harding C. A. (2013). 'Overgrowth' mutants in barley and wheat: new alleles and phenotypes of the 'Green revolution' DELLA gene. *J. Exp. Bot.*, 64: 1603-13.

Chantret N., Pavoine M. T., Doussinault G. (1999). The race specific resistance gene to powdery mildew, MIRE, has a residual effect on adult plant resistance of winter wheat line RE714. *Phytopathology*, 89: 533-39.
<http://dx.doi.org/10.1094/PHYTO.1999.89.7.533>

Chen H., Wang S., Xing Y., Xu C., Hayes P., and Zhang Q. (2003). Comparative analyses of genomic locations and race specificities of loci for quantitative resistance to *Pyricularia grisea* in rice and barley. *Proc. Natl. Acad. Sci. USA*, 100: 2544-49

Chen, S., Rouse, M. N., Zhang, W., Jin, Y., Akhunov, E., Wei, Y., and Dubcovsky, J. (2015). Fine mapping and characterization of Sr21, a temperature-sensitive diploid wheat resistance gene effective against the Puccinia graminis f. sp. tritici Ug99 race group. *Theor. Appl. Genet.* 128: 645-56.

Choi J. J., Alkharouf N. W., Schneider K. T., Matthews B. F., and Frederick R. D. (2008). Expression patterns in soybean resistant to *Phakopsora pachyrhizi* reveal the importance of peroxidases and lipoxygenases. *Funct. Integr. Genomics*, 8: 341-59.
doi:10.1007/s10142-008-0080-0

Day B., Dahlbeck D., Huang J., Chisholm S. T., Li D., and Staskawicz B. J. (2005). Molecular basis for the *RIN4* negative regulation of *RPS2* disease resistance. *Plant Cell*, 17: 1292-305.

Delledonne M., Xia Y., Dixon R. A., and Lamb C. (1998). Nitric oxide functions as a signal in plant disease resistance. *Nature*, 394: 585-88.

Delledonne M., Zeier J., Marocco A., and Lamb, C. (2001) Signal interactions between nitric oxide and reactive oxygen intermediates in the plant hypersensitive disease resistance. *Proc. Natl Acad. Sci. U.S.A.*, 98: 13454-459.

Diaz-Pendon J. A., Truniger V., Nieto C., Garcia-Mas J., Bendahmane A., and Aranda M. A. (2004). Advances in understanding recessive resistance to plant 103

viruses. *Mol. Plant Pathol.*, 5: 223–33. doi: 10.1111/j.1364-3703.2004.00223.x

Dubcovsky, J., Luo, M., and Dvorak, J. (1995). Differentiation between homoeologous chromosomes 1A of wheat and 1Am of *Triticum monococcum* and its recognition by the wheat Ph1 locus. *Proc. Natl. Acad. Sci.* 92: 6645-49.

Dubcovsky, J., Luo, M.-C., Zhong, G.-Y., Bransteiter, R., Desai, A., Kilian, A., Kleinhofs, A., and Dvorak, J. (1996). Genetic map of diploid wheat, *Triticum monococcum* L., and its comparison with maps of *Hordeum vulgare* L. *Genetics*, 143: 983-99.

Duprat A., Caranta C., Revers F., Menand B., Browning K. S., Robaglia C. (2002). The *Arabidopsis* eukaryotic initiation factor *ISO4E* is dispensable for plant growth but required for susceptibility to potyviruses. *Plant J.*, 32: 927–34. doi: 10.1046/j.1365-313X.2002.01481.x.

Durner J., Wendehenne D., Klessig D. F. (1998). Defense gene induction in tobacco by nitric oxide, cyclic GMP, and cyclic ADP-ribose. *Proc. Natl. Acad. Sci. U.S.A.*, 95: 10328–333. 10.1073/pnas.95.17.10328.

Dvorak, J. (1976). The relationship between the genome of *Triticum urartu* and the A and B genomes of *Triticum aestivum*. *Can. J. Genet. Cytol.* 18: 371-77.

Dyck, P. L. (1992). Transfer of a gene for stem rust resistance from *Triticum araraticum* to hexaploid wheat. *Genome*, 35: 788-92.

Eckardt N. A. (2002). Plant disease susceptibility genes? *Plant Cell* 14: 1983–86.

Edwards K., Johnstone C., and Thompson C. (1991). A simple and rapid method for preparation of plant genomic DNA for PCR analysis. *Nucleic Acids Res.*, 19: 1349.

Edwards H. H. and Bonde M. R. (2011). Penetration and establishment of *Phakopsora pachyrhizi* in soybean leaves as observed by transmission electron microscopy. *Phytopathology*, 101: 894-900. doi:10.1094/PHYTO-09-10-0248.

Ellis J. G., Lagudah E. S., Spielmeyer W., Dodds P.N. (2014). The past, present and future of breeding rust resistant wheat. *Front. Plant Sci.*, 5: 641.

FAO. 2013. Wheat-world yield totals. Online Publication. <http://faostat3.fao.org/faostat-gateway/go/to/download/Q/QC/E>

Faris, J. D., Xu, S. S., Cai, X., Friesen, T. L., and Jin, Y. (2008). Molecular and cytogenetic characterization of a durum wheat *Aegilops speltoides* chromosome translocation conferring resistance to stem rust. *Chromosome Res.*, 16: 1097-105.

Fung R. W., Gonzalo M., Fekete C., Kovacs L. G., He Y., Marsh E., McIntyre L. M., Schachtman D. P., and Qiu W. (2008). Powdery mildew induces defense-oriented reprogramming of the transcriptome in a susceptible but not in a

resistant grapevine. *Plant Physiol.*, 146: 236–49. doi: 10.1104/pp.107.108712

Figuerola M., Alderman S., Garvin D. F., and Pfender W. F. (2013). Infection of *Brachypodium distachyon* by Formae Speciales of *Puccinia graminis*: Early Infection Events and Host-Pathogen Incompatibility. Xu M., ed. *PLoS ONE*, 8(2):e56857. doi:10.1371/journal.pone.0056857.

Gao X., Brodhagen M., Isakeit T., Brown S. H., Göbel C., Betran J., Feussner I., Keller N. P., and Kolomiets M. V. (2009). Inactivation of the lipoxygenase *ZmLOX3* increases susceptibility of maize to *Aspergillus* spp. *Mol. Plant Microbe Interact.*, 22: 222-31.

Gao L., Turner M. K., Chao S., Kolmer J., Anderson J. A. (2016). Genome Wide Association Study of Seedling and Adult Plant Leaf Rust Resistance in Elite Spring Wheat Breeding Lines. *PLoS ONE* 11(2):e0148671. doi:10.1371/journal.pone.0148671

Garnica D., Upadhyaya N., Dodds P., and Rathjen J. (2013). Strategies for wheat stripe rust pathogenicity identified by transcriptome sequencing. *PLoS ONE*, 8:e67150. doi: 10.1371/journal.pone.0067150.

Gaspar Y. M., Nam J., Schultz C. J., Lee L. Y., Gilson P. R., Gelvin S. B., and Bacic A. (2004). Characterization of the Arabidopsis lysine-rich arabinogalactan-protein *AtAGP17* mutant (*rat1*) that results in a decreased efficiency of *agrobacterium* transformation. *Plant Physiol.*, 135(4): 2162-71.

Gerechter-Amitai, Z. K., Wahl, I., Vardi, A., and Zohary, D. (1971). Transfer of stem rust seedling resistance from wild diploid einkorn to tetraploid durum wheat by means of a triploid hybrid bridge. *Euphytica*, 2: 281-85.

Giorgi, B., and Bozzini, A. (1969). Karyotype analysis in Triticum I. Analysis of Triticum turgidum (L.) Thell. and some related tetraploid wheats. *Caryologia* 22: 249-58.

Goellner M., Wang X., and Davis E. (2001). Endo- β -1,4-Glucanase Expression in Compatible Plant–Nematode Interactions. *Plant Cell*, 13(10): 2241-56. doi: 10.1105/tpc.010219

Goodstein D. M., Shu S., Howson R., Neupane R., Hayes R. D., Fazo J., Mitros T., Dirks W., Hellsten U., Putnam N., and Rokhsar D. S., (2012). Phytozome: a comparative platform for green plant genomics, *Nucleic Acids Res.*, 40 (D1): 1178-86

Green A. J., Berger G., Griffey C.A., Pitman R., Thomason W. and Balota M. (2014). Genetic resistance to and effect of leaf rust and powdery mildew on yield and its components in 50 soft red winter wheat cultivars. *Crop Protection*, 64: 177–86.

Guerrero-Chavez R., Glover K. D., Rouse M. N., and Gonzalez-Hernandez J. L. 105

(2015). Mapping of two loci conferring resistance to wheat stem rust pathogen races TTKSK (Ug99) and TRTTF in the elite hard red spring wheat line SD4279. *Mol. Breeding*, 35: 8 DOI 10.1007/s11032-015-0198-4.

Gupta K. J., Fernie A. R., Kaiser W. M., van Dongen J. T. (2011). On the origins of nitric oxide. *Trends Plant Sci.*, 16: 160–68. 10.1016/j.tplants.2010.11.007.

KBioscience (2009). PrimerPicker Lite for KASPar v.0.26. KBioscience Ltd, Hoddesdon

Hayes H.K., Ausemus E.R., Stakman E.C., Bailey C.H., Wilson H.K., Bamberg R.H., Markley M.C., Crim R.F., and Levine M.N. (1936). Thatcher Wheat. Minnesota Agricultural Experiment Station. Retrieved from the University of Minnesota Digital Conservancy, <http://hdl.handle.net/11299/163794>.

Hewezi T., Howe P., Maier T. R., Hussey R. S., Mitchum M. G., Davis E. L., and Baum T. J. (2008). Cellulose Binding Protein from the Parasitic Nematode *Heterodera schachtii* Interacts with *Arabidopsis* Pectin Methylesterase: Cooperative Cell Wall Modification during Parasitism. *Plant Cell*, 20(11): 3080–93. doi: 10.1105/tpc.108.063065.

Hiebert C. W., Kolmer J. A., McCartney C. A., Briggs J., Fetch T., Bariana H., Choulet F., Rouse M. N., and Spielmeier W. (2016). Major Gene for Field Stem Rust Resistance Co-Locates with Resistance Gene Sr12 in ‘Thatcher’ Wheat. *PLoS ONE*, 11(6): e0157029.

Hooker A. L. (1962). Corn leaf diseases. *Proc. 17th Annu. Hybrid Corn Ind. Res. Conf.*, pp. 24–36.

Houterman P. M., Cornelissen B. J. C., Rep M. (2008). Suppression of Plant Resistance Gene-Based Immunity by a Fungal Effector. *PLoS Pathog.*, 4(5): e1000061. doi:10.1371/journal.ppat.1000061

Huckelhoven R. (2007). Cell wall-associated mechanisms of disease resistance and susceptibility. *Annu. Rev. Phytopathol.*, 45: 101–27.

Humphry M., Reinstädler A., Ivanov S., Bisseling T., and Panstruga R. (2011). Durable broad-spectrum powdery mildew resistance in pea *er1* plants is conferred by natural loss-of-function mutations in *PsML01*. *Mol. Plant Pathol.*, 12: 866–78.

Jin, Y., and Singh, R. P. (2006). Resistance in U.S. wheat to recent Eastern African isolates of *Puccinia graminis* f. sp. *tritici* with virulence to resistance gene Sr31. *Plant Dis.*, 90: 476-80.

Jin, Y., Szabo, L. J., Pretorius, Z. A., Singh, R. P., Ward, R., and Fetch, T., Jr. (2008). Detection of virulence to resistance gene Sr24 within race TTKS of *Puccinia*

graminis f. sp. tritici. *Plant Dis.*, 92: 923-26.

Jin Y., Szabo L. J., Rouse M. N., Fetch T. Jr, Pretorius Z. A., Wanyera R., and Njau P. (2009). Detection of virulence to resistance gene Sr36 within the TTKS race lineage of *Puccinia graminis* f. sp. tritici. *Plant Dis.*, 93: 367–70.

Johnson T. (1961). Man-guided evolution in plant rusts. *Science*, 133: 357–62.

Johnson, B. L., and Dhaliwal, H. S. (1976). Reproductive isolation of *Triticum boeoticum* and *Triticum urartu* and the origin of the tetraploid wheats. *Am. J. Bot.*, 63: 1088-94.

Jupe F., Witek K., Verweij W., Sliwka J., Leighton P., Etherington G. J., Maclean D., Cock P. J., Leggett R. M., Bryan G. J., Milne L., Hein I., and Jones J. D. G. (2013). Resistance gene enrichment sequencing (RenSeq) enables re-annotation of the NB-LRR gene family from sequenced plant genomes and rapid mapping of resistance loci in segregating populations. *Plant J.*, 76: 530–44.

Kerber, E. R., and Dyck, P. L. (1979). Resistance to stem and leaf rust of wheat in *Aegilops squarrosa* and transfer of a gene for stem rust resistance to hexaploid wheat. *Proc. 5th International Wheat Genetics Symposium*, New Delhi, India.

Kerber, E. R., and Dyck, P. L. (1990). Transfer to hexaploid wheat of linked genes for adult-plant leaf rust and seedling stem rust resistance from amphiploid of *Aegilops speltoides* × *Triticum monococcum*. *Genome*, 33: 530-37.

King Z. R., Harris D. K., Wood E. D., Buck J. W., Boerma H. R., and Li. Z. (2016). Registration of Four Near-Isogenic Soybean Lines of G00-3213 for Resistance to Asian Soybean Rust. *J. Plant. Reg.*, 10: 189-94. doi:10.3198/jpr2015.04.0027crg.

Kleinhofs A, Kilian A, Saghai MA, Biyashev RM, Hayes P, Chen FQ, Lapitan N, Fenwick A, Blake TK, Kanazin V (1993) A molecular, isozyme and morphological map of the barley (*Hordeum vulgare*) genome. *Theor. Appl. Genet.*, 86: 705–12.

Knott DR (1990) Near-isogenic lines of wheat carrying genes for stem rust resistance. *Crop Sci.*, 30: 901–05.

Knott D.R. (2000). The inheritance of stem rust resistance in Thatcher wheat. *Can. J. Plant Sci.*, 80: 53–63.

Knott D.R. (2001). The relationship between seedling and field resistance to two races of stem rust in Thatcher wheat. *Can. J. Plant Sci.*, 81: 415–18.

Koch M. F. and Mew T. W. (1991). Effects of plant age and leaf maturity on the quantitative resistance of rice cultivars to *Xanthomonas campestris* pv. *oryzae*. *Plant Dis.*, 75: 901-04.

Kolmer J. A., Garvin D. F., and Yin J. (2011). Expression of a Thatcher wheat adult plant stem rust resistance QTL on chromosome arm 2BL is enhanced by Lr34. *Crop Sci.*, 51: 526–33. doi: 10.2135/cropsci2010.06.0381.

La Mantia J., Klapste J., El-Kassabi Y. A., Azam S., Guy R. D., Douglas C. J., Mansfield S. D., and Hamelin R. (2013). Association analysis identifies *Melampsora xcolumbiana* poplar leaf rust resistance SNPs. *PLoS One*, 8:e78423.

Lander, E. S., Green, P., Abrahamson, J., Barlow, A., Daly, M. J., Lincoln, S. E., and Newburg, L. (1987). MAPMAKER: An interactive computer package for constructing primary genetic linkage maps of experimental and natural populations. *Genomics*, 1: 174-81.

Lellis A. D., Kasschau K. D., Whitham S. A., and Carrington J. C. (2002). Loss-of-susceptibility mutants of *Arabidopsis thaliana* reveal an essential role for *elfISO4E* during potyvirus infection. *Curr. Biol.*, 12:1046–51. doi: 10.1016/S0960-9822(02)00898-9.

Leonard, K. J. (2001). Stem rust: future enemy? in: Stem Rust of Wheat: From Ancient Enemy to Modern Foe, pp. 119-146. P. D. Peterson, ed. American Phytopathological Society, St. Paul, MN.

Li Z. K., Luo L. J., Mei H. W. Paterson A. H., Zhao X. Z., Zhong D. B., Wang Y. P., Yu X. Q., Zhu L., Tabien R., Stansel J. W. and Ying C. S. (1999). A “defeated” rice resistance gene acts as a QTL against a virulent strain of *Xanthomonas oryzae* pv. *oryzae*. *Mol. Gen. Genet.*, 261: 58–63. DOI: 10.1007/s004380050941.

Li Z. K., Arif M., Zhong D. B., Fu B. Y., Xu J. L., Domingo-Rey J., Ali J., Vijayakumar C. H., Yu S. B., Khush G. S. (2006). Complex genetic networks underlying the defensive system of rice (*Oryza sativa* L.) to *Xanthomonas oryzae* pv. *oryzae*. *Proc. Natl. Acad. Sci. USA*, 103(21): 7994–99.

Ling K. S., Harris K. R.; Meyer J. D., Levi A., Guner N., Wehner T.C., Bendahmane A., and Havey M.J. (2009) Non-synonymous single nucleotide polymorphisms in the watermelon *elf4E* gene are closely associated with resistance to *zucchini yellow mosaic virus*. *Theor. Appl. Genet.*, 120: 191–200.

Liu, R., and Meng, J. (2003.) MapDraw: A Microsoft Excel macro for drawing genetic linkage maps based on given genetic linkage data. *Hereditas*, 25: 317-321.
Lorieux M (2012) MapDisto: fast and efficient computation of genetic linkage maps. *Mol. Breeding*, 30: 1231-1235 (DOI 10.1007/s11032-012-9706-y)

Luo, M.-C., Dubcovsky, J., and Dvorak, J. (1996). Recognition of homology by the wheat Ph1 locus. *Genetics*, 144: 1195-203.

Maccaferri M., Ricci A., Salvi S., Milner S. G., Noli E., Martelli P. L., Casadio R., Akhunov E., Scalabrin S., Vendramin V., Ammar K., Blanco A., Desiderio F., Distelfeld A., Dubcovsky J., Fahima T., Faris J., Korol A., Massi A., Mastrangelo A., Morgante M., Pozniak C., Xu S., and Tuberosa R. (2015). A high-density, SNP-based consensus map of tetraploid wheat as a bridge to integrate durum and bread wheat genomics and breeding. *Plant Biotech. J.*, 13(5): 648-63.

Marais, G. F., Wessels, W. G., Horn, M., and du Toit, F. (1998). Association of a stem rust resistance gene (Sr45) and two Russian wheat aphid resistance genes (Dn5 and Dn7) with mapped structural loci in common wheat. *S. Afr. J. Plant Soil*, 15: 67-71.

Marcel T. C., Gorguet B., Ta M. T., Kohutova Z., Vels A., Niks R. E. (2008). Isolate specificity of quantitative trait loci for partial resistance of barley to *Puccinia hordei* confirmed in mapping populations and near-isogenic lines. *New Phytol.*, 177: 743–55.

McIntosh R. A., Luig N. H., and Baker E.P. (1967). Genetic and cytogenetic studies of stem rust, leaf rust, and powdery mildew resistances in Hope and related wheat cultivars. *Aust. J. Biol. Sci.*, 20: 1181-92.

McIntosh, R. A., and Gyrfas, J. (1971). *Triticum timopheevi* as a source of resistance to wheat stem rust. *Zeit. Pflaz.*, 66: 240-48.

McIntosh, R. A., Dyck, P. L., The, T. T., Cusick, J., and Milne, D. L. (1984). Cytogenetical studies in wheat. XIII. Sr35_a 3rd gene from *Triticum monococcum* for resistance to *Puccinia graminis tritici*. *Zeit. Pflaz.*, 92: 1-14.

McIntosh, R. A., Wellings, C. R., and Park, R. F. (1995). *Wheat Rusts: An Atlas of Resistance Genes*. CSIRO Publications, East Melbourne, Australia.

McIntosh, R. A., Yamazaki, Y., Dubcovsky, J., Rogers, J., Morris, C., Appels, R., and Xia, X. C. (2013). Catalogue of gene symbols for wheat.
<http://www.shigen.nig.ac.jp/wheat/komugi/genes/macgene/2013/GeneSymbol.pdf>

Mergoum M., Frohberg R. C., Stack R. W., Rasmussen J. W., Friesen T. L. (2008). Registration of ‘Faller’ spring wheat. *J. Plant Regist.*, 2(3): 224–29.

Modolo L. V., Augusto O., Almeida I. M. G., Pinto-Maglio C. A. F., Oliveira H. C., Seligman K., and Salgado I. (2006). Decreased arginine and nitrite levels in nitrate reductase-deficient *Arabidopsis thaliana* plants impair nitric oxide synthesis and the hypersensitive response to *Pseudomonas syringae*. *Plant Sci.*, 171: 34-40.

Morrissey J. P., and Osbourn A. E. (1999). Fungal resistance to plant antibiotics as a mechanism of pathogenesis. *Microbiol. Mol. Biol. Rev.* 63: 708–24. 109

Mueller A. N., Ziemann S., Treitschke S., Assmann D. and Doehlemann G. (2013). Compatibility in the Ustilago maydis–maize interaction requires inhibition of host cysteine proteases by the fungal effector Pit2. *PLoS Pathog* 9:e1003177.

Nath, J., Hanzel, J. J., Thompson, J. P., and McNay, J. W. (1984). Additional evidence implicating Triticum searsii as the B-genome donor to wheat. *Biochem. Genet.*, 22: 37-50.

Nazareno N.R.X. and Roelfs A.P. (1981) Adult plant resistance of Thatcher wheat to stemrust. *Phytopathology*, 71: 181-85.

Newcomb M., Olivera P. D., Rouse M. N., Szabo L. J., Johnson J., Gale S., Luster D. G., Wanyera R., Macharia G., Bhavani S., Hodson D., Patpour M., Hovmøller M. S., Fetch T. G. Jr., and Jin Y. (2016). Kenyan isolates of *Puccinia graminis* f. sp. *tritici* from 2008 to 2014: Virulence to *SrTmp* in the Ug99 race group and implications for breeding programs. *Phytopathology*, 106(7): 729-36.

Nicaise V., German-Retana S., Sanjuán R., Dubrana M-P., Mazier M., Maisonneuve B., Candresse T., Caranta C., and LeGall O. (2003). The eukaryotic translation initiation factor 4E controls lettuce susceptibility to the potyvirus *Lettuce mosaic virus*. *Plant Physiol.*, 132: 1272–82.

Oh S. K., Baek K. H., Park J. M., Yi S. Y., Yu S. H., Kamoun S., Choi D., (2008). Capsicum annuum WRKY protein CaWRKY1 is a negative regulator of pathogen defense. *New Phytol.*, 177: 977–989.

Oliveira H. C., Justino G. C., Sodek L., and Salgado I. (2009). Amino acid recovery does not prevent susceptibility to *Pseudomonas syringae* in nitrate reductase double-deficient *Arabidopsis thaliana* plants. *Plant Sci.*, 176: 105-11.

Olivera P., Newcomb M., Szabo L. J., Rouse M. N., Johnson J., Gale S., Luster D. G., Hodson D., Cox J. A., Burgin L., Hort M., Gilligan C. A., Patpour M., Justesen A. F., Hovmøller M. S., Woldeab G., Hailu E., Hundie B., Tadesse K., Pumphrey M., Singh R. P., and Jin Y. (2015). Phenotypic and genotypic characterization of race TKTTF of *Puccinia graminis* f. sp. *tritici* that caused a wheat stem rust epidemic in southern Ethiopia in 2013-14. *Phytopathology*, 105(7): 917-28.

Olson, E. L., Rouse, M. N., Pumphrey, M. O., Bowden, R. L., Gill, B. S., and Poland, J. A. (2013a). Simultaneous transfer, introgression, and genomic localization of genes for resistance to stem rust race TTKSK (Ug99) from *Aegilops tauschii* to wheat. *Theor. Appl. Genet.*, 126: 1179-88.

Olson, E. L., Rouse, M. N., Pumphrey, M. O., Bowden, R. L., Gill, B. S., and Poland, J. A. (2013b). Introgression of stem rust resistance genes SrTA10187 and SrTA10171 from *Aegilops tauschii* to wheat. *Theor. Appl. Genet.*, 126: 2477-84. 110

Panter S. N., and Jones D. A. (2002). Age-related resistance to plant pathogens. *Advances in Botanical Research incorporating Advance in Plant Pathol.*, 38: 251-80.

Parlevliet J.E. (2002). Durability of resistance against fungal, bacterial and viral pathogens; present situation. *Euphytica*, 124: 147-56.

Patpour M., Hovmøller M. S., Justesen A. F., Newcom M., Olivera P., Jin Y., Szabo L. J., Hodson D., Shahin A. A., Wanyera R., Habarurema I., and Wobibi S. (2015). Emergence of Virulence to *SrTm*p in the Ug99 Race Group of Wheat Stem Rust, *Puccinia graminis* f. sp. *tritici*, in Africa. *Plant Dis.*, 105(2): 522.
<http://dx.doi.org/10.1094/PDIS-06-15-0668-PDN>

Pavan S., Jacobsen E., Visser R. G. F., and Bai Y. (2010). Loss of susceptibility as a novel breeding strategy for durable and broad-spectrum resistance. *Mol. Breeding*, 25(1): 1-12. doi:10.1007/s11032-009-9323-6.

Pavan S., Schiavulli A., Appiano M., Marcotrigiano A. R., Cillo F., Visser R. G. F., Bai Y., Lotti C., and Ricciardi L. (2011). Pea powdery mildew *er1* resistance is associated to loss-of-function mutations at a MLO homologous locus. *Theor. Appl. Genet.*, 123: 1425-31. doi: 10.1007/s00122-011-1677-6.

Perchepped L., Balagué C., Riou C., Claudel-Renard C., Rivière N., Grezes-Besset B., and Roby D. (2010). Nitric oxide participates in the complex Interplay of defense-related signaling pathways controlling disease resistance to *Sclerotinia sclerotiorum* in *Arabidopsis thaliana*. *Mol. Plant-Microbe Interact.*, 23: 846-60.

Periyannan S., Moore J., Ayliffe M., Bansal U., Wang X., Deal K., Luo M., Kong X., Bariana H., Mago R., McIntosh R., Dodds P., Dvorak J., and Lagudah E. (2013). The gene *Sr33*, an ortholog of barley *Mla* genes, encodes resistance to wheat stem rust race Ug99. *Science*, 341: 786-88.

Periyannan S. K., Bansal U. K., and Bariana H. S. (2011). A robust molecular marker for the detection of shortened introgressed segment carrying the stem rust resistance gene *Sr22* in common wheat. *Theor. Appl. Genet.*, 122: 1-7.

Peterson P. D., Leonard K. J., Roelfs A. P., and Sutton T. B. (2005). Effect of barberry eradication on changes in populations of *Puccinia graminis* in Minnesota. *Plant Dis.*, 89: 935-40.

Pham T. A., Miles M. R., Frederick R. D., Hill C. B., and Hartman G. L., (2009). Differential responses of resistant soybean entries to isolates of *Phakopsora pachyrhizi*. *Plant Dis.*, 93: 224-28.

Pike S., Gao F., Kim M. J., Kim S. H., Schachtman D. P., Gassmann W. (2014). Members of the NPF3 transporter subfamily encode pathogen-inducible

nitrate/nitrite transporters in grapevine and Arabidopsis. *Plant Cell Physiol.*, 55: 162-70.

Poland JA, Balint-Kurti PJ, Wisser RJ, Pratt RC, Nelson RJ. (2009). Shades of gray: the world of quantitative disease resistance. *Trends Plant Sci.*, 14:21–29

Pretorius Z. A., Rijkenberg F. H. J., and Wilcoxson R. D. (1988). Effects of growth stage, leaf position, and temperature on adult-plant resistance of wheat infected by *Puccinia recondita* f.sp. *tritici*. *Plant Pathol.*, 37: 36-44.

Pretorius Z. A., Singh R. P., Wagoire W. W., and Payne T. S. (2000). Detection of Virulence to Wheat Stem Rust Resistance Gene Sr31 in *Puccinia graminis* f. sp. *tritici* in Uganda. *Plant Dis.* 84(2): 203.

Pretorius, Z. A., Szabo, L. J., Boshoff, W. H. P., Herselman, L., and Visser, B. (2012). First report of a new TTKSF race of wheat stem rust (*Puccinia graminis* f. sp. *tritici*) in South Africa and Zimbabwe. *Plant Dis.*, 96: 590.

Rietman H., Bijsterbosch G., Cano L. M., Lee H. R., Vossen J. H., Jacobsen E., Visser R. G., Kamoun S., and Vleeshouwers V. G. (2012). Qualitative and quantitative late blight resistance in the potato cultivar Sarpo Mira is determined by the perception of five distinct RXLR effectors. *Mol. Plant Microbe Interact.*, 25: 910–19. doi: 10.1094/MPMI-01-12-0010-R.

Rasul S., Dubreuil-Maurizi C., Lamotte O., Koen E., Poinssot B., Alcaraz G., Wendehenne D., and Jeandroz S. (2012). Nitric oxide production mediates oligogalacturonide-triggered immunity and resistance to *Botrytis cinerea* in *Arabidopsis thaliana*. *Plant Cell Environ.*, 35: 483–99.

Rockel P., Strube F., Rockel A., Wildt J. and Kaiser W.M. (2002). Regulation of nitric oxide (NO) production by plant nitrate reductase in vivo and in vitro. *J. Exp. Bot.*, 53: 103–10.

Röder, M. S., Korzun, V., and Wendehake, K. (1998). A microsatellite map of wheat. *Genetics*, 149: 2007-23.

Rodriguez-Ardon R., Scott G. E. and King S. B. (1980). Maize Yield Losses Caused by Southern Corn Rust. *Crop Science*, 20(6): 812-14. doi: 10.2135/cropsci1980.0011183X002000060035x

Roelfs, A. P. (1978). Estimated losses caused by rust in small grain cereals in the United States_1918-76. U.S. Dept. Agric. Agric. Res. Serv., Misc. Publ. 1363.

Roelfs, A. P. (1982). Effects of barberry eradication on stem rust in the United States. *Plant Dis.*, 66: 177-81.

Roelfs, A. P. (1985). Wheat and rye stem rust. In: The Cereal Rusts Vol. II; Diseases, Distribution, Epidemiology, and Control. pp. 22-29. A. P. Roelfs and W. R. Bushnell, eds. Academic Press Inc., Orlando, FL.

Roelfs A. P., Singh R. P., and Saari E. E., (1992). *Rust Diseases of Wheat: Concepts and Methods of Disease Management*. Mexico, DF: CIMMYT.

Rouse, M. N., and Jin, Y. (2011a). Genetics of resistance to race TTKSK of *Puccinia graminis* f. sp. *tritici* in *Triticum monococcum*. *Phytopathology*, 101: 1418-23.

Rouse, M. N., and Jin, Y. (2011b). Stem rust resistance in A-genome diploid relatives of wheat. *Plant Dis.* 95: 941-44.

Rouse M. N., Wanyera R., Njau P., and Jin Y. (2011c). Sources of resistance to stem rust race Ug99 in spring wheat germplasm. *Plant Dis.* 95: 762-66.

Rouse, M. N., Nirmala, J., Jin, Y., Chao, S., Fetch, T. G., Jr., Pretorius, Z. A., and Hiebert, C. W. (2014). Characterization of Sr9h, a wheat stem rust resistance allele effective to Ug99. *Theor. Appl. Genet.*, 127: 1681-88.

Rouse, M. N., Wanyera, R., Njau, P., and Jin, Y. (2011). Sources of resistance to stem rust race Ug99 in spring wheat germplasm. *Plant Dis.*, 95: 762-66. doi:10.1094/PDIS-12-10-0940

Rouse M. N., Talbert L. E., Singh D., Sherman J. D. (2014) Complementary epistasis involving Sr12 explains adult resistance to stem rust in Thatcher wheat (*Triticum aestivum* L.) *Theor. Appl. Genet.*, 127(7): 1549-59. doi:10.1007/s00122-014-2319-6.

Ruffel S., Dussault M. H., Palloix A., Moury B., Bendahmane A., Robaglia C., and Caranta C. (2002). A natural recessive resistance gene against potato virus Y in pepper corresponds to the eukaryotic initiation factor 4E (eIF4E). *Plant J.*, 32(6): 1067-75.

Russell W. A. (1965). Effect of corn leaf rust on grain yield and moisture in corn. *Crop Sci.*, 5: 95-96.

Rutkoski J. E., Poland J. A., Singh R. P., Huerta-Espino J., Bhavani S., Barbier H., Rouse M. N., Luc Jannink J., Sorrells, and M. E. (2014). Genomic selection for quantitative adult plant stem rust resistance in wheat. *Plant Gen.*, 7: 1-10.

Saintenac, C., Zhang, W., Salcedo, A., Rouse, M. N., Trick, H. N., Akhunov, E., and Dubcovsky, J. (2013). Identification of wheat gene Sr35 that confers resistance to Ug99 stem rust race group. *Science*, 341: 783-86.

Vrána J., Kubaláková M., Krattinger S. G., Wicker T., Doležel J., Keller B., and Wulff B. H. (2016). Rapid gene isolation in barley and wheat by mutant chromosome sequencing. *Genome Biol.*, 17: 221, doi: 10.1186/s13059-016-1082-1

Sato M., Nakahara K., Yoshii M., Ishikawa M. and Uyeda I. (2005). Selective involvement of members of the eukaryotic initiation factor 4E family in the infection of *Arabidopsis thaliana* by potyviruses, *FEBS Letters*, 579, doi: 10.1016/j.febslet.2004.12.086

Schneider K. T., Van de Mortel M., Bancroft T. J., Braun E., Nettleton D., Nelson R. T., Frederick R. D., Baum T. J., Graham M. A., and Whitham S. A. (2011) Biphasic gene expression changes elicited by *Phakopsora pachyrhizi* in soybean correlate with fungal penetration and haustoria formation. *Plant Physiol.*, 157: 355–71.

Sharma, R. K., Singh, P. K., Vinod, Joshi, A. K., Bhardwaj, S. C., Bains, N. S., and Singh, S. (2013). Protecting South Asian wheat production from stem rust (Ug99) epidemic. *J. Phytopathol.*, 161: 299-307.

Sheen, S.J., and L.A. Snyder. (1964). Studies on the inheritance of resistance to six stem rust cultures using chromosome substitution lines of a Marquis wheat selection. *Can. J. Genet. Cytol.*, 6: 74-82.

Shi F. M., and Li Y. Z. (2008). *Verticillium dahliae* toxins-induced nitric oxide production in *Arabidopsis* is major dependent on nitrate reductase. *BMB Rep.*, 41: 79-85.

Singh, R. P., Hodson, D. P., Huerta-Espino, J., Jin, Y., Bhavani, S., Njau, P., Herrera-Foessel, S., Singh, P. K., Singh, S., and Govinda, V. (2011). The emergence of Ug99 races of stem rust fungus is a threat to world wheat production. *Annu. Rev. Phytopathol.*, 49: 465-81.

Singh R. P., Herrera-Foessel S., Huerta-Espino J., Singh S., Bhavani S., Lan C., and Basnet B. R. (2014). Progress towards genetics and breeding for minor genes based resistance to Ug99 and other rusts in CIMMYT high-yielding spring wheat. *J. Integr. Agric.*, 13: 255-61.

Somers, D. J., Isaac, P., and Edwards, K. (2004). A high density microsatellite consensus map for bread wheat (*Triticum aestivum* L.). *Theor. Appl. Genet.* 109: 1105-14.

Song, Q. J., Shi, J. R., Singh, S., Fickus, E. W., Costa, J. M., Lewis, J., Gill, B. S., Ward, R., and Cregan, P. B. (2005). Development and mapping of microsatellite (SSR) markers in wheat. *Theor. Appl. Genet.* 110: 550-60.

Spanu P. D. (2012). The genomics of obligate (and nonobligate) biotrophs.

Annu Rev Phytopathol., 50: 91–109.

Stakman, E. C., Stewart, D. M., and Loegering, W. Q. (1962). Identification of physiological races of *Puccinia graminis* var. *tritici*. U.S. Dept. Agric. Agric. Res. Serv. E-617.

Steffenson B. J., Zhou H., Chai Y., and Grando S. (2013). Vulnerability of cultivated and wild barley to African stem rust race TTKSK. *Advance in Barley Sciences* (Springer: The Netherlands), pp. 243–55.

Steuernagel B., Periyannan S. K., Hernández-Pinzón I., Witek K., Rouse M. N., Yu G., Hatta A., Ayliffe M., Bariana H., Jones J. D. G., Lagudah E. S., and Wulff B. B. H. (2016). Rapid cloning of disease-resistance genes in plants using mutagenesis and sequence capture. *Nat. Biotechnol.*, 34: 652–55.

Sun W., Dunning F. M., Pfund C., Weingarten R and Bent A. F. (2006). Within-Species Flagellin Polymorphism in *Xanthomonas campestris* pv *campestris* and Its Impact on Elicitation of Arabidopsis FLAGELLIN SENSING2–Dependent Defenses. *The Plant Cell*, 18(3): 764–79. doi: <http://dx.doi.org/10.1105/tpc.105.037648>

The, T. T. (1973). Chromosome location of genes conditioning stem rust resistance transferred from diploid to hexaploid wheat. *Nat. New Biol.*, 241: 256.

The International Wheat Genome Sequencing Consortium (IWGSC). (2014). A chromosome-based draft sequence of the hexaploid bread wheat (*Triticum aestivum*) genome. *Science*, 345: 286–87.

Tremblay A., Hosseini P., Alkharouf N., Li S., Matthews B. F. (2010). Transcriptome analysis of a compatible response by *Glycine max* to *Phakopsora pachyrhizi* infection. *Plant Science*, 179: 183–93.

Truman W., Torres de Zabala M. and Grant M. (2006). Type III effectors orchestrate a complex interplay between transcriptional networks to modify basal defence responses during pathogenesis and resistance. *The Plant Journal*, 46: 14–33. doi: 10.1111/j.1365-3113X.2006.02672.x

Uppalapati S. R., Ishiga Y., Doraiswamy V., Bedair M., Mittal S., Chen J., Nakashima J., Tang Y., Tadege M., Ratet P., Chen R., Schultheiss H., and Mysore K. S. (2012). Loss of Abaxial Leaf Epicuticular Wax in *Medicago truncatula* *irg1/palm1* Mutants Results in Reduced Spore Differentiation of *Anthraco*se and Nonhost Rust Pathogens. *The Plant Cell*, 24(1): 353–70.

van de Mortel M., Recknor J. C., Graham M. A., Nettleton D., Dittman J. D., Nelson R. T., Godoy C. V., Abdelnoor R. V., Almeida A. M. R., Baum T. J., and Whitham S. A. (2007). Distinct biphasic mRNA changes in response to Asian

soybean

rust infection. *Mol. Plant Microbe Interact.*, 20: 887–99.

van Esse P., van't Klooster J. W., Bolton M. D., Yadeta K. A., van Baarlen P., Boeren S., Vervoort J., de Wit P. J. G. M., and Thomma B. P. H. J. (2008). The Cladosporium fulvum Virulence Protein Avr2 Inhibits Host Proteases Required for Basal Defense. *The Plant Cell*, Vol. 20: 1948–1963. doi: 10.1105/tpc.108.059394

Vanegas G., Garvin D. F., and Kolmer J.A. (2008). Genetics of stem rust resistance in the spring wheat cultivar Thatcher and the enhancement of resistance by Lr34. *Euphytica*, 159: 391–401.

Veronese P., Nakagami H., Bluhm B., Abuqamar S., Chen X., Salmeron J., Dietrich R. A., Hirt H., Mengiste T., (2006). The membrane-anchored BOTRYTIS-INDUCED KINASE1 plays distinct roles in Arabidopsis resistance to necrotrophic and biotrophic pathogens. *Plant Cell*, 18: 257–273.

Wang Y., Cheng X., Shan Q., Zhang Y., Liu J., Gao C., and Qiu J.-L. (2014a). Simultaneous editing of three homoeoalleles in hexaploid bread wheat confers heritable resistance to powdery mildew. *Nature Biotechnology*, 32: 947–51. doi:10.1038/nbt.2969

Wang C. X., El-Shetehy M., Shine M. B., Yu K. S., Navarre D., Wendehenne D., Kachroo A., and Kachroo P. (2014b). Free radicals mediate systemic acquired resistance *Cell Rep.*, 7: 348–55.

Wang S. C., Wong D. B., Forrest K., Allen A., Chao S. M., Huang B. E., Maccaferri M., Salvi S., Milner S. G., Cattivelli L., Mastrangelo A. M., Whan A., Stephen S., Barker G., Wieseke R., Plieske J., Lillemo M., Mather D., Appels R., Dolferus R., Brown-Guedira G., Korol A., Akhunova A. R., Feuillet C., Salse J., Morgante M., Pozniak C., Luo M. C., Dvorak J., Morell M., Dubcovsky J., Ganai M., Tuberosa R., Lawley C., Mikoulitch I., Cavanagh C., Edwards K. J., Hayden M., Akhunov E. (2014c). International Wheat Genome Sequencing Consortium Characterization of polyploid wheat genomic diversity using a high-density 90 000 single nucleotide polymorphism array. *Plant Biotechnol. J.*, 12: 787–96. <http://doi.org/10.1111/pbi.12183>

Whitham S. A., Yamamoto M. L., and Carrington J. C. (1999). Selectable viruses and altered susceptibility mutants in *Arabidopsis thaliana*. *Proceedings of the National Academy of Sciences*, 96(2): 772–77.

Winfield M. O., Wilkinson P. A., Allen A. M., Barker G. L., Coghill J. A., Burridge A., Hall A., Brenchley R. C., D'Amore R., Hall N., Bevan M. W., Richmond T., Gerhardt D. J., Jeddloh J. A., Edwards K. J. (2012). Targeted re-sequencing of the allohexaploid wheat exome. *Plant Biotechnol. J.*, 10: 733–42.

- Wu Y., Bhat P. R., Close T. J., and Lonardi S. (2008). Efficient and Accurate Construction of Genetic Linkage Maps from the Minimum Spanning Tree of a Graph. *PLoS Genet.*, 4(10): e1000212. doi:10.1371/journal.pgen.1000212.
- Yamamoto-Katou A., Katou S., Yoshioka H., Doke N., and Kawakita, K. (2006). Nitrate reductase is responsible for elicitor-induced nitric oxide production in *Nicotiana benthamiana*. *Plant Cell Physiol.*, 47: 726-35.
- Yang B., Sugio A. & White F. F. (2006). *Os8N3* is a host disease-susceptibility gene for bacterial blight of rice. *Proc. Natl. Acad. Sci. USA*, 103:10503–08.
- Yoshii M., Yoshioka N., Ishikawa M., and Naito S. (1998). Isolation of an *Arabidopsis thaliana* mutant in which accumulation of *cucumber mosaic virus* is delayed. *Plant J.*, 13: 211-19.
- Yoshii M., Nishikiori M., Tomita K., Yoshioka N., Kozuka R., Naito S., and Ishikawa M. (2004). The *Arabidopsis cucumovirus* multiplication 1 and 2 loci encode translation initiation factors 4E and 4G. *J. Virol.*, 78: 6102–111. doi: 10.1128/JVI.78.12.6102-6111.2004.
- Young ND. (1996). QTL mapping and quantitative disease resistance in plants. *Annu. Rev. Phytopathol.*, 34: 479–501
- Yu L. X., Lorenz A., Rutkoski J., Singh R. P., Bhavani S., Huerta-Espino J., and Sorrells M. E. (2011) Association mapping and gene-gene interaction for stem rust resistance in spring wheat germplasm. *Theor. Appl. Genet.*, 123: 1257-68
- Yu L. X., Barbier H., Rouse M. N., Singh S., Singh R. P., and Bhavani S. (2014). A consensus map for Ug99 stem rust resistance loci in wheat. *Theor. Appl. Genet.*, 127: 1561–81. 10.1007/s00122-014-2326-7.
- Yu, J. B., Bai, G. H., Zhou, W. C., Dong, Y. H., and Kolb, F. L. (2008). Quantitative trait loci for *Fusarium* head blight resistance in a recombinant inbred population of Wangshuibai/Wheaton. *Phytopathology*, 98: 87-94.
- Zago E., Morsa S., Dat J. F., Alard P., Ferrarini A., Inze D., Delledone M., and Van Breusegem F. (2006). Nitric oxide and hydrogen peroxide responsive gene regulation during cell death induction in tobacco. *Plant Physiol.*, 141: 404-11.
- Zhang, W., Olson, E. L., Saintenac, C., Rouse, M., Abate, Z., Jin, Y., Akhunov, E., Pumphrey, M. O., and Dubcovsky, J. (2010). Genetic maps of stem rust resistance gene *Sr35* in diploid and hexaploid wheat. *Crop Sci.*, 50: 2464-74.
- Zhang D., Bowden R. L., Yu J., Carver B. F., and Bai G. (2014). Association analysis of stem rust resistance in U.S. winter wheat. *PLoS ONE* 9(7):e103747. doi:10.1371/journal.pone.0103747

Zheng Z., Nonomura T., Appiano M., Pavan S., Matsuda Y., Toyoda H., Wolters A.-M. A., Visser R. G. F., and Bai Y. (2013). Loss of function in Mlo orthologs reduces susceptibility of pepper and tomato to powdery mildew disease caused by *Leveillula taurica*. *PLoS One*, 8(7): e70723. doi: 10.1371/journal.pone.0070723.